.

MAGNETIC FIELD ASSISTED ULTRA-PRECISION MACHINING FOR IMPROVING MACHINABILITY OF TITANIUM ALLOYS

YIP WAI SZE

Ph.D

The Hong Kong Polytechnic University

2018

The Hong Kong Polytechnic University

Department of Industrial and Systems Engineering

Magnetic Field Assisted Ultra-Precision Machining for Improving Machinability of Titanium Alloys

YIP WAI SZE

A thesis submitted in partial fulfillment of the requirements for the degree of Doctor of Philosophy

January 2018

CERTIFICATE OF ORIGINALITY

I hereby declare that this thesis is my own work and that, to the best of my knowledge and belief, it reproduces no material previously published or written, nor material that has been accepted for the award of any other degree or diploma, except where due acknowledgement has been made in the text.

_____(Signed)

Yip Wai Sze_____(Name of student)

Abstract

Ultra-precision machining (UPM) is a promising machining technology for manufacturing precise components with nanometric surface roughness and sub-micron form accuracy without the need for a subsequent process. As the machined components generated by UPM are extremely precise, UPM involves various machining and material factors. Those machining and material factors such as high cutting temperature, machining vibration, and tool wear, as well as material swelling, are potentially dominant to the machined surface quality of fabricated components, the complexity of the interaction between each factor adds challenges to UPM.

Titanium alloys are widely applied in the biomedical industry for precise components due to their excellent material properties. However, titanium alloys are difficult to cut materials because of their low thermal conductivity and high sustainability of work hardening at the elevated temperature, causing the localized cutting heat and the machining vibration at the tool/workpiece interface during machining, leading to serious tool wear, a high level of material swelling, and unsatisfactory surface finishing of the machined titanium alloys. Therefore, an evolutional machining technology should be adopted to uplift the machining performances of titanium alloys in UPM.

This thesis therefore proposes a novel machining technology that introduces a magnetic field into the UPM process with the aim of overcoming the machining difficulties of

titanium alloys encountered in UPM. In the experimental set up, a magnetic field was superimposed onto titanium alloys in single point diamond turning (SPDT) by positioning titanium alloys in between of two permanent magnets. An eddy current damping effect and a magnetic field effect were then induced in the machining processes to positively influence the machining performances by suppressing the machining vibration and enhancing the thermal conductivity at the tool/workpiece interface. The unique benefits of the proposed research can be categorized and summarized as follows:

(1) A magnetic field was superimposed onto static titanium alloys during SPDT in order to exert the core influence of the magnetic field, which is the enhancement of thermal conductivity at the tool/workpiece interface. During SPDT in the presence of magnetic field, the magnetic dipolar energy inside the materials is sufficient to overcome the thermal energy. The paramagnetic particles generated at the tool/workpiece interface tend to align along the direction of the external field due to the positive value of magnetic susceptibility of titanium alloys. These aligned titanium alloy particles act as linear chains, which are highly conductive paths for transferring heat and enable the promotion of the fast heat transference along the path of the fluid carrier. Using this principle, SPDT was conducted in between of two permanent magnets for the purpose of uplifting the thermal conductivity of

titanium alloys and consequently minimizing the material swelling effect on the machined surface.

(2) A magnetic field was superimposed onto rotating titanium alloys in SPDT in order to exert an eddy current damping effect. When a conductive metal rotates within a magnetic field, an eddy current is generated through a stationary magnetic field inside the conductor. The eddy current will create its own magnetic field in the opposite direction of the external magnetic field, it generates a repulsive force called the Lorentz force, which the Lorentz force compensates the vibration displacement of machining system. Using this principle, rotating titanium alloys within a magnetic field in SPDT were subjected to the eddy current damping effect, which functionally counteracts the vibration force and energy from the turning system.

(3) SPDT of titanium alloys was influenced by the integral effects of an eddy current damping and a magnetic field. The eddy current damping effect reduces the machining vibration of the rotating workpieces, while the magnetic field effect enhances the thermal conductivity at the tool/workpiece interface in SPDT. Both help to reduce damages to the diamond tool in SPDT of titanium alloys, even in a dry machining environment. The positive influences from the magnetic field on SPDT inspire and facilitate the implementation of ultra-precision manufacturing process in the green and clean directions.

The research findings and subsequent works in this thesis contribute to enhance the current machining performances of titanium alloys in UPM by resolving the problems of machining vibration, tool wear, and material recovery. The proposed novel machining technology provides a new cutting approach that not only uplifts the existing precision level of machined products using titanium alloys, but which also contributes to the feasibility of green and clean manufacturing processes.

Publication arising from this study

Journal papers

1. **Yip, W. S.**, & To, S. (2018) Ductile and brittle transition behavior of titanium alloys in ultra-precision machining. Scientific Reports, 8, 3934. (SCI Impact factor: 4.259)
2. **Yip, W. S.**, & To, S. (2017). Tool life enhancement in dry diamond turning of titanium alloys using an eddy current damping and a magnetic field for sustainable manufacturing. *Journal of Cleaner Production*, *168*, 929-939. (SCI Impact factor: 5.715, Q1, 19/229, Environment Science, Top 10%)
3. **Yip, W. S.**, & To, S. (2017). Reduction of material swelling and recovery of titanium alloys in diamond cutting by magnetic field assistance. *Journal of Alloys and Compounds*, 722, 525-531. (SCI Impact factor: 3.133, Q1, 5/74, Metallurgy & Metallurgical Engineering, Top 10%)
4. **Yip, W. S.**, & To, S. (2017). An application of eddy current damping effect on single point diamond turning of titanium alloys. *Journal of Physics D: Applied Physics*, *50*(43), 435002. (SCI Impact factor: 2.588, Q2, 44/148, Applied Physics)
5. **Yip, W. S.**, & To, S. Control of tool tip vibration in single point diamond turning using eddy current damping effect. *Journal of Physics D: Applied Physics (Under review)*.

6. **Yip, W. S.**, & To, S. Sustainable manufacturing of ultra-precision machining of titanium alloys using a magnetic field and its sustainability assessment. *Sustainable Materials and Technologies (Under review).*

7. **Yip, W. S.**, & To, S. Sustainable manufacturing of ultra-precision machining using social network analysis. *Complexity (Under review).*

8. **Yip, W. S.**, & To, S. Experimental and theoretical investigations of tool tip vibration induced by material swelling in single point diamond turning of titanium alloys. *Mechanical Systems and Signal Processing (submitted to journal)*.

9. **Yip, W. S.**, & To, S. Reduction of size effect by altering friction coefficient using a magnetic field in ultra-precision diamond cutting of titanium alloys. *Materials Science and Engineering: C (submitted to journal)*.

Conference papers

1. **Yip, W. S.**, To, S., & Deng, Y. (2015). Preliminary experimental study on ultrasonic assisted diamond turning Ti6Al4V alloy. In *Proceedings of the 15th International Conference of the European Society for Precision Engineering and Nanotechnology, EUSPEN 2015*. Euspen.

2. **Yip, W. S.**, & To, S. (2015). Influence of electropulsing treatment on microstructures and surface integrity of ti-6Al-4V alloys in ultra-precision diamond turning. *In Proceedings of the 6th International Conference of Asian*

Society for Precision Engineering and Nanotechnology, ASPEN 2015, Harbin, China, 2015.

Acknowledgements

Foremost, I would like to express the deepest thanks to my chief supervisor, Dr. Sandy To. She continuously encourages and supports me to adventure the new idea in the research and the excitement during the progress of PhD study. Without her patient guidance and persistent supports this thesis would not have been possible.

I would like to thank all of the staffs in State Key Laboratory of Ultra-precision Machining Technology of The Hong Kong Polytechnic University, they provide me a supportive platform to conduct all the experiments in this thesis. Special thanks to all of the classmates and my friends who are still working hard to finish the PhD study, they share the valuable knowledge and research approaches with me and so that I can continuously improve myself to conduct better researches.

Last but not least, I would like to express my honest thanks to my mother, who waits for the graduation day of PhD for several years, she gives me the supports and encouragements as always.

Table of Contents

List of figures

List of tables

List of acronyms

AFM = Atomic force microscopy

CBN = Cubic boron nitride

CCP = Computer controlled polishing

CV = Coefficient of variation

DMFS = Dry magnetic field sample

DNMFS = Dry non-magnetic field sample

ECDM = Electrochemical discharge machining

EDM = Electric discharge milling

EMF = Electromotive force

FFT = Fast Fourier transform

LPMM = Laser induced plasma micro-machining

MFS = Magnetic field sample

NMFS = Non-magnetic field sample

PZT = Piezoelectric actuator

RadCrV = Radius of curvature of cutting profile

SPDT = Single point diamond turning

SEM = Scanning electron microscopy

TC4 = Ti6Al4V

TEM = Transmission electron microscopy

UPM = Ultra-precision machining

VB = The maximum width of wear mark on the flack face

XRD = X-ray diffraction

Chapter 1 Introduction

1.1 Background research

Owing to the excellent material properties of two phase (α+β) titanium alloys Ti6Al4V such as excellent strength-to-weight ratio and extraordinary corrosion resistance, they are widely used in biomedical and automobile industries (Maurotto et. al., 2014). Despite the increased applications of titanium alloys, they are relatively expensive in comparison to other traditional metals and alloys because of the complicacy of production in the raw stage (Bomberger and Froes, 1984; Hayes et al., 1984). On the other hand, titanium alloys are difficult to cut materials because of the low thermal conductivity at the elevated temperature, causing the unfavorable effects on machinability of the materials especially in ultra-precision machining (UPM). Titanium alloys hold the material property of low thermal conductivity, this material properties hinders the cutting heat transference from the cutting zone, the cutting heat cannot be dissipated from the working surface effectively. Consequently, the localized heat is accumulated at the diamond tool tip which accelerate tool wear. The dispersion of cutting heat is inhibited, and the high cutting temperature is intensified at the tool/workpiece interface under the continuous cutting process which deteriorates the tool condition ultimately, leading to unsatisfactory surface finishing and surface integrity. The above undesired cutting characteristics outweigh the benefit of high

precise effect from UPM.

On the other hand, some machining technologies in UPM such as drilling and turning processes are also unlikely to machine titanium alloys with good surface finishing because of the accumulation of high machining heat at the tool/workpiece interface, therefore, the machined surface appears poor surface quality and form accuracy (Maurotto et. al., 2014). Utilizing of liquid lubricants have been proposed to solve the problem of heat localization in machining of titanium alloys. Lubricants enable to disperse the cutting heat from the cutting zone to the surrounding in the faster rate, improving and lengthening tool life. However, the effectiveness of heat dissipation using traditional lubricants is still low, the surface integrity and diamond tool life are only improved with few extensions according to literature, which the machining results in the wet machining environment remain unsatisfied the requirement of precise products made by titanium alloys in the current market. On the other hand, uses of lubricants cause environmental and cost concerns. All of the above contribute the needs of evolution of machining technologies for machining titanium alloys in UPM.

Siekmann (1955) mentioned that “machining of titanium and its alloys would always be a problem, no matter what techniques are employed to transform this metal into chips". Titanium alloys motivates several famous companies such as Rolls-Royce and General Electrics to put large investments in advancing machining techniques to reduce

the machining costs, aiming to reach the reasonable material removal rate and surface quality of titanium alloys simultaneously (Ezugwu and Wang, 1997). The evolutional machining technology should be adopted to resolve the above problematic machining and material factors induced from the machining processes of titanium alloys for uplifting the machining performances of these metals in UPM.

The machining and material factors are potentially dominant to affect the surface quality of fabricated components made of titanium alloys. Machining factors including high cutting temperature, machining vibration and the induced tool wear inevitably happen in the machining process which provide challenges in UPM. On the other hand, titanium alloys hold the low thermal conductivity and high sustainability of work hardening at the elevated temperature, those material factors additionally rise the machining difficulties. In addition, the material factor of low elastic modulus of titanium alloys causes a high level of material recovery, it leads form accuracy of machined components always largely different from the assigned machining parameters, resulting in unsatisfactory surface integrity. Therefore, there exists a research gap in enhancing the machinability of titanium alloys in UPM, promoting the motivation on modifying the current technologies in UPM in order to enhance the machining performances of these excellent metals – titanium alloys.

In this thesis, a novel machining technique - a magnetic field was firstly introduced

into UPM area which delivered the positive influences on the machining processes in UPM of titanium alloys.

The application of magnetic field delivers three major machining outcomes in UPM which contribute to resolve the problematic sources of machining difficulties of titanium alloys in UPM. First, the magnetic field enhances the thermal conductivity of titanium alloys at the tool/workpiece interface in single point diamond cutting once the workpiece has a positive reaction toward the magnetic field. The cutting heat localized at the tool edge could be dissipated efficiently in the presence of magnetic field, thus minimizes tool wear and the material recovery effect. Second, an eddy current damping effect would be generated inside the workpiece in single point diamond turning (SPDT) based on the principle of rotating conductor within a magnetic field, which suppresses the machining vibrations in the turning system. Third, the combining effects of thermal conductivity enhancement and suppression of machining vibration induced by the eddy current damping effect minimize tool wear and enhance diamond tool life even in dry machining condition, which promotes the development of UPM in the green and environmental friendly directions.

The above benefits induced from the magnetic field resolve the underlying sources of machining difficulties in UPM. The application of magnetic field in UPM facilitates the machinability of titanium alloys as well as supporting the green manufacturing

concept.

1.2 Research objectives

As the machining difficulties and negative machining outcomes in UPM of titanium alloys subsist, therefore, in this study, an appropriate machining technology is adapted in order to provide the objectives of following:

(1) To propose a novel machining technology – magnetic field assisted ultra-precision machining to increase the machinability of titanium alloys

In response to the material properties of titanium alloys causing low machinability of titanium alloys in UPM, the functions of increasing the cutting heat dissipation and minimizing the machining vibration should be delivered by the proposed machining technology. In this study, magnetic field assisted ultra-precision machining is introduced to deliver the influence of a magnetic field and an eddy current damping effect, which the captioned effects benefit to reduce the negative machining outcomes in UPM of titanium alloys.

(2) To study the machinability of titanium alloys in magnetic assisted ultra-precision machining

Magnetic field assisted ultra-precision machining enables to increase the machinability of titanium alloys. A serious of experiments would be conducted in this study in order to investigate and examine the effectiveness of magnetic field

assistance on the machining performance on UPM of titanium alloys systematically. The machining performance indicators in term of diamond tool condition, surface roughness, form accuracy, cutting force and machining vibration under the magnetic field influences would be investigated extensively in this study.

(3) To examine the effect of a magnetic field on material swelling in SPDT of titanium alloys

A magnetic field enables to increase the thermal conductivity of titanium alloys which are classified as paramagnetic materials. Lowering cutting temperature in diamond cutting enables to suppress the material swelling effect on the machined surface. The surface integrity in term of surface roughness, form accuracy and form error of cutting profile generated under magnetic field assisted diamond cutting are examined in order to investigate the effects of a magnetic field on the material swelling effect.

(4) To investigate the effects of eddy current damping effect on ultra-precision machining of titanium alloys

The precise level of machined titanium alloys components is always the challenging issue in UPM. The low thermal conductivity of titanium alloys causes serious tool wear and the low level of surface integrity of machined titanium alloys in UPM. By employing the proposed machining technology, surface finishing and form accuracy

of the machined titanium alloys increase, consequently upgrading the precise level of machined titanium alloys in UPM and widening the applications of titanium alloys in the related industries.

1.3 Organization of the thesis

This report includes six chapters, they are arranged as follow:

CHAPTER 1 is an introduction; it describes the background research of the thesis; this chapter includes the current research gap of machining titanium alloys in UPM and the methodology planned to be used in the study.

CHAPTER 2 is the part of literature review which it states all of the reference materials that are related to the thesis. The materials include the basic information of ultra-precision machining, material properties of titanium alloys, review of hybrid machining technologies using a magnetic field and an eddy current damping effect.

CHAPTER 3 is the report about the application of eddy current damping effect on SPDT. The theory and basic principles of eddy current damping effect are demonstrated in this chapter. Also, the experimental investigations in term of cutting force, surface roughness, vibration amplitude, chip formation and diamond tool condition using the eddy current damping effect are written in this chapter.

CHAPTER 4 reports the effectiveness of magnetic field on the suppression of material recovery of titanium alloys in diamond cutting. In this chapter, the errors in

form accuracy, cutting width, cutting depth and cutting radius for both magnetic sample and nonmagnetic sample are examined. The comparison of the level of material recovery on the machined titanium alloys surface between both magnetic sample and nonmagnetic sample is also made.

CHAPTER 5 reports the environmental concerns in UPM of titanium alloys. In this chapter, it reports that an utilization of magnetic field to SPDT of titanium alloys in dry machining environment, which aims to apply the magnetic field to remove the use of lubricant in the SPDT process. The experimental results related to adhesive diamond tool wear are reported, also the surface quality of machined surface of titanium alloys in dry SPDT is discussed in this chapter. This chapter offers the preliminary guideline of green concept in UPM.

CHAPTER 6 is the conclusion part, the summaries of research work of the whole thesis. The contributions of the research to the existing ultra-precision machining area are also described. Future research plans and the extended works related to magnetic field assisted UPM are stated.

Chapter 2 Literature review

2.1 Overview of ultra-precision machining

With the speed development of various high technology products, the demands of products with high surface quality are increasing. One of advanced manufacturing techniques, ultra-precision machining (UPM) provides the feasible approach to fabricate the precise components which fulfill the needs. UPM enables to generate the surface with non-rotational symmetry with small scale topologies. Several core industries such as optic and medical manufacture their precise products by UPM technology. The machined surface generated by UPM enables to achieve sub-micrometer form accuracy and nanometric surface roughness. Compared with the conventional machining technologies, the machining costs in UPM are relatively higher. On the other hand, form accuracy and surface roughness of fabricated surface generated by UPM accomplish 100 times and 1000 times respectively in comparison to that of the conventional machining technologies (Cheung and Lee, 2000a).

UPM technology is normally categorized as four types, they are single point diamond turning (SPDT), ultra-precision grinding, ultra-precision raster milling and ultra-precision raster grinding. SPDT enables to give out machined products with the final shape by only one cutting step without the second machining step. SPDT in UPM is used for generating edges and final cutting of semi-finish products which the

geometries of the machined surface are varied continuously in the controllable manner. Figure 2.1 shows the applications of four types ultra-precision machining technologies with the corresponding machining processes. Figure 2.2 illustrates the evolutions of machining accuracy of machining technology in the past decade.

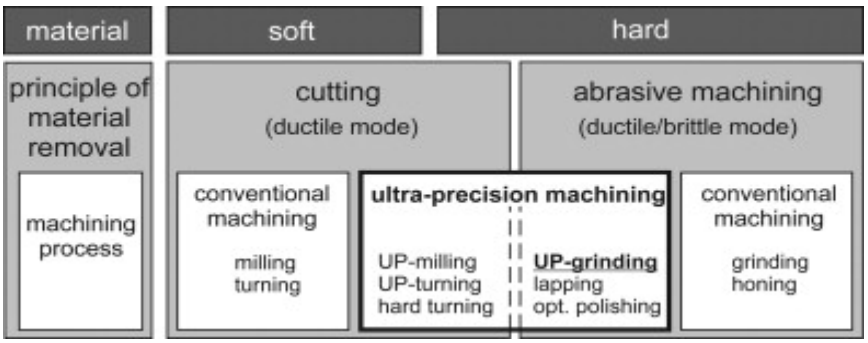

Figure 2.1 The applications of four types ultra-precision machining technologies according to the processing method (Brinksmeiera et. al., 2010).

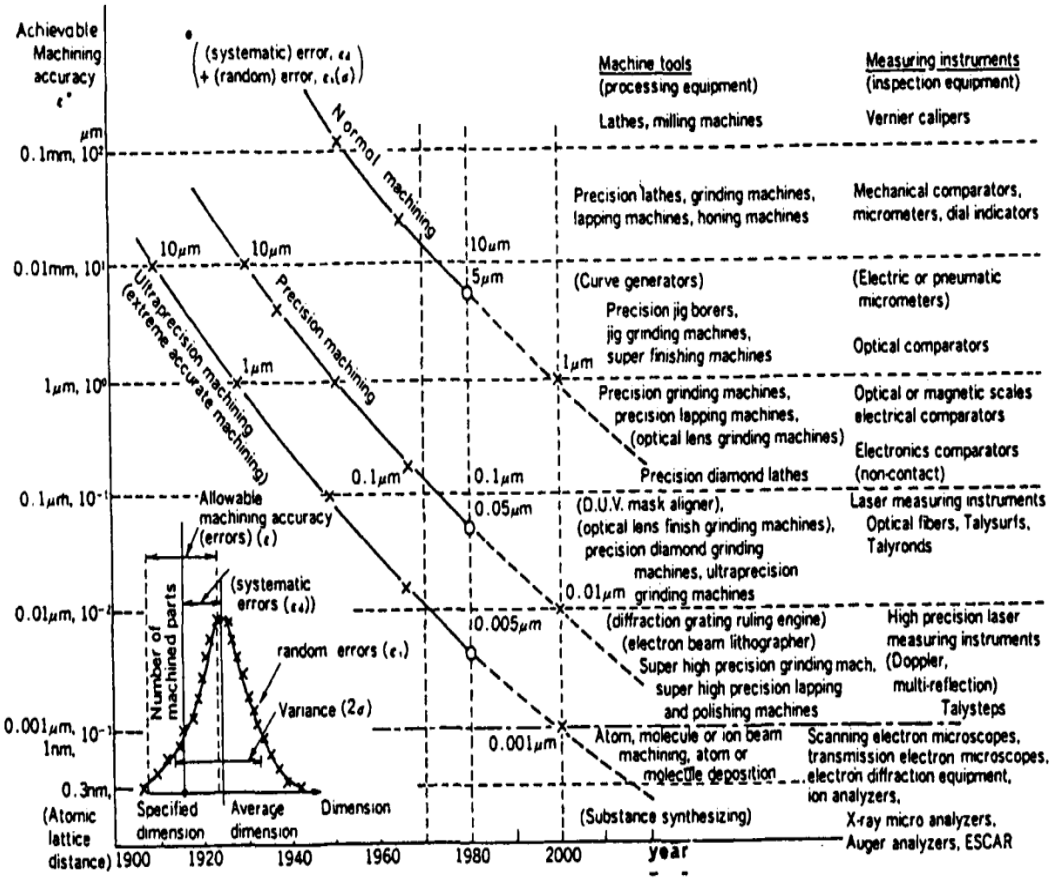

Figure 2.2 The evolution of machining accuracy in the past decade (Taniguchi, 1983).

Conventional machining technologies are still applied nowadays in some industries although they are unable to generate surface finishing with similar surface roughness and form accuracy as UPM technology. Various industries require different types of machining approach depending on their own products. Figure 2.3 shows the applications of different machining technologies including conventional machining technologies and UPM in various industries nowadays.

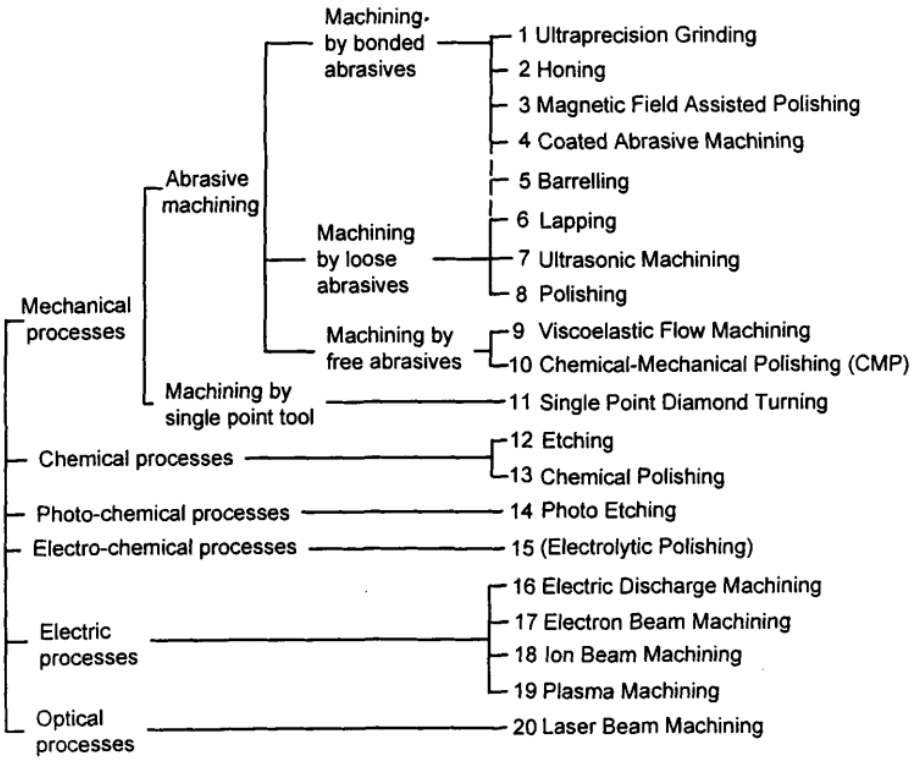

Figure 2.3 Machining technologies for different processing approaches (Nogawa, 1988).

2.1.1 Single point diamond turning

Single-point diamond turning (SPDT) is treated as a valid technique in the UPM area which it is available to fabricate a surface with high form accuracy profile and the

excellent surface integrity without second finishing, therefore the products manufactured by SPDT enable to achieve to the optical grade quality (Li et. al., 2014). SDPT is applied to fabricate high precise products such as optical, electronic and mechanical components (Ikawaa et. al., 1991).

During the SPDT process, a workpiece is locked into the fixture and rotated by an ultra-precision machine while the diamond tool is moved according to the controller input. SPDT presents an accurate surface profile and a small step control. It enables to generate the freeform shape components in a single cutting process without a further polishing process. Materials can be machined with a good surface integrity by choosing the suitable parameters in SPDT, which the chip formations are followed by the deformation process instead of fracture (Goel et. al.,2013).

A monocrystalline diamond tool is used in SPDT which it obtains nanoscale edge sharpness and excellent wear resistance. Depth of cut involved in SPDT process is smaller than the mean grain size of polycrystalline machined materials, therefore, the diamond cutting is performed within a single grain. Consequently, the process is capable of generating components with submicrometric form accuracy and nanometric surface roughness. Problematic diamond tool wear exists in SPDT as the rapid degradation of diamond tool occurs, especially when it is used to machine difficult to cut materials. Tool wear leads to an abrupt change in the material removal mechanism

and finally the quality of machined surface is affected. Tool wear also causes other problems unrelated to the wear condition such as chipping and machine setting difficulties which induce high machining costs in SPDT ultimately (Goel et. al.,2013). Therefore, a better grasp of tool wear mechanism is necessary in monitoring diamond tool life. Many studies have been conducted to investigate on recognizing and enhancing the tool condition in SPDT by experimental and observational approaches (Shimada et al., 2004; Paul et al., 1996; Zhang et al., 2014). The width of tool flank wear is normally applied to be an indicator of diamond tool wear in the experimental studies of SPDT process. Furthermore, the diamond tool used in SPDT is highly chemical sensitive to some particular metallic materials. When the turning process is started and the diamond tool contacts with the materials containing carbon element, the transition of diamond to graphite is driven because of the high cutting temperature. This causes rapid tool wear because the diamond tool begins to degrade and change in the mechanical properties, which are not suitable for the further cutting process. Therefore, SPDT is commonly used to machine of nonferrous materials.

Chip morphology is one of the important features in SPDT. The chip formation is highly related to the machining condition and machining parameters. Furthermore, in SPDT, it is essential to understand the cutting mechanisms and machining factors which are dominant to the saw-tooth chip formation. It is also critical to study the mechanism

about the transitions from continuous chips to serrated chips and the effects of machining parameters and material properties on that transitions. On the other hand, the diamond tool geometry is proven to be one of influencing factors of chip formation. Chips are normally divided into four types, they are continuous, segment, serrated and fragmented. One of the most concern areas for studying of the chip formation is the chip segmentation. The chip segmentation is originated by adiabatic shear bands which are induced from the fluctuation of cutting force, surface roughness variation, and tool condition.

Mechanisms of chip formation have been deeply studied by many researchers, Bayoumi and Xie (1995) focused on the chip formation of titanium alloy Ti6Al4V by utilizing scanning electron microscopy (SEM) image and X-ray diffraction (XRD) with chemical methodology approaches, they observed the phase transformation within the shear bands. On the other hand, for high speed machining of hard metals, the cutting temperature is reached to extremely high that it induces the phase transformation of titanium alloys. The shear band inside the chip was changed to hard layer when it was undergone fast cooling after machining (Shaw and Vyas, 1998). The generation of saw tooth on chip tip is also one of the concerned topics in the chip formation, some researchers stated that the saw tooth chip formation was initiated by the formation of adiabatic shear band in the cutting process. By analyzing the free surface of the chip,

the phase transformation of materials could be predicted (Barry and Byrne, 2002). By understanding the chip formation mechanism especially, the cutting mechanism could be examined deeply, and it assists the investigation of improving machinability of titanium alloys.

2.1.2 Ultra precision grinding technology

The needs for high precise components are significantly up. Ultra-precision grinding is one of UPM technologies aims to produce components with a high surface integrity especially for the board applications such as optical, automobile, medical and aerospace industries.

Ultra-precision grinding is normally applied to produce excellent surface finishing and high form accuracy components. Commonly, difficult to cut materials such as ceramics, carbides and glasses are machined and shaped by an abrasive process.

Ultra-precision grinding belongs to the abrasive process which is highly related to the type of machined material. The process demands the equipment of fine grain wheel, abrasives particles and spindle. Ultra-precision grinding adapts extremely small depth of cut with sub-micrometer small feedrate and low cutting speed in order to generate a high precise surface.

Ultra-precision grinding machines are built up by the combination of grinding spindle and diamond turning machine. This set up enables to enhance the grinding

performance to generate accurate aspheric optics which are highly demanding in the current market. Also, machining time is surprisingly decreased. Installation of grinding spindle to the diamond turning machine contributes to wide applications (Nicholas and Boon, 1981).

Diamond and cubic boron nitride (CBN) is popularly used as an abrasive tool in grinding process (Chen et. al., 2002). For diamond type abrasive materials, they are classified as two types, they are natural and artificial types. They both have excellent wear resistance, and low coefficient of friction. However, the diamond abrasive tool is highly chemical sensitive to metallic materials, it causes the transition of diamond inside the wheel in the grinding process under high grinding temperature, and this induces rapid tool wear. Therefore, ultra-precision grinding normally uses to machine nonferrous materials. Because of the problem, the researchers proposed that diamond grains should be coated by different materials which they acted as a protective layer to separate the diamond grain and the working surface in the grinding process, the coated layer avoids diamond from oxidation induced by the chemical reaction (Wang et. al., 2003). Coated diamond grains enable to enhance the grinding ratio, decreasing wear out of diamond grains in the machining process.

2.1.3 Ultra precision polishing technology

Ultra-precision polishing is the UPM process which involves the plastic deformation of

workpieces with extremely small step. The polishing process has been evaluated time by time with the sequence of hand polishing, machining polishing and UPM.

Some materials such as biomedical materials, ferrous materials are not satisfactory to be machined by SPDT and ultra-precision grinding to achieve surface finishing with the nanometer range. For the above reason, ultra-precision polishing is suggested to be a substitutional machining technology for fabricating ferrous materials. Some researchers reported that there were several types of computer controlled polishing such as water jet polishing and ion beam polishing (Cheung et. al., 2011). Because of the superior influences of ultra-precision polishing on the surface generation, many attentions have been paid on the researches of understanding the material removal mechanism in ultra-precision polishing. Ultra-precision polishing provides advanced benefits on the machining performances in comparison to traditional hand polishing, the comparisons between traditional hand polishing and ultra-precision polishing are shown in Table 2.1

Table 2.1 Comparisons of traditional hand polishing and ultra-precision polishing.

Traditional hand polishing	Ultra-precision freeform polishing
•Quality varies with workers •NO guarantee •NO repeatability •Inefficiency, time-consuming and higher cost •Cannot ensure the texture formation for self-cleaning effect •Difficult to ensure form accuracy	•Computer controlled polishing (CCP) •Quality can be guaranteed •Repeatability •Once success in forming the texture, the texture formation can be guaranteed •Improve and ensure form accuracy

Under the fast development of technology, the polishing technology has been stepped into computer controlled ultra-precision polishing with multiple axis. This technology enables to generate a freeform surface with higher form accuracy and lower surface roughness. Ultra-precision polishing can be implemented to machine difficult to machine materials such as glass and ferrous materials which they are not recommended to machine by SPDT in UPM. Nowadays, ultra-precision polishing is used to generate super mirror surface finishing by removing the surface imperfections (Cheung et. al., 2011). Zeeko Ltd company from United Kingdom offers a freeform polishing machine with 7-axis movement, to monitor the movements of workpiece and polishing head by 4 axes and 3 axes respectively. Figure 2.4 shows the direction of 7 axes in the ultra-precision polishing process.

The polishing process is divided into two types, they are mechanical polishing, and another is fluid jet polishing. The mechanical polishing utilizes the plastic made bonnet with a cloth in polishing. Figure 2.5 shows the polishing mechanism in mechanical polishing

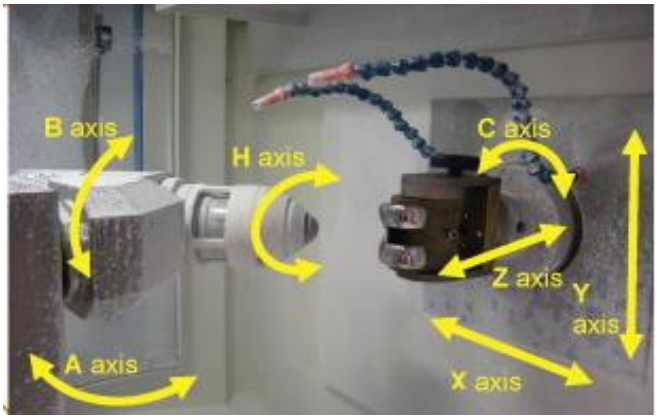

Figure 2.4 The direction of 7 axes of freeform ultra-precision polishing machine (Cheung et. al., 2011).

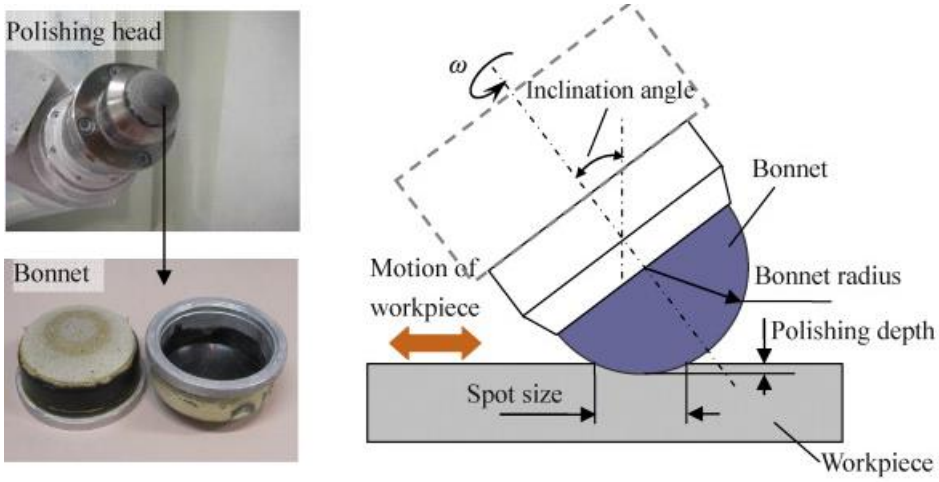

Figure 2.5 Polishing mechanism in mechanical polishing (Cheung et. al., 2011).

For fluid jet polishing, it uses the principle of quick erosion induced by abrasive water jet, acting as the machining tool to generate high quality surface finishing (Zhu et. al., 2009). This technology enables to operate in a high material removal rate and results of low surface roughness with free thermal distortion (Huang et. al., 2006). The fluid jet polishing could be applied to machine various materials such as ceramic, glass and hard alloys. Apart from mechanical and fluid jet polishing, some researchers applied the vibration assisted system into ultra-precision polishing. The vibration

assisted spherical polishing system operated by a piezoelectric actuator (PZT) was built, and the machined components showed a significant enhancement of surface roughness in polishing the hardened STAVAX mold, tool wear of the polishing ball also decreased (Shiou and Ciou, 2008).

Ultra-precision polishing enables to give out high quality surface with high surface integrity which are the basic requirement to fabricate the optical grade components. The geometries of machined surface could be flat, aspheric and even freeform. This technology contributes to the board industries nowadays.

2.1.4 Ultra precision raster milling technology

Ultra-precision raster milling is treated as fly cutting. A diamond tool is rotated with circle locus using high speed spindle which the movement creates the cutting motion. Figure 2.6 shows the cutting mechanic of ultra-precision raster milling. A diamond tool is moved by the connectable movement of the spindle and acts as the fly cutting machining technology. Ultra-precision raster milling is applied for generating a non-rotational symmetric surface with high quality and high form accuracy. The components generated by ultra-precision raster milling generally do not need to undergo a further machining process. It is one of the important machining technologies for offering highly precise products.

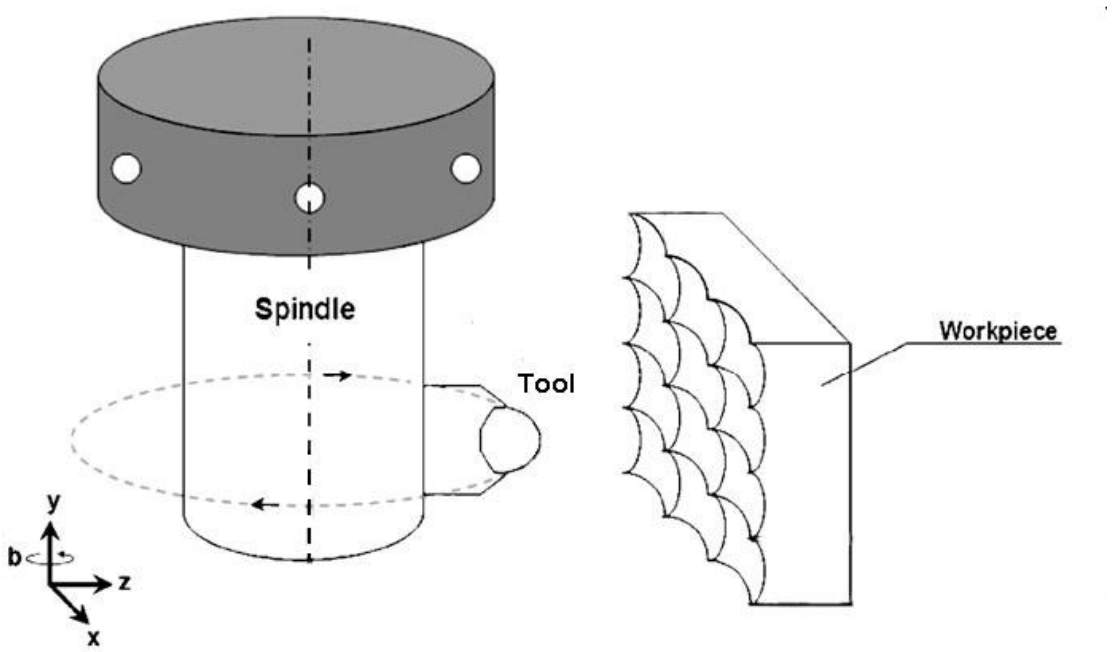

Figure 2.6 The movement of diamond tool in ultra-precision raster milling (Kong et al., 2009).

Ultra-precision raster milling is an unconventional machining process which enables to offer a nanometric surface generation (Chen et. al., 1998). Ultra-precision raster milling causes the phase transformation and plastic deformation on the machined layer. If the machining parameters are set with appropriate values, normally the affected layer is about 250nm (Zhu et. al., 2010). In general, the plastic deformation and phase transformation of machined surface do not occur when feedrate increases up to the certain value. Other machining parameters such as depth of cut and tool radius are also essential for generating a high quality surface in ultra-precision raster milling. Furthermore, the level of plastic deformation decreases with the cutting distance increase. On the other hand, the elastic modulus increases when the machining distance

is larger than a critical value. In ultra-precision raster milling process, the feed direction and raster milling direction are always perpendicular to each other. Consequently, the machined surface is appeared as semi arc profile with a pre-determined distance between each step of cutting process.

The machining strategy of ultra-precision raster milling can be classified by two types, they are horizontal cutting and vertical cutting. Their differences are lied on the milling direction, which the milling direction in horizontal cutting is conducted in the direction of perpendicular to that of vertical cutting. Figure 2.7 shows the vertical and horizontal cutting in ultra-precision raster milling.

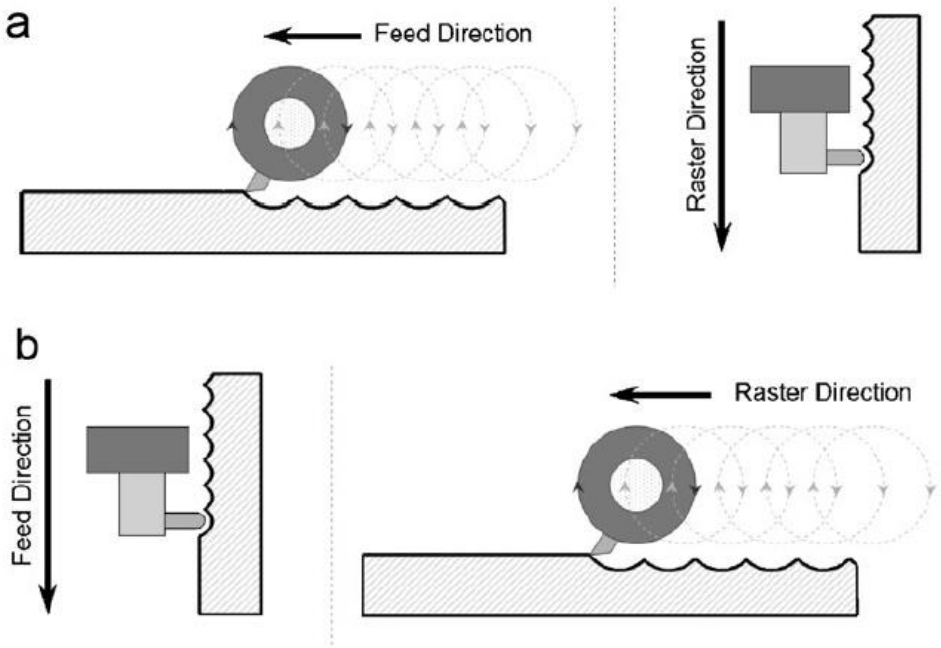

Figure 2.7 The cutter in both vertical and horizontal cutting in ultra-precision raster milling. (Kong et al., 2009).

Precitech Ltd company from United States offers a machine for an intensive ultra-precision raster milling process, Freeform 705G, which enables to provide non-

axisymmetric freeform milling and grinding functions. It is an ultra-precision raster machine with 2 axis turning directions. Optical parts with freeform surface and microstructures can be generated by Freeform 705G, surface roughness of those parts can achieve to the nanometer range and form accuracy can be up to sub-micrometer.

2.2 Material and mechanical properties of titanium alloys

2.2.1 Mechanical properties and applications of titanium alloys

The updated records of tensile and yield strength, elongation and Vickers hardness of different titanium alloys are shown in Table 2.2.

Table 2.2 Tensile strength, yield strength, elongation and Vickers hardness of different titanium alloys (Niinomi, 1998).

Alloy	Process	Tensile strength (Mpa)	Yield strength (Mpa)	Elongation (%)	Vickers hardness (Hv)
1. Ti–20Cr–0.2Si	Casting	874	669	6	318
2. Ti–25Pd–5Cr	Casting	880	659	5	261
3. Ti–13Cu–4.5Ni	Casting	703	—	2.1	—
4. Ti–6Al–4V	Casting	976	847	5.1	—
5. Ti–6Al–4V	Superplastic forming	954	729	10	346
6. Ti–6Al–7Nb	Casting	933	817	7.1	
7. Ti–Ni	Casting	470	—	8	190

According to Table 2.2, the data shows that the yield stress of Ti6Al4V is normally

higher than that of other two phase titanium alloys. Similarly, the elongation percentage of Ti6Al4V is also higher than that of two phase titanium alloys too. The demanded yield stress of biomedical titanium alloys for the practical biomedical use is between 500 and 1000MPa which the mechanical properties of two phase titanium alloys enable to fulfill the requirements of most medical components.

The commercial uses of titanium alloys were started in the late 1940s. From that year, titanium alloys were evaluated to be the main surgical implant materials. Pure titanium and titanium alloys are now used widely in many industries because of their attractive material and mechanical properties. They have become the most attractive materials for biomedical applications (Niinomi, 1998). Especially for Ti6Al4V, it has been applied into the biomedical field and became one of the most popular titanium alloys for the medical purpose. However, Ti6Al4V consist of toxic components inside alloys, so several undesired responses may be induced when the alloys are implanted into a human body. Other types of titanium alloys such as Ti6Al7Nb and Ti5Al2.5Fe also appear in the current market and they are currently under examined for the advanced uses in other fields (Semlitsch, 1987). Another type of titanium alloys β type alloys, they can provide a larger strength and toughness with an even distribution throughout the whole alloys' structure in comparison to α+β type alloys. They compose of a larger biocompatibility which they are suggested to substitute Ti6Al4V. Therefore,

β type alloys recently are investigated for the wider applications.

Although other types of titanium alloys are now focused in researches, two phase titanium alloys, Ti6Al4V, are still utilized the most in the biomedical industries. Actually, pure titanium provides superior corrosion resistance, the capability of tissue adaptation of pure titanium is higher than many other metallic materials such as stainless steel. However, pure titanium is low in strength, it causes rapid wear of devices when it is putting in some particular applications such as pacemaker cases, heart valve cages and reconstruction components (Wang, 1996). Consequently, the strength of commercial pure titanium is needed to enhance by further treatments such as cold processing in order to obtain the suitable material properties for the safe dental implant and other artificial bones. Therefore, Ti6Al4V alloys are still the proper alloy for fabricating components in the medical purposes. The joint part inside a human body mostly is Ti6Al4V alloys, these alloys consist of low elastic modulus, superior corrosion resistance and high tissue adaptation. Now the applications of Ti6Al4V alloys are expended to hip and knee prostheses, trauma components, instruments, and dental implants. Ti6Al4V alloys provide the outstanding material properties for biomedical uses.

2.2.2 Microstructures and phase transformation of Ti6Al4V alloys

The superior material properties such as light weight and outstanding corrosion

resistance of two phase titanium alloys Ti6Al4V are due to their microstructures and geometrical allocations of the phase elements inside the alloys. Their crystallographic arrangements of the hexagonal shape β phase grain are originated after the fabrication method. The traditional transformation route of two phase titanium alloys is related to the temperature change during the fabrication process. Figure 2.8 shows the influences of temperature on the phase transformation of titanium alloys (Lütjering, 1998). The phase transformation of titanium alloys could be divided into four stages, which are homogenization of β phrase, grain deformation in the α+β phase, recrystallization of grains into the α+β phase and stabilization of α+β phase. The most important factor of affecting the phase change inside alloys is the processing temperature.

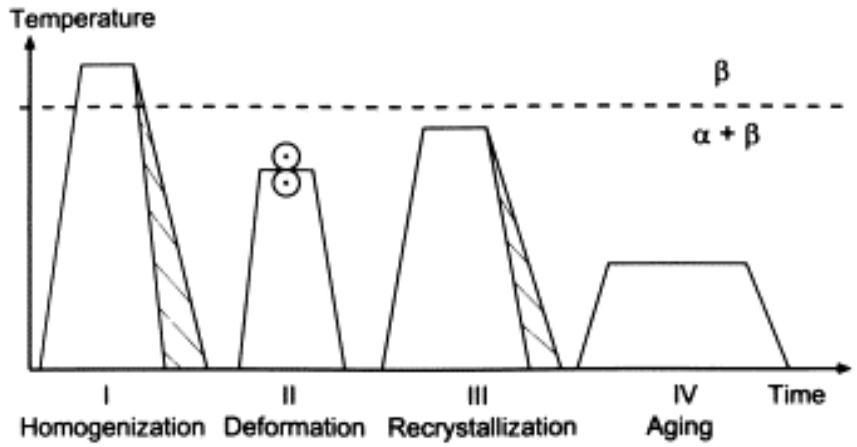

Figure 2.8 The influences of temperature on different steps in the phase transformation (Lütjering, 1998).

Suggested by Lütjering (1998), the change in the temperature provided the energy to generate different microstructural features inside titanium alloys. In the step of homogenization of β phase, the cooling rate during processing resulted to the

particular α-lamellae structures within the lamellar structures inside β grains and the growth of α-layer in between of β grain boundaries. In this case, β grains are in the moderate size when the homogenization temperature and processing time are set as small. Figure 2.9 shows different structures of α+β phase inside titanium alloys under the different processing temperatures.

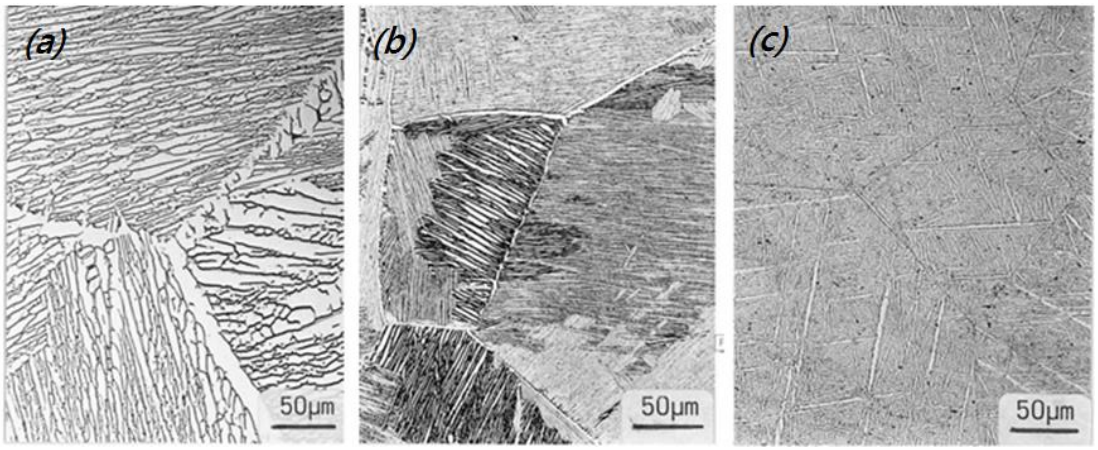

Figure 2.9 Different structures α+β phase combinations by different processing temperature: (a)1°C min^{-1}; (b) 100°C min^{-1}; (c) 800 °C min^{-1} (Lütjering, 1998).

In the deformation process of the α+β phase, the lamellar structures are formed plastically by continuously supplying of energy. The plastic deformation occurs in a high rate and it induces the sufficient dislocation to give out the process of recrystallization of α and β phases. In the deformation process under the low processing temperature, the deformation grains, which are treated as basal/transverse texture, are formed with a high volume fraction of *α* phase inside the alloys. For the part of a high-volume fraction β phases which contain α+β phase grains with β grains are formed with the subsequent transformation to α phase. Finally, the transverse type of

transformational grain is generated. The deformation level determines the intensity of α grains and β grains *(*Zhecheva et. al., 2005).

2.3 Ultra-precision machining of titanium alloys

Titanium alloys become the selective materials that are utilized in the biomedical industries. Titanium alloys have excellent material properties such as high corrosive resistance, light weight and superior biocompatibility (Niinomi, 2003; Pervaiz et al., 2014). However, they are difficult to cut materials because of their low thermal conductivity; high cutting heat is localized at the tool/workpiece interface which cannot be dissipated effectively, it ultimately causes serious tool wear and relatively unsatisfactory surface finishing of the machined surface.

Ultra-precision machining (UPM) is a promising machining technology to fabricate a high quality surface. For such high demanding machining performances in UPM, only a slight change in machining environment would cause an unacceptable surface generation (Ruibin and Wu, 2016). Therefore, UPM of titanium alloys is still in the progress as the machining difficulties of titanium alloys remain unsolved.

Serious tool wear has been reported by many scholars academically. Schneider et al. (2014) presented the works about the investigation of the effects of chip formation on the surface integrity of titanium alloys by using quick-stop tests. The chip formation in single point diamond turning is one of the main machining indicators which could be

used as predicting the surface topography of machined surface. They examined the effects of cutting force and the force ratio on the chip formation. The segment chip was formed when the cutting thickness was below 10μm while the continuous chip was generated above this critical cutting thickness. Zareena AR (2012) examined the tool wear mechanism of titanium alloys in UPM. They discovered that the features of tool, chip and workpiece materials were highly related to the diamond tool condition, which they affected the rate of adhesive tool wear and determined the level of adhesive material on the diamond tool. They also reported that the diamond tool would undergo the graphitization if the tool/chip interface was at the high temperature and high pressure. After the graphitization, build-up edge was formed which increased the amount of diamond materials pulling out from the tool, consequently unsatisfactory surface integrity was resulted in UPM of titanium alloys because of serious tool wear. Zhu et al. (2016) studied the chip morphology and milling vibration characteristics generated during various tool condition in machining of titanium alloys, the experimental results showed that the degree of tool wear was directly proportional to the vibration amplitude and induced cutting friction at the tool/workpiece interface.

Academic concerns are arisen on machining titanium alloys and the related cutting mechanism especially in UPM in order to solve the underlying sources of the machining challenges. Oliaei and Karpat (2016) implemented micro cutting of titanium alloys and

examined the relationship between built-up edge, cutting force and surface integrity in micro cutting. They concluded that several machining parameters especially depth of cut, cutting velocity and tool clearance angle were highly related to the size of built-up edge, contributing the negative influences on the machining outcomes if they were adjusted improperly. Jackson et al. (2017) studied the thermal effect generated in micro machining, and they demonstrated that the coated tool enabled to keep the surface integrity. Bai et al. (2016) investigated the microstructures of machined surface of titanium alloys in UPM. The experimental results showed that the refined grains were formed on the machined surface which the dislocations happened within the fine grain boundaries. Researchers investigated the cutting mechanism and underlying sources causing the unsatisfactory surface integrity of machined titanium alloys' surface in UPM. However, these works only defined the existence of problematic sources but have not provided the exact solution on them. Therefore, the modification of UPM for titanium alloys is urged to adapt in order to uplift the machinability of titanium alloys in UPM.

2.4 Hybrid machining technologies using a magnetic field

Various machining technologies using a magnetic field influence are recorded in literature, the hybrid machining technologies have been reported to deliver the excellent

machining outcomes. Mostly, the machining technologies using the magnetic field influences include electrochemical discharge machining (ECDM), electric discharge milling (EDM), and laser induced plasma micro-machining (LPMM).

2.4.1 Magnetic assisted electrochemical discharge machining (ECDM)

A magnetic field always combines with electrochemical discharge machining (ECDM) to deliver the unexpected machining performances. Fan et al. (2004) conducted the experiments about magnetic assisted ECDM by installing permanent magnets into the tool during electrochemical discharge machining, they discovered that the extra energy was offered to ECDM by the magnetic field influence, the critical voltage decreased with the level of excited particles at the higher energy level. They indicated that the electric flux was inclined to focus because of the regular alignment of magnetic moments of processing ions. Cheng et al. (2010) applied a magnetic field into ECDM to solve the problem of unstable spark discharge, which was uncontrolled when the machining depth increased. After utilizing a magnetic field to ECDM, the electrolyte circulation was highly enhanced, contributing an improvement of machining accuracy and material removal rate. Without requiring complicated machining setup, the improvement of overall machining time in their studies reached 57.4% under the magnetic field influence. Pa (2009) utilized a magnetic field into an ultrasonic assisted ECDM to enhance the dreg out of discharging in electrodes' gap, which assisted the

machining performances in term of super finishing. The author discovered that the frequency and ultrasonic vibration amplitude, the magnetic field strength and the rotational speed of magnetic field system deeply affected the machining performances of ECDM. The author concluded that surface finishing of machined surface was highly improved under the rotational magnetic field assistance. Long et al. (2017) investigated the relationship between a magnetic field and an electric field in ECDM, they examined the rules of three main factors including a magnetic field, an electric field, and an electrolyte motion in the machining process, and their influences on the material removal rate of ECM by using Navier-Stokes equation.

In conclude, ECDM assisted by the magnetic field resulted of enhancing the material removal efficiency and surface accuracy without applying the complicated change in the machining setup (Cheng et al., 2010).

2.4.2 Magnetic assisted electric discharge milling (EDM)

A magnetic field is integral with electric discharge milling (EDM) to enhance the machining performances of EDM. Yeo et al. (2004) used a magnetic field into micro EDM process in order to obtain a better aspect ratio of micro holes in EDM of hardened steel. The experimental results showed that the debris circulation was significantly improved in comparison to the traditional EDM. The supplied magnetic field should be in the direction of perpendicular to the rotational force of electrodes. The depth of

drilling hole achieved to 26% higher than that of the conventional micro EDM in the absence of magnetic field, contributing fewer deteriorations of surface integrity of side wall. Joschi et al. (2011) introduced a hybrid dry EDM integrated with a pulsed magnetic field to improve the machining performances of dry EDM. The pulsed magnetic field was supplied in the direction which was tangential to the electric field, offering the increase in the electron movements and the level of ionization of plasma. They successfully demonstrated the improvement of productivity over 130% and nearly no tool wear in comparison to dry EDM without using the magnetic field, the surface quality of machined surface was also uplifted. Teimouri and Baseri (2013) conducted the cutting test of ultrasonic assisted dry EDM under the influences of rotary magnetic field, they discovered that the machining parameters involving a pulse current, tool rotational speed and the power magnitude of ultrasonic vibration were highly related to the material removal rate of dry EDM. Also, they suggested that the application of magnetic field offered the positive effects on surface roughness of machined layer. Lin and Lee (2008) added the magnetic force into EDM process, conducting a hybrid magnetic force assisted EDM. The machining parameters including peak current and pulse duration were adjusted to offer positive influences on the material removal rate, electrode wear rate, contributing to generate a high quality machined surface with high efficiency EDM.

2.4.3 Magnetic assisted laser induced plasma machining (LPMM)

Hybrid machining technology of magnetic field combined with laser induced plasma micro machining (LPMM) has been also concerned academically. Malhotra et al. (2013) presented a hybrid machining process, plasma micro machining with the laser assistance (LPMM) integrated with a magnetic field. They described that the manipulation of plasma shape as well as the machining flexibility was enhanced by the applied magnetic field. In the experimental setup of this study, the transverse magnetic field was superimposed in the plasma therefore the plasma expanded in the direction of magnetic force, resulting in a larger conversion of plasma energy into heat energy. Saxena et al. (2015) proposed LPMM using an unidirectional magnetic field, which aimed to change the plasma feature. A higher material removal rate in LPMM of steel using a magnetic field was resulted in comparison to the conventional LPMM. The plasma energy was measured, and it was counted with an increase level of 70% compared with that of the conventional LPMM. Also, the micro features of machined pattern were also facilitated about 50% in the presence of transverse magnetic field. Wolff and Saxena (2014) conducted the experiments on LPMM with superimposing a magnetic field, the experiential results showed that the magnetic field facilitated the material capability, machined depth and complexity of machined geometry involving in LPMM; the aspect ratio of laser spot was improved which contributed to horizontal

squeezing of plasma channel.

In conclude, a magnetic field offers the function of generating high-aspect ratio of micro features with an efficient material removal rate. A magnetic field contributes to enhance accuracy and the intensity of laser induced plasma, which causes firmer features of machined micro patterns with complicated geometries.

2.5 An eddy current damping effect and its practical applications

An eddy current is created in a conductor within a varying magnetic field. It is initiated by the motion of conductor within the magnetic field or the change in the magnetic field intensity, which all of these movements induce electromotive force (EMF). The created eddy current further induces the repulsive force which is highly depended on the moving velocity of the conductor. The applications of eddy current damping effect have been examined recently. The eddy current damping effect is broadly applied into magnetic braking devices (Cadwell, 1996; Heald 1988; Wiederick et al. 1987), vibration reduction of machines (Genta et al. 1992), vibration controls (Bae et al. 2005; Sodano et al., 2005; Sodano et al., 2006) and vibration separations of magnetic levitation systems (Elbuken et al., 2006; Teshima et al., 1997).

Various novel designs for the eddy current dampers have been examined in the recent years. The advantages of applying the eddy damping factors for suppressing mechanical

vibrations are that, the eddy current damping effect is functioned without contacting the components of the mechanical system; also, no external power supply is required, and applicable to various vibrational structures. As fewer external components are needed for functioning of the eddy current damping effect, the device using the eddy current damping effect offered high reliability and durability. Furthermore, the eddy current damper does not require of damping fluid and relatively stable to the change in the temperature

2.5.1 Principle of eddy current damping effect

When a conductor suffers from a time varying magnetic field, an eddy current is created inside the conductor. The varying magnetic field is enabled to introduce through the motion of conductor within the magnetic field, or the alterations of magnetic field strength and the distance between the magnetic source and the conductor. When the eddy current is generated inside the conductor, it circulates within the conductor which further induces a magnetic field in the direction opposite to the supplied magnetic field, leading a repulsive force which the direction of the repulsive force is opposite to the vibration directions of conductor. On the other hand, as there exists electrical resistance inside the conductor, the induced eddy current will dissipate the heat by using the kinetic energy of moving conductor which the dissipation energy follows the ohms law. In dynamic mechanical systems, the conductor is continuously moving within the

external magnetic field, suffering the dynamic variation of magnetic field which it further introduces EMF. The EMF generates the induced current and creates the repulsive force which the magnitude of the created repulsive force is directly proportional to the moving conductor. Under the dissipation of heat energy because of the induced current, the kinetic energy of vibration motion in the dynamic system is acted as a source and it is extracted for the heat dissipation, consequently, the vibration energy is minimized, and the vibration amplitude of mechanical system is suppressed.

As a result, the overall system with the magnet and the moving conductor is similar to a viscous damper. The overall condition of generating an eddy current damping effect is shown in Figure 2.10.

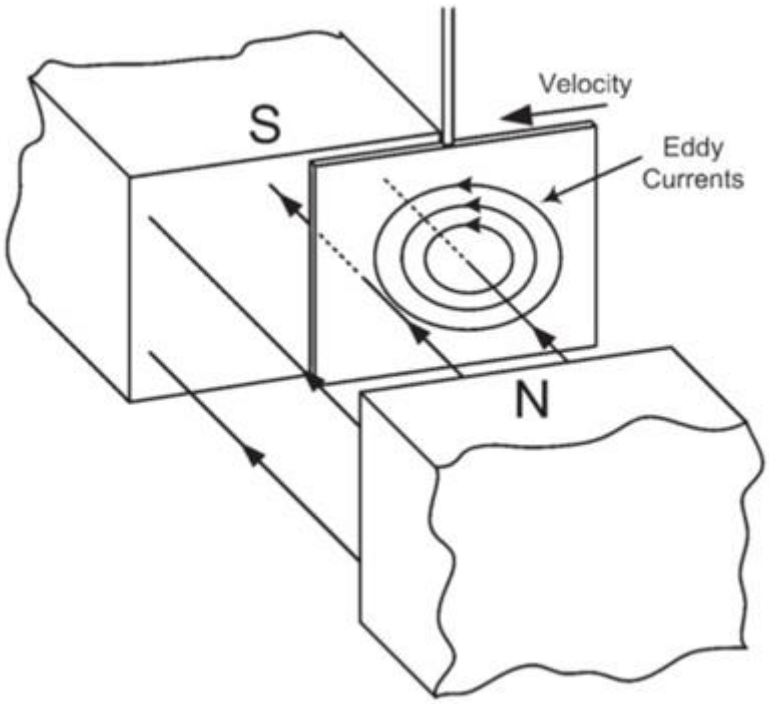

Figure 2.10 The overall condition of generating an eddy current damping in a general mechanical system (Sodano and Bae, 2004).

In literature, the Lorentz force and electromagnetic force are employed to stabilize the maglev motion, as the Lorentz force contributes the advantage of better linearity that is essential for the high precision while the nonlinear electromagnetic force enables to provide bigger current-force ratio per applicable volume. The moving-magnet design is proposed for various applications which are light weight requirements. Especially for the application in the magnetic levitation, the eddy current damping effect is also employed to provide excellent performance in high degree of freedom motion within short stroke, the performance of the overall system can achieve ± 1 nm error for constant velocity operation.

2.5.2 The applications of eddy current damping effect

The applications of using eddy current for a damping function were started from 1800s. An eddy current damping effect has been applied widely into magnetic braking systems. Davis and Reitz (1971) investigated the principle of eddy current braking system, they studied about the force induced by a magnet moving on the surface with semi-infinite and finite medium. The calculation was based on the theory concluded by Sommerfeld (1889), which indicated that the induced eddy current should be determined in the situation of finite conducting disk. The study contributes the preliminary concept to the case of generating the eddy current within the finite dimension object with a finite conductivity, which is the main course for the decay of eddy current intensity in joule

heating.

Schieber (1974) conducted the study about the braking effect of conductive sheet moving within the magnetic field which was composed of electromagnets with rectangular surface. With an improvement on the pole design, the braking force and the material cost were both improved. One year later, Schieber (1975) investigated the same topic of the eddy current breaking effect. They successfully determined the optimal size of the rectangular electromagnetic used in braking systems, the optimal ratio of the length to the width of the rectangular electromagnet was approximate about 0.34-0.44 for the moving conductor with an infinitely long beam structure, while the ratio was 0.5 for an infinite large plate. Nagaya et al. (1984) examined the force induced by an eddy current damping effect on a conducting plate moving with the direction parallel to the magnetic surface. The boundary condition of conductive plate was determined by using Fourier expansion method, mentioning the restrictions of the conductor shape in the calculation of eddy current braking force. The boundary condition and the optimal shape of the moving conductor in the eddy current braking system were successfully obtained under the fast pace of academical concerns on eddy current braking.

In the real application, Lee and park (1999) developed a non-contacted eddy current damping brake to enhance the performance of fast antilock braking of hydraulic

brake system. They built up a theoretical model for determining the usage of eddy current damping brake in the actual vehicle. The optimal torque of reducing braking distance was determined by keeping the slip ratio regarding to the real road condition. Gosline and Hayward (2008) investigated the new design of eddy current brake by applying the programmable damper for the operation in the haptic interface. The programmable eddy current damping brake enabled to offer the linear and physical damping capability which operated at the high frequency mode, which provided the same function as the dissipative actuators in the haptic interface. An optimal condition related to the design and physical relationship with the braking components was obtained, which it contributed to the improvement of stability of stiff wall in the braking system. Karakoc et al. (2014) used stochastic algorithm to optimize the braking torque generated in the eddy current damping braking system. Under the consideration of requirements of comfort and the induced skin effect at the braking system, they discovered that an utilization of AC magnetic field with multiple pole projection configurations increased the braking torque remarkably in comparison to the braking system using DC magnetic field, the novel eddy current braking can improve the braking torque of the existing braking system in the current market.

Other than the magnetic braking system, an eddy current damping effect has also been utilized into other practical applications, Lu et al. (2017) proposed an approach

using an eddy current damping effect to enhance the vibration performance of high rise building. They employed a vibration control device using the principle of eddy damping effect. They conducted the reduced scale and field tests which demonstrated the dynamic features of the eddy current damping device with supporting results, which the condition of eddy current generation in the vibration control device by the interactive motion between a magnet and a conductor, as shown in Figure 2.11. The results showed that, by using the device, the wind induced the structural acceleration of Shanghai Center Tower, which is a high building in China, was significantly reduced up to 60% and the displacement from the earthquake-induced structural decreased up to 15%. The proposed device had been already installed in the building and the performance of the device was reported to be excellent. Chen et al. (2013) used the passive eddy current damper to minimize the vibration occurred in the calibration and measurement of force sensor. The eddy current damping device composed of eight permanent magnets, conductive copper rods with the position of Halbach array, which aimed to induce an eddy current damping effect to the force sensor. The operational mechanism of the device was determined by developing an energy approach using pseudo-rigid body, which directed to obtain the optimal design. Without consuming the external electric source, the damping coefficient of eddy current damping device increased to $4.3 Nsm^{-1}$, which delivered the proper amount of damping force to suppress

the force sensor vibration only in 0.1s.

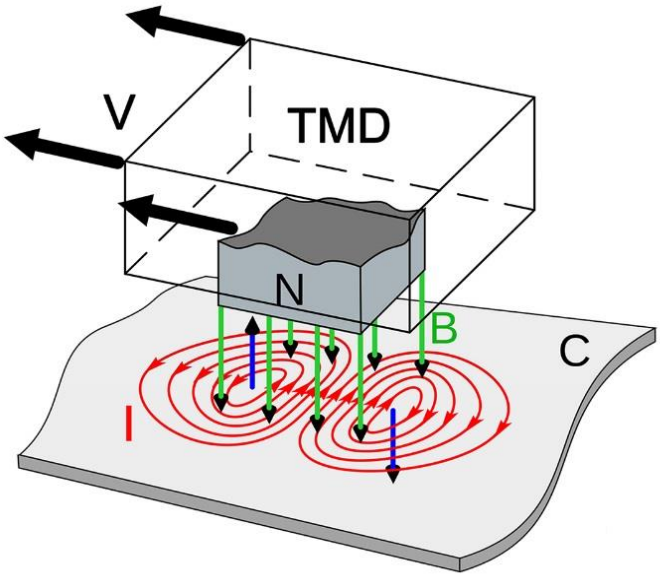

Figure 2.11 An eddy damping damper used in high building, Lu et al. (2017).

2.6 Thermal conductivity of magnetic materials under the magnetic field influence

Fluids containing of magnetic materials consist of a suspension of domain magnetic particles within carrier fluid. In the absence of magnetic field, the particles may aggregate each particle closely because of the van der Waals forces and dipole–dipole interactions within molecules and dipole–dipole interactions between each particle. Therefore, the particles are randomly positioned without the magnetic field influence, and the liquid carrier has no net magnetization. In the presence of magnetic field, the magnetic particles obtain the enough energy to react with the applied magnetic field. The magnetic particles inside the liquid carrier would move with the direction of the applied magnetic field.

Many researchers reported the same phenomenon as above. Gavili et al (2012) described the thermal conductivity of ferrofluid which had Fe_3O_4 nanoparticles was enhanced 200% at the maximum in the presence of magnetic field. The authors conducted the experiments by creating the magnetic field by Helmholtz coils, which the magnetic intensity was enabled to adjust by the electric current given to the coils. Other than the enhancement of thermal conductivity of the ferrofluid, the average diameter of magnetic particle increased under the magnetic field. Choi et al. (2003) examined the thermal conductivity and the electrical conductivity of single wall carbon nanotube in the magnetic field environment, the experimental results showed that the both thermal and electrical properties of single wall carbon nanotube remarkably increased under the magnetic field influence. They confirmed that the electrical and thermal transport properties of conductive particles were highly related to the ratio of localization length of particle to bundle diameter, which this ratio was promoted by the magnetic field influence. Parekh and Lee (2010) analyzed the thermal conductivity of the magnetic nanofluid in the presence of magnetic field. XRD and transmission electron microscopy (TEM) were implemented for showing the spinel structure of nanofluid under the magnetic field influence. They concluded that the thermal conductivity of magnetic nanofluid had the direct relationship with the transverse magnetic field. They reported that an increase percentage of thermal conductivity

reached to 30% under the condition of 4.7% volume fraction of the magnetic field, which the underlying reason of an increase in thermal conductivity was the formation of 3D zippered structure of magnetic particles inside nanofluid. Peacor et al. (1991) conducted the measurement of the thermal conductivity of single crystal $YBa_2Cu_30_7$ under the magnetic field influence. The thermal conductivity of the crystal was sensitive to the transition temperature under the magnetic field, meaning the great importance of magnetic field on the crystal structures and thus affected the thermal conductivity of the crystal.

Literature reported the close relationship about the magnetic field and the thermal conductivity of magnetic particles in the liquid state, which the thermal conductivity of fluid with magnetic particles increased entirely under the magnetic field influence

2.7 Summary

Ultra-precision machining technology is discussed deeply in this chapter. The reasons of poor machineability of titanium alloys in UPM are mainly their low thermal conductivity and low elastic modulus, which they are the interstice properties induced from their microstructures in the raw stage.

In order to maintain their superior material properties and improve the machinability of titanium alloys simultaneously, an indirect approach should be made.

An eddy current damping effect is a widely adapted method to suppress the vibration in mechanical systems. Furthermore, a magnetic field is proven to enable to uplift the thermal conductivity of magnetic materials at their liquid stages. Combining with these two effects, an application of magnetic field into UPM is believed to take an effectiveness on improving the machinability of titanium alloys, and it enables to response to the underlying sources of poor machinability of titanium alloys in UPM, which are the low heat transference at the tool/workpiece and the high level of induced machining vibration.

Chapter 3 Single point diamond turning using a magnetic field

3.1 Introduction

Because of the superior material properties of two phase (α + β) titanium alloys Ti6Al4V (TC4) such as excellent strength-to-weight ratio and excellent corrosion resistance, they are widely used in the medical area. Although the rapid development of machining technology which increases the uses of titanium alloys, machining of titanium alloys is still a difficult task especially in UPM. Titanium alloys difficult to cut materials which their machinability is relatively poor in comparison to other metals because of various internal physical and material properties. The main causes for the poor machinability are their low thermal conductivity, high chemical reactivity and low elastic modulus (Khettabi et al., 2013). Especially for the material properties of low thermal conductivity, titanium alloys prevents the heat transference from the cutting zone in machining processes, so the heat generated cannot be dissipated from the machined surface effectively (Komanduri and Von Turkovich, 1981). Hence, the localized heat at the tool flank and rake surfaces diminishes the tool life, leading to unsatisfactory surface finishing and surface integrity. The machining costs unavoidably increase due to rapid tool damage and the low surface integrity in UPM of titanium alloys.

Apart from localization of cutting heat in UPM of titanium alloys, the high level

of machining vibration is another main factor that damages the machined surface and the machining performances in UPM of titanium alloys. Vibration is inevitable in machining processes. The high strength of titanium alloys causes the high cutting force and the high cutting friction in the machining process, which they further generate vibration and chattering eventually (Tlusty, 2000). Basically, the vibration in the turning process can be divided as two types: forced vibration and self-excited vibration. Normally, the forced vibration is caused by the generation of periodic cutting force at the tool/workpiece interface. The cutting tool vibrates at the frequency of the cutting force as the existence of periodic cutting force, which the vibration amplitude is higly related to the frequency ratio of the cutting force to the natural frequency of the cutting tool (Lee et al. 2001; Wang et al., 2010). On the other hand, the vibration receptively occurs because of the self-excited vibration at the machined surface and the tool, resulting from the acyclic force as well as localized shearing, causing the dynamic instability in the turning process (Pramanik, 2014; Fan et al., 2011). The machining vibration generates a wavy surface on the machined component, causing an advanced cutting force variation and discontinuous chips, further generating an extensive machining vibration at the tool/workpiece interface apart from the self-excited vibration. Moreover, the waviness regeneration occurs if the tool vibration is not in the phase with the surface waviness, causing an increase in tool tip vibration and instability in the

machining processes. In addition, chatter vibration exists in the turning process, and it increases with an increase in cutting thickness in the machining processes (Smith and Tlusty, 1990; Rao and Shin, 1999). Chatter vibration is magnified at the particular combination of depth of cut and spindle speed, therefore, changes in spindle speed and depth of the cut are implemented in order to suppress chatter vibration which lead to sacrifice in material removal rate. It is critical to choose the right cutting condition in order to manipulate the cutting vibration and the induced chattering. For the machining aspect, the stability lobe is one of the feasible approaches to avoid chatter vibration generated from the spindle with a high rotational speed. Although there is a large space inside the stable zones of the stability lobe diagram, the maximum spindle speed is still restricted by the high cutting temperature in machining of titanium alloys, the unstable cutting condition still exists in the machining processes especially for titanium alloys. Therefore, the approach of stability lobe is seldom applied in resolving chatter vibration in UPM of titanium alloys.

The machining vibration causes adverse effects on the machined components of titanium alloys in UPM, causing unsatisfactory surface integrity of machined products and high machining costs; thus, the applications of these excellent alloys for precise products are limited. Therefore, the suppression of machining vibration of titanium alloys becomes the main issue for enhancing the machining performances of titanium

alloys.

SPDT is one of the machining technologies used in UPM and is widely used for producing optical grade surface finishing within 10 nm of surface roughness. Titanium alloys have superior properties such as great strength-to-weight ratio, so the uses of titanium alloys are popularly in the medical applications with precise specifications, which are commonly manufactured by SPDT to reach the excellent surface quality. On the other hand, diamond turning of titanium alloys has been extensively investigated by researchers, especially for the aspect of diamond tool wear, it is one of the most concerned topics in UPM. Ruibin and Wu (2016) studied the optimum machining parameter for diamond cutting of titanium alloys, and they verified that low feedrate and small depth of cut should be adopted in diamond cutting in order to provide a better surface quality of machined components. Zareena and Veldhuis (2005) examined the tool wear mechanisms involved in diamond turning of titanium alloys, and they found that serious adhesive diamond tool wear occurred on the rake face due to the high localized cutting temperature. Hu and Zhou (2016) conducted cutting tests on diamond cutting of titanium alloys and reported the wear patterns, showing uniform wear and chemical wear because of trapping high cutting heat at the cutting zone. The reported reason for serious adhesive tool wear in diamond turning of titanium alloys was principally the low thermal conductivity of titanium alloys, which caused the high

cutting vibration, cutting friction and thereby strong adhesion of materials on the diamond tool.

Consequently, researchers have focused on resolving problematic tool wear, and the underlying sources of tool wear. Zhang et al (2014) indicated that the tool vibration induced from the high cutting friction as well as the high cutting heat were the main factors affecting tool wear; therefore, they proposed ultrasonic vibration diamond turning to lower the cutting force and vibration in machining. Sales et al (2017) proposed different cooling approaches to lower the cutting temperature in diamond machining of titanium alloys in response to the low thermal conductivity of the materials, and the results showed that the use of cryogenic cooling altered the tribological behavior of the machining interface, reducing tool wear and surface roughness. They also showed that adhesive titanium alloys resulted in the plucking out of hard diamond materials from the diamond tool, causing a high level of abrasive wear. According to literature, the high cutting vibration and adhesive tool wear in diamond turning of titanium alloys should be resolved in order to improve diamond tool condition in machining titanium alloys.

On the other hand, researches on machining technologies related to physical fields have been getting attentions recently. Several studies have shown the successful application of a magnetic field to machine different materials. Li et al (2015)

demonstrated an improvement of machining performance of TC4 by a pulsed magnetic field treatment. The phase transformation from beta to alpha of titanium alloys was facilitated and the dislocation density decreased under the influence of magnetic field intensity of 4T. El Mansori et al (2003*)* confirmed that tool wear was significantly reduced with the application of a coaxial electromotive force which was explained by the principle of magnetic alignment induced by an irreversible rotation of the domain wall of ferromagnetic materials. Actually, an eddy current damping effect has been already proven to be effective in suppressing the vibration of structural mechanical systems. Teshima et al. (1997) examined the effectiveness of eddy current damper on the performance of vibration separation in a superconducting levitation, which the experimental results showed the damping performance in the vertical direction of the levitation system was enhanced about hundred times by the designed eddy current dampers in comparison to the conventional levitation system. Elbuken et al. (2006) used an eddy current damping on the magnetic levitation in order to increase the precision of levitation. Karnopp (1989) proposed a new electromechanical damper and utilized it into a vehicle. The author reported that the electrodynamic variable shock absorbers were practical in the vehicle suspensions. Schmid and Varaga (1992) built a system for supporting the development of high resolution nanotechnology patterns by applying of eddy current dampers. The magnetic spring effect has been also reported to deliver the

excellent performance to the vibration suppression (Patt, 1985). Bae et al (2005) demonstrated the theoretical and experimental results, which they showed that the vibration of beam structure was remarkably minimized using the eddy current damper effect.

Existing literature has reported that machining of titanium alloys results in unsatisfactory surface roughness due to the low machinability of the materials especially thermal conductivity, high strength at high temperatures, and low Young's modulus. The smallest surface roughness was demonstrated to be 416nm for diamond turned titanium alloys (Colafemina et al., 2007), which the obtained surface roughness is much larger than the requirement of surface roughness in ultra-precision machining. Actually, machining titanium alloys is still in the progressive stage and different machining technologies should be adopted in order to fill up the research gap. An eddy current damping has never been applied in the machining area especially UPM to provide the exceptional effects to increase the machining performances of difficult to cut materials in SPDT. In this chapter, the investigations of the effects of eddy current damping effect on SPDT are demonstrated. By employing the eddy current damping effect in SPDT, a suppression of cutting force variation, a continuous chip formation and a reduction of adhesive tool wear were shown experimentally in comparison to normal SPDT. Furthermore, the proposed experimental setup in the research is cost-

efficient and flexible for the further modification, only two extremely low cost permanent magnets are used. The small size of the magnets enables them to be installed inside the ultra-precision machine. The proposed modified UPM technology overcomes the restriction of insufficient space of the ultra-precision machine, simultaneously, the machinability of titanium alloys in SPDT is enhanced without alternating the excellent material properties of titanium alloys.

3.2 Theory of eddy current damping effect in single point diamond turning

When a conductive metal rotates within a magnetic field, an eddy current is generated through a stationary magnetic field inside the conductor. The eddy current generates its own magnetic field with the opposite direction of external magnetic field leading the repulsive force called the Lorentz force (Sodano et al., 2005; Sodano et al., 2006; Teshima et al., 1997). Ebrahimi et al (2010) reported that the repulsive force generated by the eddy current was corresponding to the velocity of the moving conductor, therefore the magnet and moving conductor became as a viscous damper system. The phenomenon of acting force reduction by the repulsive force induced from the eddy current is called the eddy current damping effect.

Faraday's law indicates that an electromagnetic force ε is generated within a conductor once the occurrence of a change in the magnetic field, the electromagnetic force is expressed as the rate of change in the magnetic field, the electromagnetic force

is denoted as

$$\epsilon = -\frac{d\emptyset_B}{dt} \quad (3.1)$$

where $\emptyset_B$ is the magnetic flux density. The EMF creates a current I which is inversely proportional to the resistance R of the moving conductor. The current is expressed as:

$$I = \frac{\epsilon}{R} \quad (3.2)$$

Lentz's law indicated that the induced currents will further generate a magnetic field with an opposite direction to the original magnetic field. Consequently, the Lorentz force F is created, and it is termed

$$F = E \times q + q \times V_e \times B \quad (3.3)$$

where V_e is the turning velocity of the conductor, q is the charge carried by the conductor, E is the electric field and B is magnetic field.

$$F \alpha V_e \text{ and } F\alpha B \quad (3.4)$$

Therefore, the Lorentz force is proportional to the turning velocity of the rotating titanium alloys and the magnetic field intensity. On the other hand, the machining parameters involved in the SPDT process are always in small scale, depth of cut and feedrate used in the experiments were 4μm and 8 mm/min, respectively. Hence, the cutting force as well as the turning vibration generated was small accordingly. The eddy current damping force was used to suppress millimeter range vibration force. Therefore, the magnetic field intensity was set as 0.01T – 0.03T in the experiments in order to

generate the proper Lorentz force to suppress the small vibration force in the experiments. Matsuzaki et al (1997) discussed the active approach of vibration control using a moving-coil type actuator using an eddy current damping principle. They determined the velocity of the driving current and confirmed a reduction in system vibration by proposing a novel vibration control system which successfully suppressed the vibration of partially magnetized beam using an EMF. In the practical applications, an eddy current damping effect has already been used in the automobile and elevator systems. Liu et al (2011) designed an eddy current retarder for automobiles and it decreased the brake torque and enhanced the braking efficiency of the main brake system. Jou et al (2006) designed an upright magnetic braking system, applying permanent magnets for elevators to reduce the inside vibration and hence to enhance the safety of the elevator.

For the experiments mentioned in this chapter, titanium alloys were rotated in between of two magnets in this study, and a Lorentz force was generated which caused the opposite force acting on the rotating direction and compensated the vibrational force of the unstable turning system. The eddy current damping effect suppressed the turning vibration caused by the interaction between the diamond tool and workpiece in SPDT.

3.3 Experimental investigation of an application of eddy current damping effect

on single point diamond turning

In the proposed machining technology, two phase titanium alloys, Ti6Al4V, were used as the materials for the experiments. Ti6Al4V has 6% aluminum, 4% beta phase stabilizer vanadium, 0.25% iron, 0.2% oxygen and the remaining parts are titanium. Titanium alloys were cylindrical in shape with a length of 40mm and a diameter of 15mm. One group of titanium alloys, NMFS (non-magnetic field sample), processed normal SPDT in the absence of a magnetic field, while another group of titanium alloys MFS (magnetic field sample) processed SPDT in the presence of a magnetic field. In the experiment, the special fixture was needed in the experimental setup. The self-developed fixture for holding permanent magnets was installed in the ultra-precision turning machine. MFSs were located in the middle of two magnets during SPDT in order to suffer from an eddy current damping effect. The particular part of the fixture is made by steel, which is a ferromagnetic material, it aims to provide the uniform magnetic field intensity passing through titanium alloys so that the steady magnetic torque could be generated in SPDT. The radius and height of diamond tool were 1.468 mm and 10.172 mm, respectively. The chip formation was observed with SEM (Hitachi HT3030). The force sensor Kistler 9256c was used to capture the cutting force, the corresponding cutting force would be transferred into fast Fourier transform (FFT) for determining the turning vibration in SPDT of both sets of samples. A Moore Nanotech

350FG (4 axis ultra-precision machine) was used for SPDT. The magnetic field intensity provided in the experiments was adjusted for three values as 0.01T, 0.02T and 0.03T. Feedrate, depth of cut and spindle speed were set as 8mm/min, 4μm and 1500 rpm, respectively, and they were remained unchanged throughout the experiments. The tool conditions at the cutting distances of 75m and 150m were observed under the SEM. The experimental setup is illustrated in Figure 3.1.

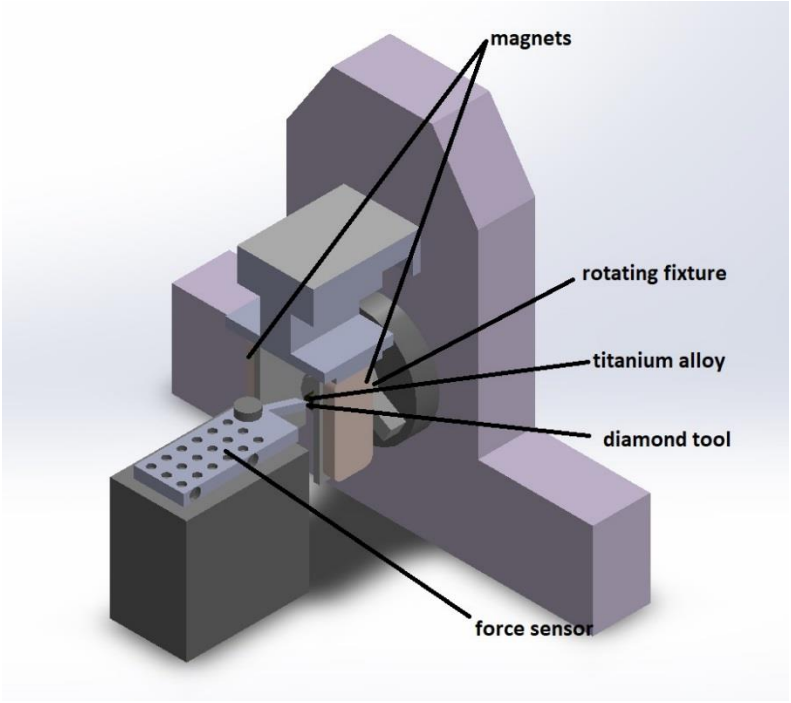

Figure 3.1 Experimental setup of magnetic assisted diamond.

3.3.1 Suppression of machining vibration using eddy current damping effect

The selection of magnetic field intensity was on the basis of the estimation of cutting force needed to be damped. The Lorentz force contributes to an eddy current damping force, which is shown in equations 3.1 and 3.2. The Lorentz force is proportional to the turning velocity of rotating titanium alloys and the magnetic field intensity. The cutting

parameters involved in SPDT are in the small scale, depth of cut and feedrate used in the experiments were at the micron range and micron displacement per second, hence, the cutting force as well as the turning vibration generated in SPDT would be small. On the other hand, a serious of pilot experiments are conducted in order to determine the suitable range of the magnetic field intensity using in SPDT. Therefore, the eddy current damping force used to suppress the vibration force in the experiments is planned to be small also. Consequently, the magnetic field intensity was set to 0 - 0.03T which are in the millimeter range in order to generate an adaptive Lorentz force to compensate the small vibration force in the turning system.

In ultra-precision SPDT, the thrust force is the dominant indicator to show the tool vibration as the material recovery of machined surface affects mostly the thrust force (Cheung and Lee, 2000b; Wang et al., 2013). Therefore, the FFT of thrust force generated at different magnetic field intensity was examined to investigate the turning vibration. The FFT of thrust force is shown in Figures 3.2. The sample frequency of FFT is 50KHz. Under the influence of eddy current damping effect, the kinetic energy of turning vibration was converted to heat energy which heated up titanium alloys, as a result, it suppressed the magnitude of turning vibration. Therefore, the vibration amplitudes generated by the MFSs are expected to be lower than that of the NMFS. Comparing the peak amplitudes between NMFS and MFSs as shown in Figures 3.2 (a-

c), all peak amplitudes of NMFS in the FFT were higher than that of MFSs. The maximum peak value of magnetic field intensity at 0.02T was only 0.0047N while that of 0T magnetic field intensity was 0.0088N, the maximum peak value decreased 87.2% under the influence of magnetic field intensity 0.02T. The above provided the solid evidence that the overall turning vibration was suppressed by an eddy current damping effect.

The area under FFT curve of cutting force represents the total vibration energy of measured data. It was determined in order to prove the dissipation of vibration energy of the turning system by an eddy current damping effect. Table 3.1 shows the results of the area under FFT curve at magnetic field intensity 0 - 0.02T. The vibration power generated in SPDT in the absence of magnetic field was 0.945W, the vibration energy of MFSs generated at magnetic field intensity 0.01T and 0.02T was reduced to 0.795W and 0.706W respectively which the reduction percentages were 15.9% and 25.3% respectively.

Table 3.1 The area under FFT curve at magnetic field 0-0.02T.

	H=0	H=0.01T	H=0.02T
Area/ Vibration power (W)	0.945	0.795	0.706

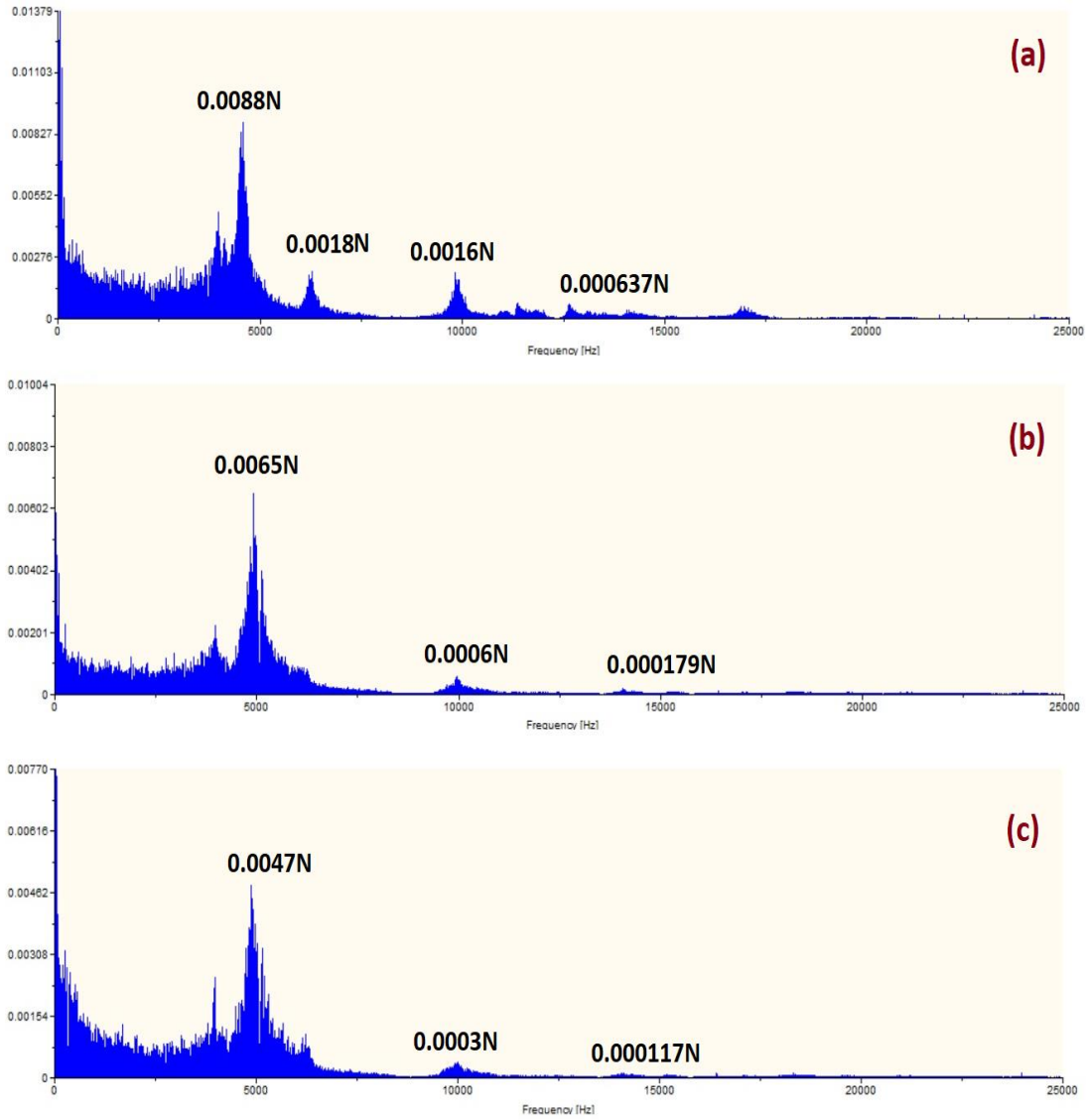

Figure 3.2 The FFT of thrust force generated at magnetic field (a) 0T, (b) 0.01T and (c) 0.02T.

3.3.2 Chip formation analysis

Figures 3.3 (a-d) show the SEMs of chip formation generated in SPDT at the magnetic field intensity 0 - 0.03T with different magnifications. Refer to Figure 3(c), the long, flat and continuous chips were generated at the magnetic field intensity 0.02T. The free surface of chips showed entire and glossy with the unserrated side tips. This type of

chip suggests the steady cutting mode as well as non-interrupted turning. In the contrast, discontinuous chips were generated from the NMFS. The discontinuous chips implied the formation of defects on the machined surface due to the tool vibration, and the small movement of tool vibration initiated the tensile cracks and shear cracks at the chip. This kind of chip formation normally happens in machining materials with low modulus elasticity such as titanium alloys. The integral effects of low elastic modulus of titanium alloys and the small step removal mechanism in SPDT lead to decrease the chip stiffness at the high cutting temperature, finally the chips melted and caused the generation of segment chips of NMFS. On the other hand, the NMFS generated the chip edges with classical saw tooth tips. For the MFSs at the same machining condition, the chip edges showed flat without appearing the saw tooth shape, their free surfaces displayed lamellae layers with even width. It suggested the diamond tool lid easily with the long dislocation distance during the diamond turning process, demonstrating fewer vibration characteristics. In order to capture the entire chip of MFS at the magnetic field 0.02T, a lower magnification of MFS chip was applied in order to provide the clear view of whole chip and make the macro comparison between that of NMFS and MFSs.

The contrast of chip formation between the NMFS and MFSs was magnified in term of macro view as shown in Figures 3.4 (a-b). The length of chips generated from the MFS at the magnetic field intensity 0.02T was surprisingly long while the powder

and fragment chips were formed from the NMFS due to an extensive turning vibration in SPDT. Faraday's law explained that an electromagnetic force ε is generated within a conductor when there is a change in the magnetic field initiated by the conductor, and the ε is highly related to the change rate of magnetic field according to equation (3.1). A higher magnetic field results a higher EMF and current, consequently, the MFS at the magnetic field intensity 0.03T suffered the higher current among the other two MFSs.

Under the influence of relatively high temperature at the magnetic field intensity 0.03T, the ductile fracture occurred inside the chips generated at magnetic field 0.03T, more voids were observed on the free surface of chips. On the other hand, a reduction of turning vibration lessened the tool tip shift during SPDT, thus minimized the chip breaking in the chip removal process and the chips would be still continuous. Therefore, the chip generated at the magnetic field intensity 0.03T was still continuous with few voids.

In this study, the EMF generated was very small in the MFSs. The effect of magnetic field on the temperature change was indirectly estimated by the amount of EMF generated in the workpiece:

$$dEMF = Bvdx \quad (3.5)$$

$$\mathrm{EMF} = \int \mathrm{dEMF} = \int_0^1 \mathrm{B}(\omega \mathrm{x})\mathrm{dx} \quad (3.6)$$

where ω is the angular velocity of rotating conductor, x is the length of conductor,

$$\mathrm{EMF} = \mathrm{B}\omega\left[\frac{\mathrm{x}^2}{2}\right]_0^1$$

For magnetic field 0.03T, spindle speed 1500rpm and conductor length 28mm

$$\mathrm{EMF} = \frac{1}{2}(0.03)(157)(0.028)^2 = 1.846 \times 10^{-3}\mathrm{V}$$

The EMF generated was extremely small in the proposed machining technology. Therefore, although the induced eddy current would impose the heat into the workpiece, and it placed negative effects on the machining performances of proposed machining technology, the significance of that influence is exceptionally small. On the other hand, as ultra-precision diamond turning involves high machining accuracy (depth of cut and feedrate are normally in micron range and millimeter displacement per second respectively), a small tool vibration enables to affect the surface integrity of components. As a result, the effect of tool vibration on the machined surface would be the dominant in diamond turning. The induced eddy current affects the machined surface negatively, however, as an eddy current damping effect is dominant over the induced eddy current effect in SPDT, the overall machining performance was still improved for the MFS at magnetic field intensity 0.03T, which was proven by the showed experimental results.

Due to the stronger of eddy current damping effect in SPDT, the machining performance of SPDT was uplifted. Generally, a higher magnetic field intensity improves the machining performance of SPDT in comparison to an absence of magnetic

field. However, the optimum magnetic field intensity in SPDT may not be obtained at the relatively high magnetic field intensity because of the induced eddy current, the optimum magnetic field intensity may be obtained at the middle value in the adaptive range. The detail of optimization would involve the processes of modeling and simulation, which would be the focus of the future research.

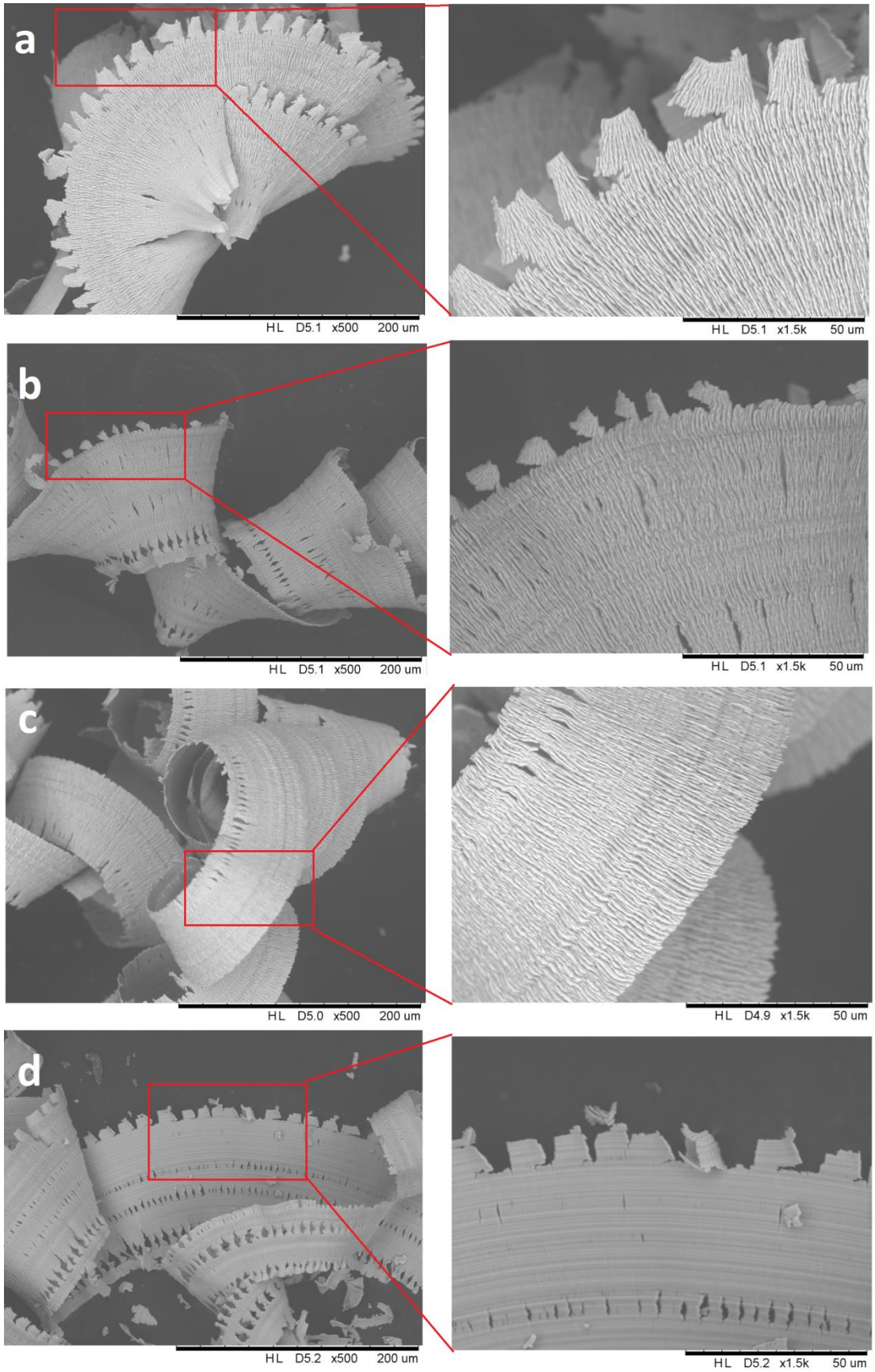

Figure 3.3 SEMs of chip generated in (a) magnetic field 0T (an absence of magnetic field), (b) magnetic field 0.01T, (c) magnetic field 0.02T, and (d) magnetic field

0.03T.

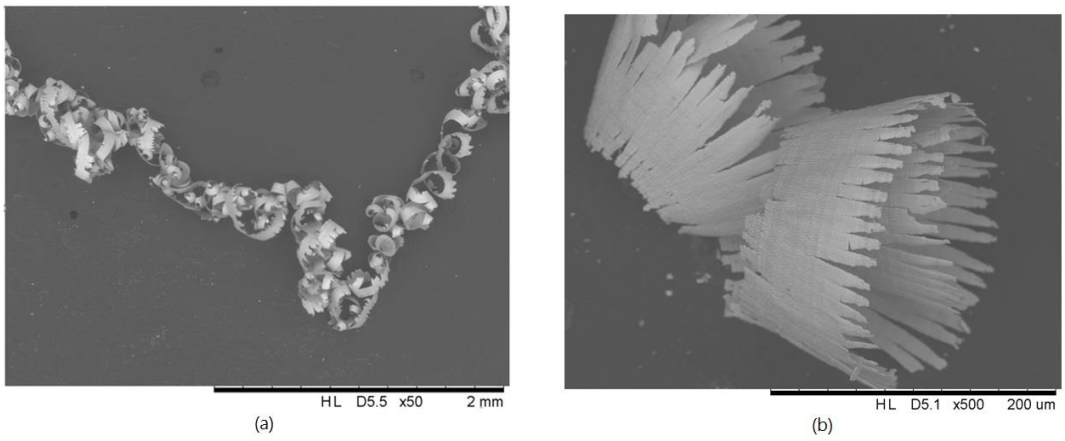

Figure 3.4 SEMs of chip generated in (a) magnetic field 0.02T, (b) magnetic field 0T (an absence of magnetic field) in a lower magnification.

3.3.3 Tool wear

The low thermal conductivity and high elastic recovery capability of titanium alloys cause heat trapping at the cutting zone during machining, results in an extensive tool vibration during SPDT which damages the diamond tool (Cadwell et al., 2008). In machining of titanium alloys, a sizable chipping of cutting edge occurs as the vibration in the machining system enlarges, causing chip tangling and welding at the tool edge (Bhatt et al., 2010). Adhesive tool wear is dominated in machining processes of titanium alloys; adhesive wear is caused by the micro welding of workpiece materials on the cutting edge. The soldering of materials is related to the high cutting force at the cutting zone which the cutting force shears the metallic junction between the cut materials and workpiece; the powder forms of chips and material particles are released at the moment of breaking the metallic junction. The metallic junction is much earlier broken because

of the tool vibration and eventually more chips are welded on the cutting edge (Devillez et al., 2004), the turning vibration especially the tool tip vibration facilities adhesive tool wear in SPDT of titanium alloys.

Titanium alloys are classified as difficult to cut materials and proven to be low machinability due to their low thermal conductivity, which restricts the dissipation of cutting heat from the tool/workpiece interface (Bordin et al., 2015; Narutaki et al., 1983; Che-Haron, 2001). In comparison to other materials, the temperature at the tool/workpiece interface during machining of titanium alloys is extremely high (Ezugwu and Wang, 1997), and tends to localize at the tool edge. Hence, during machining processes, the diamond tool wears very speedily due to the high cutting temperature and much more strong adhesion of materials at the tool/chip interface and tool/workpiece interface (Jawaid et al., 1999). Therefore, mainly, tool wear in machining of titanium alloys is due to the adhesive wear mechanism on the rake face (Dearnley and Grearson,, 1986). Adhesive wear was reported to be the dominant wear mechanism in machining of titanium alloys (da Silva et al., 2013; Huang et al., 2012; Rahim and Sasahara, 2011). Park et al. (2011) indicated the same that titanium adhesion was the dominant factor for tool wear during drilling of composite containing titanium. Combining the effects of extremely high cutting temperature and tool vibration in SPDT of titanium alloys, short chips remain contacts with the tool rake and flank surfaces,

finally they stick to the tool tip and cause serious tool wear. Therefore, the significance of adhesive wear is one of the indicators to display the intensity of tool vibration in machining processes.

Refer to the above reports, adhesive wear would be the main focus of tool condition in SPDT of titanium alloys. In order to show the clear difference between the cutting distances 75m and 150mfor the NMFS tool, Figures 3.5 and Figures 3.6 showed the size and thickness of adhesive layer which are the main indicators for adhesive wear. Although the area of welded titanium alloys in the rake surface enables revealing adhesive wear, the welded titanium alloys on the rake surface do not contribute to the cutting motion as they are not located at the cutting edge. Therefore, the adhesive titanium alloys located at the cutting edge and near the cutting edge would be accounted for tool wear and would affect the machined surface quality, we would focus on investigating the adhesive layer close to the cutting edge. Refer to Figures 3.5(a-b), adhesive/diffusive wear occurred at the tool tip regardless of the presence of magnetic field, shiny melted titanium alloys stuck to the cutting edges of both diamond tools. Although the tool wear mechanisms between MFSs and the NMFS were the same, the significances of tool wear were much different between the NMFS and MFS tools. For the NMFS tool, the area and width of welded titanium alloys at the tool tip were found to be larger and more breadth, more titanium alloys were dissolved on the tool tip in the

absence of magnetic field. The adhesive layer of titanium alloys of NMFS tool displayed much denser than that of MFS tool, which is showed in the larger magnification inside the Figures 3.5 and 3.6.

When the cutting distance increased to 150m, the characteristics of tool wear between the NMFS and MFS tools were started to be dissimilar, adhesive wear was minimized under the influence of magnetic field intensity 0.02T, which is shown in Figure 3.6(b). Once the junction between titanium alloys and the diamond tool was formed in the presence of magnetic field, the turning vibration was suppressed by an eddy current damping effect. Because of fewer machining vibrations as well as tool vibrations, as a result, fewer powder chips and material particles were welded on the tool tip firmly, reducing adhesive wear in SPDT of titanium alloys. In addition, the continuous turning motion further provided the harmony and offered the extra force to take off the stuck chips. When the chips melted again in the further turning process (the cutting distance 150m), the melted chips lost the adhesion and were flushed away from the working gap because of the magnetic torque and aerodynamic force of turning motion. In comparison to the tool edge of NMFS, the area of adhesive wear at the tool tip came to be larger and wider when the cutting distance increased to 150m. The length of adhesive titanium alloys on the tool tip at the cutting distances 150m was longer than that at the cutting distances 75m, the adhesive layer at NMFS tool tip was expanded

along to the tool edge as shown in area A of Figures 3.5(a) and 3.6(a). The small fragments of titanium alloys were welded and attached into the tool tip, that adhesive titanium alloys were deformed and enlarged to the lateral tool edge. They integrated to the tool edge and became the entire part, which contributed to the disruptive turning motion and further enhanced tool wear.

According to ISO 3685, the useful tool life is considered as end when a tool is not able to produce workpieces in the desired size and surface quality, or when it is physically incompetent for conducting further cutting (American National Standards Institute, 1996; Vagnorius et al., 2010). UPM aims to fabricate components with a high surface quality, which the surface roughness of UPM products has reached up to the nanometer level. In practice, the crack of tool edge usually has the most essential influence on the quality of the produced parts. Therefore, the appearance of crack on the tool edge is used as a tool life criterion in this study.

Tool wear at the longer cutting distances 750m was observed in order to observe the difference of tool wear significance between using an eddy current damping effect and without using an eddy current damping effect. As adhesive materials weakened the physical strength of diamond tool, the hard diamond materials were plucked out from the tool after adhesive tool wear in the longer cutting distance. Consequently, the NMFS tool appeared a crack on the cutting edge as shown in Figure 3.7(b). Therefore, tool life

of NMFS tool was likely end at the cutting distance of 750m, tool life of NMFS tool was 79.4min. In contrast to the MFS tool, the MFS tool was still in the stage of adhesive tool wear at this cutting distance, more titanium alloys covered on the tool edge of MFS tool but no observation of obvious crack. Tool life of MFS tool at the magnetic field intensity 0.02T would be longer than 79.4min.

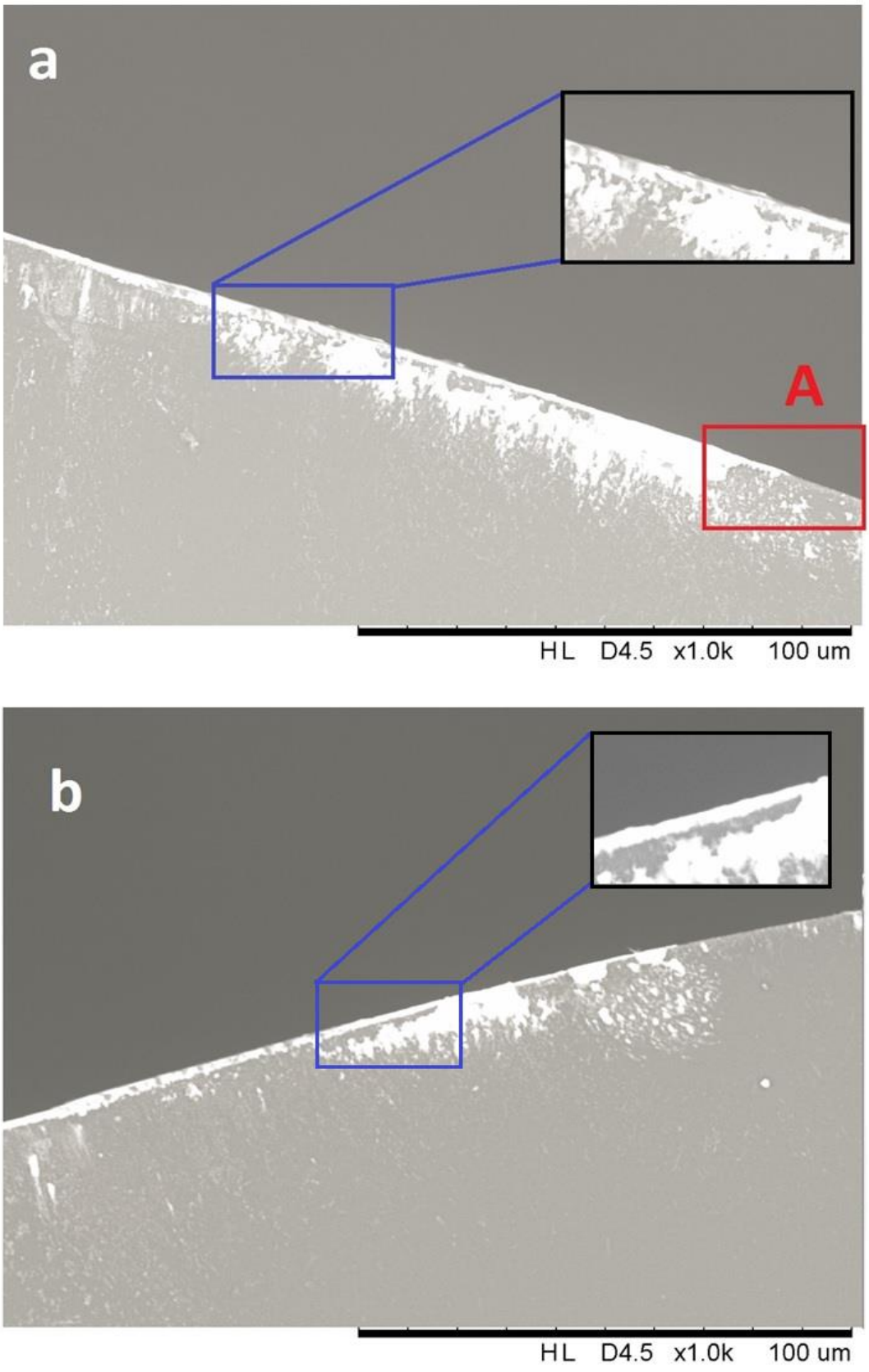

Figure 3.5 SEMs of tool edge at cutting distance 75m (a) absence of magnetic field and (b) 0.02T of magnetic field.

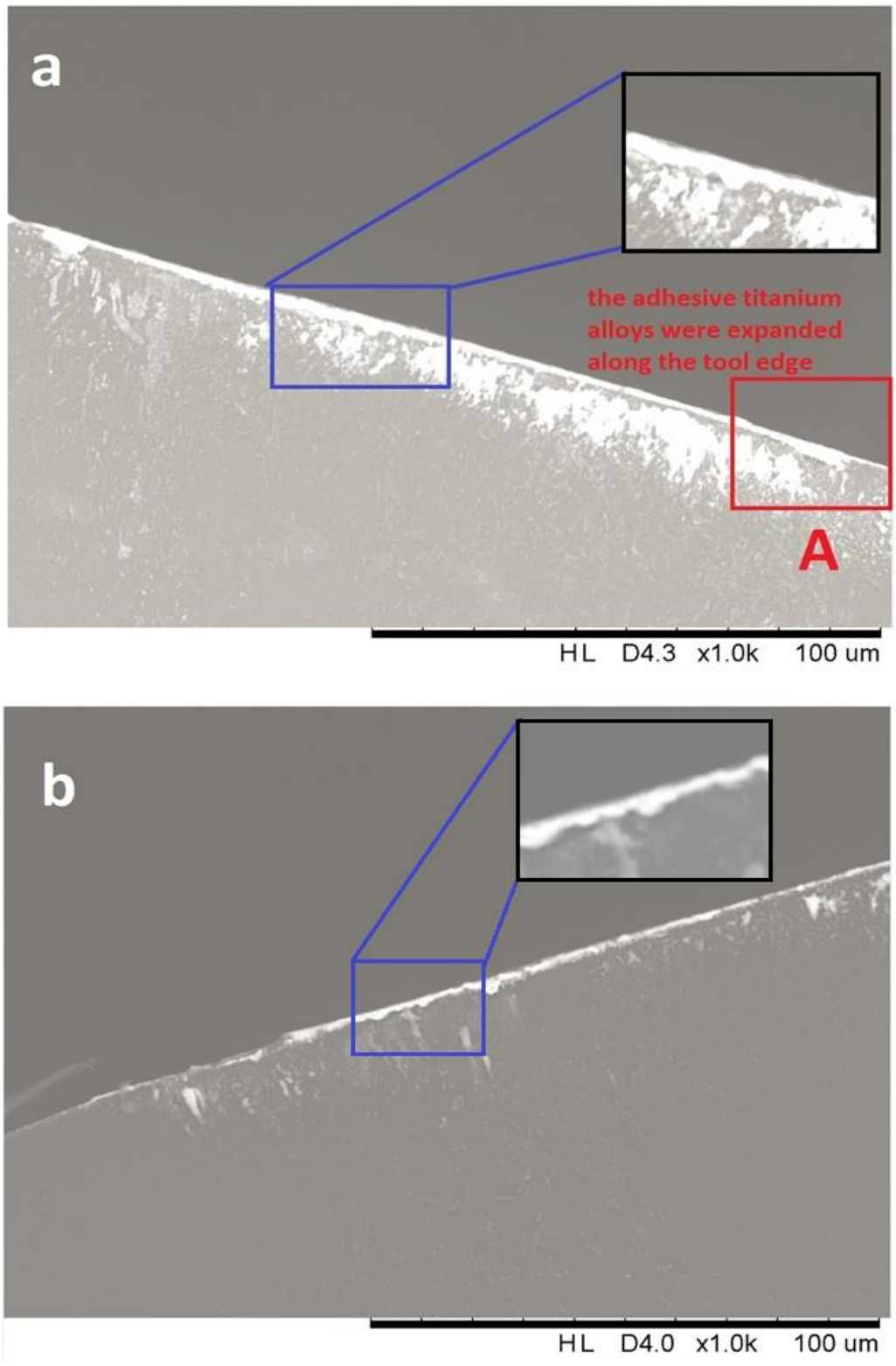

Figure 3.6 SEMs of tool edge at cutting distance 150m (a) absence of magnetic field and (b) 0.02T of magnetic field.

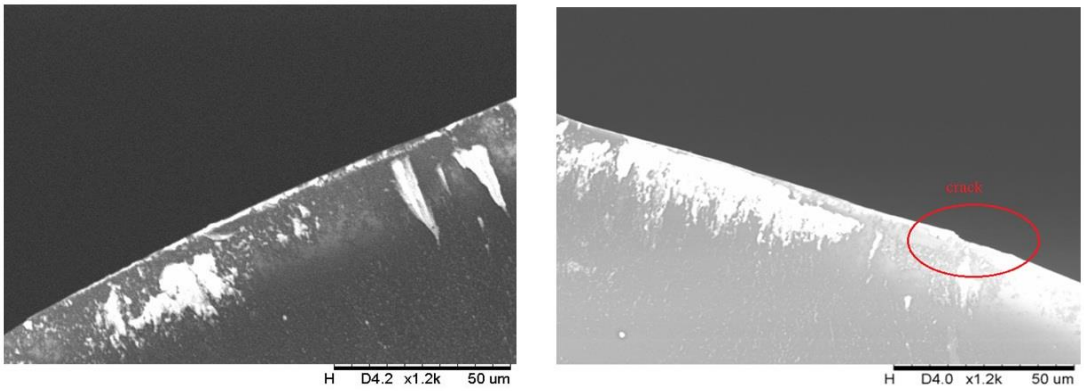

Figure 3.7 The tool edge at cutting distance 750m (a) MFS and (b) NMFS.

3.3.4 Cutting force variation

Kong et al. (2006) stated that the thrust force F_t caused material deep swelling during SPDT, it induced obvious tool marks on the final workpiece, therefore, the thrust force F_t of NMF and MFSs was measured in the experiments. The duration was 55 seconds. The mean value of overall cutting force is calculated by the software Dynoware sensor. After obtaining the mean value, each data point is used for calculating the standard deviation. The CV is then calculated by dividing the standard deviation to the mean value. The results are shown in Table 3.2. According to Table 3.2, the mean F_t magnitude of NMFS was the lowest in comparison to that of MFSs at the magnetic field intensity 0.01T - 0.03T. The mean F_t of NMFS was 1.37N while 2.92N, 5.24N and 6.28N were for the MFSs at the magnetic field intensity 0.01T, 0.02T and 0.03T respectively. The larger mean F_t of MFSs was caused by adding the repulsive force and magnetic torque in the direction of shear surface by the magnetic field. The repulsive

force increased with the magnetic field intensity increase according to Equation 3.1, therefore, the mean F_t increased with the magnetic field intensity increase. Although the mean F_t of all MFSs was larger than that of the NMFS, the F_t variation was in the contrast. The higher magnifications of F_t of both NMFS and MFSs are shown in Figures 3.9 for the visual comparison of F_t variation. According to Figure 3.9(a), the crests at the F_t curve of NMFS displayed solid and clear, each crest was shown as individual and separate. According to Figure 3.8, at the cutting time 10s - 24s, the F_t variation of NMFS was large, it fluctuated and showed many sharp crests, At the later cutting time 24s - 40s, the F_t variation was reduced, it was much stable that the height and width of the crests became smaller. The sudden change of F_t variation globally (from 10s- 24s to 24s-40s) resulted in the much higher force variation in the overall cutting process, which was unfavorable to tool life as well as the surface integrity. For the F_t of all MFSs, the crests at the F_t curve were blur with the shorter heights and width in comparison to that of NMFS. Also, there was no dramatic increase/decrease in F_t throughout the whole turning process, implying the more stable turning motion under the influence of an eddy current damping effect.

To compare the F_t variation between MFSs and NMFS in the statistical aspect, the parameter named Coefficient of variation (CV) was used and is defined as:

$$CV = \frac{\sigma}{\mu} \quad (3.7)$$

Where σ is the standard deviation and μ is the mean of all measured data values. CV is expressed as the percentage normally. The data of F_t captured at the beginning (0-4s) and the end (44s-55s) was excluded in the CV calculation for removing the effects of instability of tool motion in the stages of tool entry and exit. The cutting force data was collected by the force sensor, which the mean value and the standard deviation of cutting force were determined by the software Dynoware. The CV would be calculated by dividing the value of standard deviation to the mean value.

From Table 3.2, The CVs of MFSs at the magnetic field intensity 0.02T and 0.03T were only 5.38% and 5.48% while the NMFS was 15.77%. The CVs of MFSs at the magnetic field intensity 0.02T and 0.03T were improved by 65.88% and 65.25% respectively, suggesting less dispersive of F_t values from the mean value under the influence of eddy current damping effect. A reduction of cutting force variation was implied.

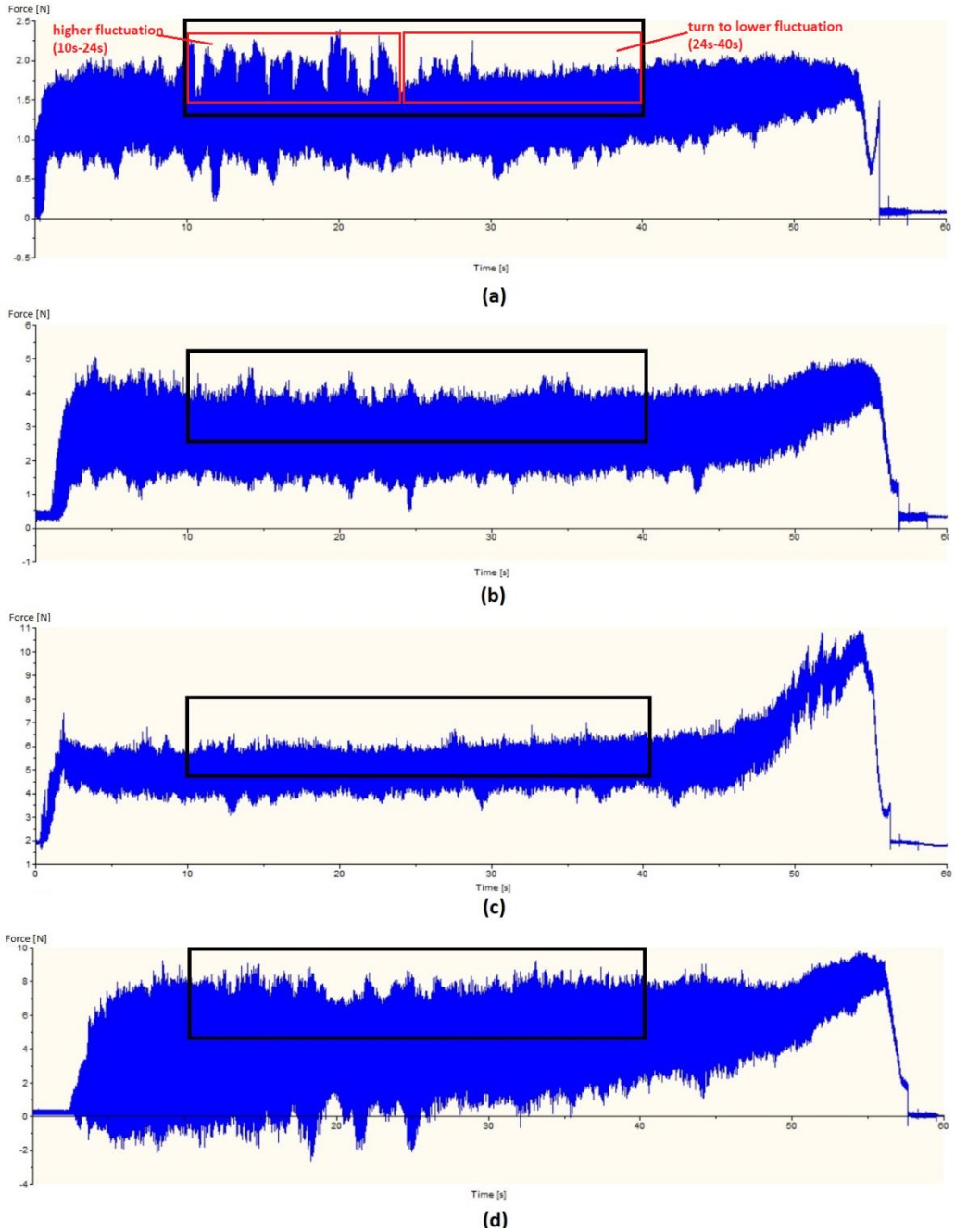

Figure 3.8 The F_t of (a) 0T (an absence of magnetic field), (b) 0.01T magnetic field, (c) 0.02T magnetic field and (d) 0.03T magnetic field.

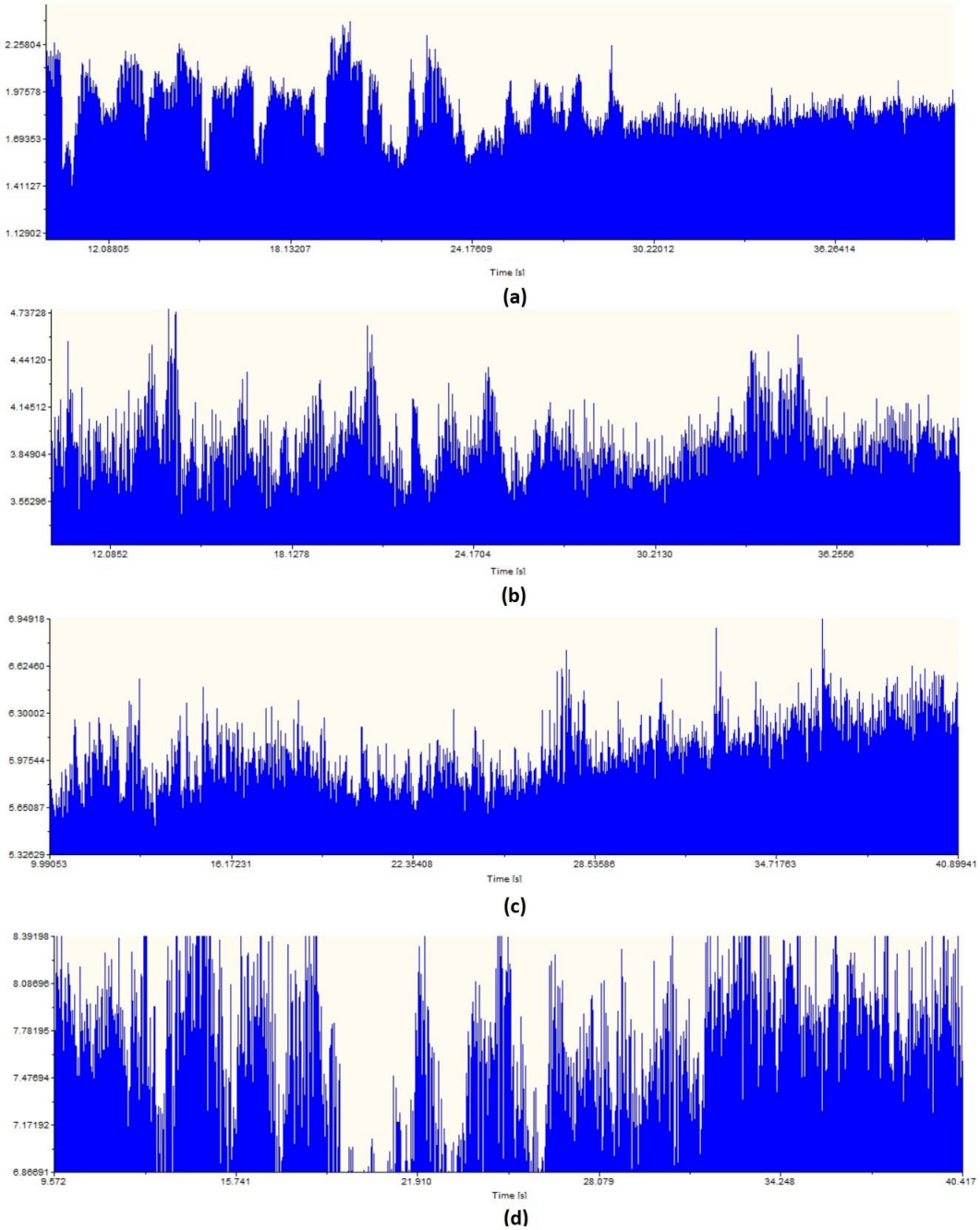

Figure 3.9 The F_t of (a) 0T (an absence of magnetic field), (b) 0.01T magnetic field, (c) 0.02T magnetic field and (d) 0.03T magnetic field in higher magnification (10s-40s).

Table 3.2 Mean, standard deviation and Coefficient of variation of thrust force in magnetic field 0T-0.03T.

	H=0	H=0.01T	H=0.02T	H=0.03T
Mean F_t (N)	1.37	2.92	5.24	6.28
Standard Deviation	0.22	0.25	0.28	0.34
Coefficient of variation (%)	15.77	8.42	5.38	5.48

3.3.5 Surface roughness and surface texture

Surface roughness of MFSs and NMFS was measured, the six areas of the machined surface were measured and averaged. The corresponding results are shown in Table 3.3. According to the results of average surface roughness of MFSs and NMFS, the lowest average surface roughness was achieved at the magnetic intensity 0.02T, which is 13nm, this further provided the proof that the optimum magnetic field intensity was 0.02T in the experiments of this thesis. On the other hand, average surface roughness of other MFSs (0.01T and 0.03T) was also lower than that of NMFS. Therefore, an application of eddy current damping effect in SPDT successfully improved surface roughness of machined surface of titanium alloys.

The particular area of the surface roughness at the magnetic field intensity 0 - 0.03T was shown in Figure 3.10. According to Figure 3.10(c), the nano-surface generation was achieved in the turning condition with the machining parameters feedrate 8mm/min, depth of cut 4μm and spindle speed 1500 rpm under the influence

of magnetic intensity 0.02T. The surface roughness is 9nm for the MFS at magnetic field intensity 0.02T. The nano-surface generation in SPDT of titanium alloys has never been reported from literature. In this study, the nano-surface generation in SPDT of titanium alloys was achieved by applying the proposed machining technology, it is a comprehensive breakthrough in UPM area.

Table 3.3 Average surface roughness of MFSs and NMFS.

	0	H=0.01T	H=0.02T	H=0.03T
Surface roughness(nm)	29	22	13	19.5

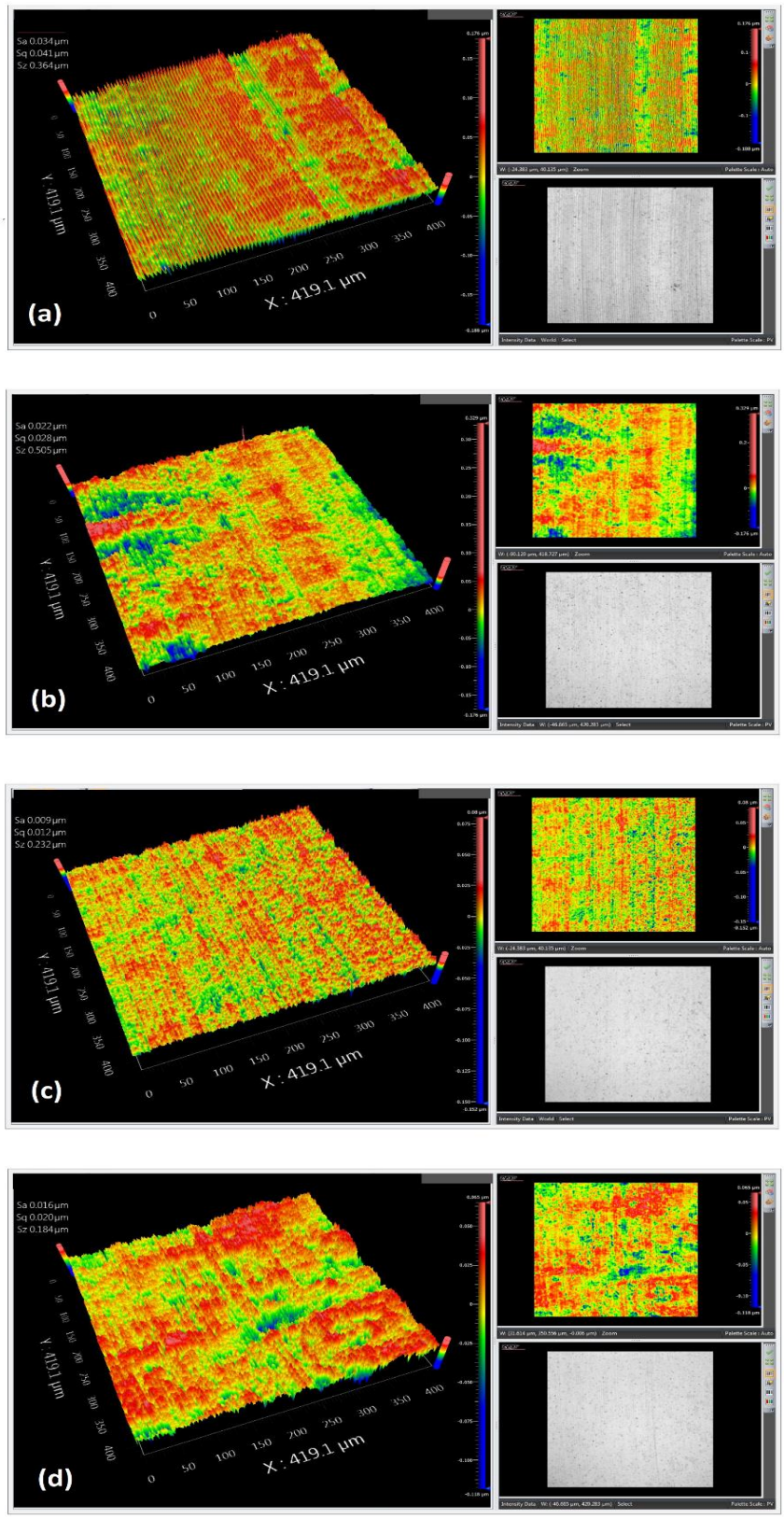

Figure 3.10 Surface roughness of particular area on the machined surface (a) 0T (an absence of magnetic field), (b) 0.01T magnetic field, (c) 0.02T magnetic field and (d) 0.03T magnetic field.

3.4 Summary

In this part of thesis, SPDT of titanium alloys assisted with an eddy current damping effect was demonstrated. The experimental results showed the long and continuous chip formations, the reductions of cutting force variation and adhesive tool wear which all are favorable to the machining performances of titanium alloys in SPDT. Under the influence of eddy current damping effect, the machining vibration as well as tool vibration was highly suppressed, thus lengthened tool life. Tool life of NMFS tool was 79.4min in SPDT of titanium alloy, which was lower than that of MFS tool. The application of an eddy current damping in SPDT successfully suppresses the machining vibration and enhances the machinability of titanium alloys in UPM.

The effectiveness of an eddy damping current effect directly affects the machinability change of titanium alloys during SPDT, the proper magnetic field should be applied in order to provide an adaptive damping force to suppress the turning vibration. The optimum magnetic field intensity in the presented experiments was 0.02T; Combining the optimum magnetic field intensity 0.02T with the machining parameters: feedrate: 8mm/min, depth of cut: 4μm, spindle speed: 1500rpm, the best machining performance displayed. In case of altering machining parameters for the particular application, the magnetic field intensity needs to be adjusted with the machining parameters in order to deliver the proper degree of an eddy current damping effect; this

issue relates to the optimization processes and will be the focus in the later research.

Because of the domination of eddy current damping effect in SPDT, the machining performance of SPDT is uplifted. Generally, the higher magnetic field intensity improves the machining performance of SPDT in comparison to the absence of magnetic field. However, the optimum magnetic field intensity in SPDT may not be obtained at the relatively high magnetic field because of the induced eddy current, the optimum magnetic field intensity may be obtained at the middle value of adaptive range. The proper magnetic field intensity was critical to provide an adaptive damping effect to suppress the turning vibration in SPDT of titanium alloys. If the values of depth of cut and feedrate in SPDT of titanium alloys increase, the cutting force as well as the vibration force will increase, in these cases, the higher eddy current damping force should be generated in order to suppress the higher vibration force, accordingly, the optimum magnetic field intensity will increase in these cases.

Chapter 4 Material swelling and recovery of titanium alloys in diamond cutting using a magnetic field

4.1 Introduction

Ultra-precision machining (UPM) is one of the most widespread machining technologies for the nano surface generation, it enables to fabricate medical products in mirror grade surface finishing with sub-micrometer form accuracy and nanometer range surface roughness. Extremely small depth of cut is always set in UPM; therefore, little bur or bur free is believed to generate on the machined surface and the shape of cutting groove is anticipated as same as the tool radius of diamond tool ideally. However, the material properties of various materials and the thermal expansion effect induce the tendency of altering in shape, volume and even the texture of machined surface in order to react the change in the temperature after machining processes. Temperature is a function of kinetic energy of an object in the molecular level. When the object is undergone the heating process, the kinetic energy within the molecules increases. After absorbing the heat energy, the molecules start to vibrate and maintain themselves with a certain separation with other molecules. Therefore, the volume of object expands. As the residue stress from the machining process is attained on the machined surface, this provides the energy for the molecules to keep the vibration, but the vibration of molecules in this stage is less serious in comparison to the original machining stage.

Finally, the machined surface has expanded, and depth of cut of actual machined surface is difference from the assigned one unavoidably. On the other hand, the level of material expansion is highly depended on the change in the temperature and material properties involved in the machining processes. The relationship between these factors is called coefficient of thermal expansion. Coefficient of thermal expansion is changed when the material properties and the rate of temperate change on the object are changed.

In UPM, as the requirement of surface finishing is relatively high, the few variations on the assigned depth of cut would make the unacceptable surface quality to the final components. The material swelling/ recovery caused the deviation from the prefect case in UPM as illustrated in Figure 4.1. Extremely high cutting temperature melts the machined materials in the cutting processes, at the same time, the exertion force and pressure from the diamond tool are sufficiently high to cause the plastic side flow of melted materials laterally, leaving the materials behind the cutting edge especially at the location of side and bottom of cutting edge. When the materials recover/swell during the solidification process, they are expanded because of the effect of thermal expansion and their volumes are enlarged, consequently tool marks are left on the machined surface randomly. Especially for low thermal conductivity and elastic modulus alloys, a huge amount of heat is trapped and cannot be dissipated effectively from the tool/workpiece interface, a higher amount of heat energy is supplied to the

molecules of that alloys, the molecules vibrate in a larger distance because they absorb much more energy. Consequently, the machined surfaces of alloys with the low thermal conductivity undergo with even large material recovery volume, they demonstrate the notable swelling marks on the machined surface thus.

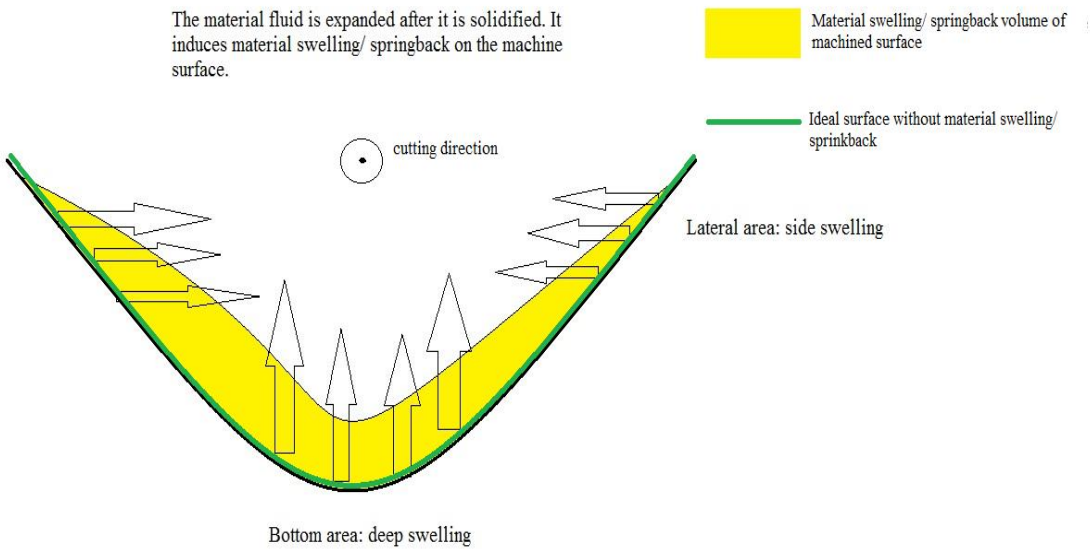

Figure 4.1 The illustration graph of material swelling/recovery of machined surface in UPM

The problems of material swelling and recovery in single point diamond cutting are treated as the natural response of materials properties. As mentioned above, the phenomenon of material swelling is related to the material properties, which the degree of recovery is proportional to coefficient of thermal expansion, they are unavoidable and uncontrollable unless the materials are undergone change of chemical compositions or change of cutting parameters in machining processes. Those methods minimized the level of material swelling and enhanced the surface integrity, at the meantime, they

generated several side effects including large investigation time, high machining costs and change of machining strategies which may lower the material removal rate, therefore, a better machining approach should be adopted to fill up the research gap which is to lower the negative impacts from the material swelling or minimize the recovery level of the machined surface without sacrificing the machining performances simultaneously. Resolving the problematic material swelling effect in UPM technology contributes the fabrication of higher precise level of components, expanding the utilizations of potential and valuable alloys in the related industries.

The material swelling effect is considered as the dominant factor to worsen surface roughness and form accuracy (Jasinevicius et al., 2003; Kong et al., 2006; Liu and Melkote, 2006; Sata et al., 1985) in machining processes. Because of the material swelling effect, the assigned machining parameters such as the cutting depth, width and radius are invariably different from the corresponding results displayed into the machined components, leading the variation between the designed and actual products; form accuracy and surface integrity of machined surface are subsequently deteriorated. Especially for the materials with low elastic modulus and thermal conductivity such as titanium alloys, the material swelling effect is reinforced because the molecules within titanium alloys vibrate in a higher level for responding the trapped heat energy inside the molecules. In this part of thesis, as titanium alloys possess material properties of

low elastic modulus and low thermal conductivity, the effect of material recovery on ultra-precision machined titanium alloys is intensified. Therefore, titanium alloys are chosen as the materials for showing the effectiveness of magnetic field on the suppression of material recovery in UPM.

Recently, researchers investigated the mechanisms of material swelling effect in order to reduce its' negative impacts induced on the machine surface. Although they investigate the formation of material recovery by experimental and theoretical approaches, these works only defined the existence of problematic recovery but provided no solution. On the other hand, there have been many academic attentions on how a magnetic field changes the isotropic and internal energy of material microstructures. The grain orientation and ordering of different materials including alloys and superconductors were obtained through the alignment in the presence magnetic field (Ferreira et al., 1988; Shimotomai et al., 2003; Tolbert et al., 1997; Ullakko et al., 1996). Kainuma et al. (2006) further discovered that NiCoMnIn alloys displayed nearly a perfect shape recovery by applying a magnetic field, showing only 3% deformation behavior during a reverse transformation. The existing empirical evidence has already showed that a magnetic field enables to alter material properties of particular materials with a positive magnetic sensitivity, providing the aligned microstructure. The next question would focus on the effect of alignment and ordering

on the thermal transference of low thermal conductivity materials, which is the main reason for the high level of material swelling in machining processes of titanium alloys

In this part of thesis, a magnetic field was superimposed on titanium alloys to increase the thermal conductivity of titanium alloys during diamond cutting in UPM, we only employ two permanent magnets additionally to give out the results of significant reduction of material recovery as well as high form accuracy and low surface roughness of machined groove. Our works only require 0.02T magnetic field intensity without utilizing of any extra source to obtain the unprecedented findings.

4.2 Theory

4.2.1 Material swelling and recovery in diamond turning

In ultra-precision diamond cutting, the material swelling/recovery is known to be reasons for the springback of machined surface and leads to tool marks on the machined surface, causing unsatisfactory surface integrity. These two effects are dominant, especially when depth of cut is extremely small. According to To et al. (2001), the material swelling is classified as two types: side swelling and deep swelling. Side swelling is the flow of liquid metal to the diamond tool side when the cutting edge exerts the high pressure and load on the machined materials; the side flow materials become viscous fluid under the continuous cutting process, the metal fluid stays at the two sides of the cutting edge and solidifies when the temperature lowers, and

consequently, they leave obvious tool marks thereby affecting surface roughness. Similar to side swelling, deep swelling is the expansion of material volume at the bottom position of machined surface when metal fluid solidifies after cutting, the expanded volume mostly locates on the bottom side of machined surface.

4.2.2 Enhancement of thermal conductivity by magnetic moment alignment under magnetic influence

Researches stated the thermal conductivity of nanofluid which containing ferroparticles /magnetite particles could be enhanced in the presence of magnetic flied (Altan et al., 2011; Gavili et al., 2012; Philip et al., 2007; Sundar et al., 2013; Younes et al., 2012). Also, the thermal conductivity of nanocomposite which contained carbon nanotubes with ferrometals or ferrofluid in the form of thin film was well enlarged in the presence of magnetic field (Gonnet et al., 2006; Han and Fina, 2011; Horton et al., 2011). The basic principles and underlying reasons for the improvement of thermal conductivity using a magnetic field of above literature are that, the ferroparticles of nanofluid or carbon nanotubes are aligned under an application of external magnetic field. In the absence of an external magnetic field, some magnetic particles position separately to each other because of the van der Waals forces and dipole–dipole interactions, causing aggregations of magnetic particles. The magnetic particles are randomly oriented and positioned as a result (Lajvardi et al., 2010; Nkurikiyimfura et al., 2013). In the presence

of magnetic field, the magnetic dipolar energy inside molecules is sufficient to come over the thermal energy, the ferroparticles inside or surrounding the nanofluid/ carbon nanotube tend to align along with the direction of the external field as the positive value of magnetic susceptibility of ferroparticles. The aligned particles or carbon nanotubes move as a chained structure, the magnetic particles act as linear chains which are highly conductive paths for transferring heat, the fast heat transference along the paths of fluid carrier is occurred (Philip et al., 2008; Li et al., 2012).

In the absence of external magnetic field, paramagnetic particles may attach to each other because of the van der Waals forces and dipole-dipole interactions. However, once a magnetic field presence, the dipole moments liked to align with an external applied magnetic field. The dipole-dipole interaction energy U_d between the magnetic particles is termed as (Li et al., 2012):

$$U_d(ij) = -\frac{3(m_i \cdot r_{ij})(m_j \cdot r_{ij})}{{r_{ij}}^5} - \frac{(m_j \cdot m_i)}{{r_{ij}}^3}\ ,\ r_{ij} = r_i - r_j \quad (4.1)$$

where r is the distance between the magnetic particles i and j, m is the mass of magnetic particle, i and j denotes to i-th and j-th magnetic particles. The coupling constant is equal to:

$$\mathrm{L} = U_d(ij)/k_B T \quad (4.2)$$

which defines the effective attraction between two magnetic particles, where k_B is Brownian constant and T is the temperature respectively. In the absence of magnetic

field, the magnetic particles are oriented in random directions and follow with Brownian motion as L < 1. When applying a magnetic field, the magnetic dipole interaction energy turns to be large enough, the magnetic particles start to align themselves parallel to the direction of magnetic field. As the magnetic field increases, the magnetic particles begin to group as short chains along the direction of the magnetic field. The chain structures of magnetic particle enhance the thermal conductivity in the magnetic field (Philip et al., 2008), the aligned particles act as linear chains which are highly conductive paths for transferring heat. The lengths of the chains increase with an increasing magnetic field (Philip et al., 2007), also, the amount of aligning magnetic particles remarkably increases with magnetic field intensity increase (Lajvardi et al., 2010).

The enhancement of thermal conductivity induced from the alignment of magnetite particles under the influence of magnetic field could be extended to UPM of titanium alloys based on the same principle. According to the sources of titanium alloys, the magnetic susceptibility of titanium alloys is 14.6ppm (Suenaga, 1984; Wichmann et al., 1997), the positive value of magnetic susceptibility represents that the classification of magnetism of titanium alloys belongs to paramagnetic, their reaction tendencies toward the magnetic field exist as long as the magnetic field is presence, meaning that the magnetic moments of titanium alloys could be aligned in the presence

of external magnetic field. Therefore, the machining process of titanium alloys is expected to take benefits from the magnetic field assistance, employing the enhancement of thermal conductivity by aligning and forming the chained structures of magnetic moment at the liquid state of melted titanium alloys in the cutting process. The formation of highly conductive paths on the machined titanium alloys surface enables the dissipation of cutting heat effectively, the material swelling / recovery consequently is reduced in the condition of less heat trapped inside the material in the solidification stage, it results of lowering the degree of molecular vibration, causing fewer expanded volumes of machined titanium alloys' surface in comparison of that under the absence of magnetic field.

This part of thesis reported a new application of using the properties of magnetic moment alignment of titanium alloys under the influence of magnetic field in UPM, to solve the problem of high level recovery in machining titanium alloys. A single groove was cut onto titanium alloys' surface under the magnetic field influence with comparison tests. The experimental results confirmed the above conclusion and the theory, they showed a significant reduction of recovery surface and improved surface roughness of machined surface by using the magnetic field during the diamond cutting in comparison to that without the magnetic assistance.

4.3 Experimental investigation of the magnetic field effect on material recovery in diamond cutting

4.3.1 Experimental setup

Two phase titanium alloys, Ti6Al4V were used as materials for the experiments. The composition of Ti6Al4V was listed in Table 4.1. A straight line was cut on the Ti6Al4V s' surface using a single point diamond tool in the presence and absence of magnetic field. The cutting parameters and tool specification were: depth of cut: 3μm, feedrate: 200mm/min and the tool radius:1.514. A magnetic field was provided by two permanent magnets. Titanium alloys were placed at the center of two permanent magnets to expose the samples to the magnetic field where magnetic field intensity was 0.02T. The experimental setup is shown in Figures 4.2(a-b). Moore Nanotech 350FG (4 axis Ultra-precision machine) was used as an equipment for the diamond cutting. Atomic force microscopy (AFM) measurement system Park's XE-70 was used for observing the bur formation. Surface roughness, cutting radius and cutting depth of samples were measured by Wyko NT8000 Optical Profiling System which is the optical profiler using non-contact measurement. The samples processed the diamond cutting test in the presence and absence of magnetic field are named MFS (magnetic field sample) and NMFS (non-magnetic field sample) respectively.

Table 4.1 The composition of titanium alloys used in the experiments.

	Element composition (%)						
	V (Vanadium)	Al (Aluminium)	N (Nitrogen)	O (Oxygen)	H (Hydrogen)	C (Carbon)	Fe (Iron)
Titanium alloys (Ti6Al4V)	4	6	0.05	0.2	0.012	0.1	0.3

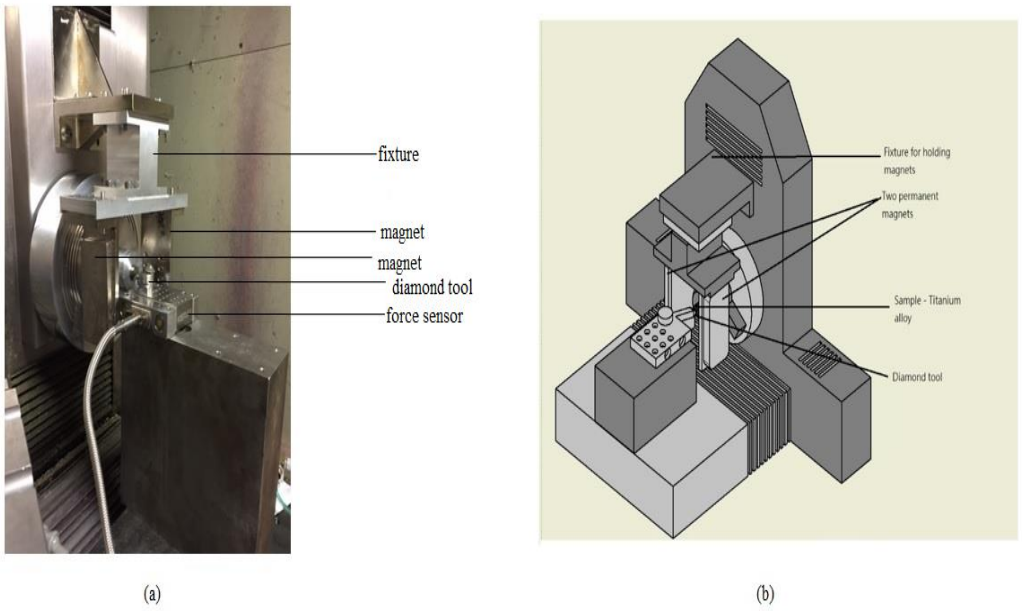

Figure 4.2 (a) Experimental setup (b) illustration graph of experimental setup.

4.3.2 The effect of magnetic field on the tool/workpiece interface

The magnetic particles inside the melted titanium alloys were aligned and moved along the direction of magnetic field. According to previous literature reported, the number of magnetic particles aligned in the direction of magnetic field is proportional to the magnetic field intensity, meaning that the number of magnetic particles migrated in the magnetic field increases with the magnetic field intensity increase.

As the magnetic field increases, the magnetic particles start to group as short chains along the direction of the magnetic field. The chain structures of magnetic particle enhance the thermal conductivity in the magnetic field (Philip et al., 2008), the aligned particles act as linear chains which are highly conductive paths for transferring heat, the fast heat transference along the paths of fluid carrier is occurred. The lengths of the chains increase with the magnetic field intensity increase (Philip et al., 2007). Also, the number of magnetic particles which have tendency to align in the direction of magnetic field remarkably increase with magnetic field intensity increase (Lajvardi et al., 2010) and considerable increase the heat transference in magnetic fluid.

Ti6Al4V are paramagnetic materials and they are magnetized as only as an existence of external magnetic field. In the cutting process, titanium alloys melted under the high cutting temperature. Melted titanium alloys consisted of suspensive paramagnetic particles in carrier fluid. Under the same logic as the above-mentioned

characteristics of magnetic particle, in the presence of magnetic field, the paramagnetic particles inside the melted titanium alloys would move with the direction of magnetic field. There should be a hint on the machined surface that the movements of paramagnetic particles in the magnetic field could be traced, which prove the migration of paramagnetic particle, they become the evidence of the formation of conductive path.

The experimental results agree with the previous reported. The plane view and the cutting profile of cutting groove under the magnetic field intensity 0.03T are shown in the Figures 4.3 and 4.4. Under the influence of stronger magnetic field intensity 0.03T, more magnetic particles were migrated along with the direction of magnetic field. Due to the paramagnetic particles alignment under an external magnetic field, the paramagnetic particles formed as chains and migrated with the direction of magnetic field. As mentioned before, the amount of magnetic particles aligned in the direction of magnetic field increases with magnetic field intensity increase (Lajvardi et al., 2010), therefore, under the influence of application of larger magnetic field intensity 0.03T, more amount of paramagnetic particles were migrated, consequently, paramagnetic particles were expected to group at the end point of magnetic field direction which was at the right hand side of groove, forming a cluster and grouped at one side of the machined groove.. Refer to Figures 4.3, there was a dark area concentrated at the right side of groove, which was the good agreement with the theoretical statement, implying

the formation of cluster of paramagnetic particles because of the stronger migration of them under the stronger magnetic field influence. From the above view, the movement of paramagnetic particle during the diamond cutting process was displayed experimentally; it further proved that the formation of conductive path of paramagnetic particles was feasible because the existence of evidence of the paramagnetic particle migration under the magnetic field.

Refer to the results given from the stronger magnetic field intensity 0.03T at Figures 4.3 and 4.4, one more conclusion is pointed out. The optimum magnetic field should be applied in order to minimize the “over grouping” of paramagnetic particles which generates the denser volume in the machined surface, consequently worsen form accuracy and the surface integrity. With the application of the magnetic field intensity 0.02T, which was the optimum magnetic field intensity in the experimental plan, it provided the formation of conductive path to minimize the material swelling effect and avoided from "over grouping" of paramagnetic particles to deteriorate the surface quality simultaneously.

Although the thermal conductivity of titanium alloys in the presence of magnetic field cannot be measured in the current state, the indirect proof was provided in this session that the paramagnetic particles were migrated and formed as conductive paths to enhance the heat transference as well as the thermal conductivity of titanium alloys.

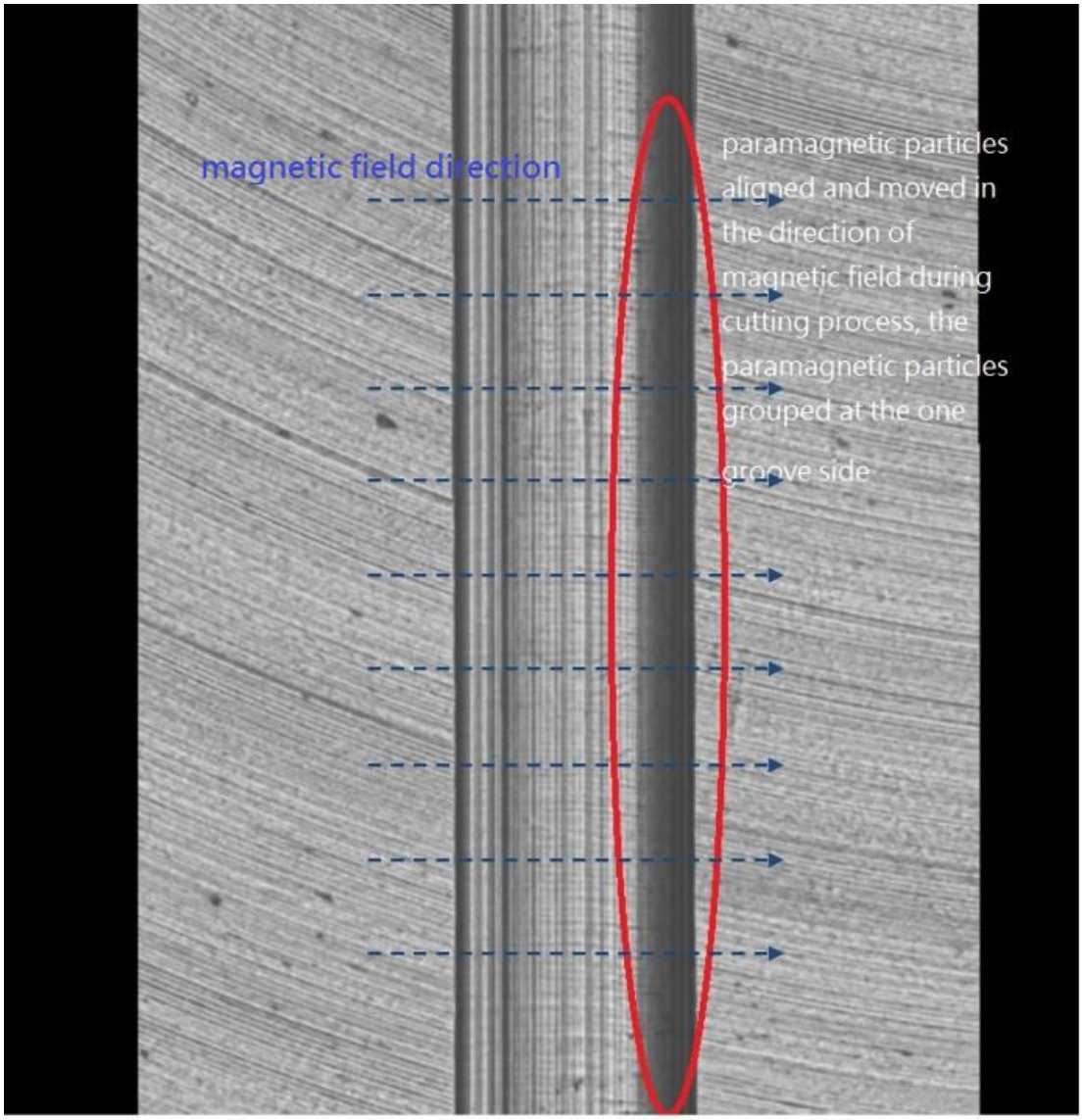

Figure 4.3 The plane view and microscope of the cutting profile of cutting groove under magnetic field intensity 0.03T.

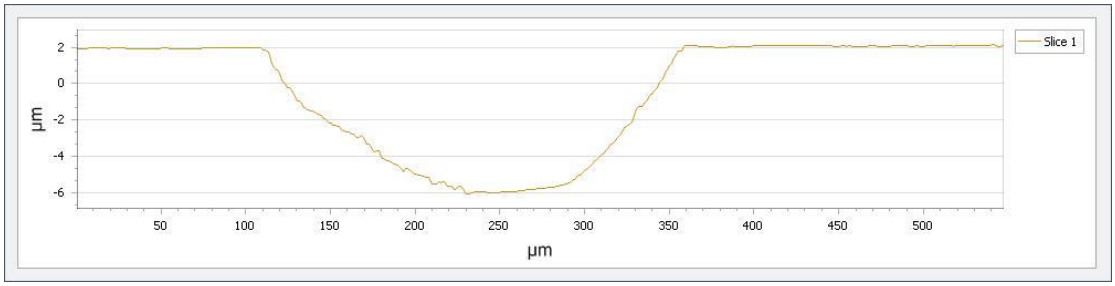

Figure 4.4 The cutting profile of the machined groove under magnetic field intensity 0.03T.

4.3.3 Form accuracy and surface integrity of machined groove under the magnetic field influence

The springback level during the solidification of metal fluid was highly reduced due to the effective transference of cutting heat by the alignments of paramagnetic particles of titanium alloys, forming the conductive paths to dissipate the cutting heat from the tool/titanium alloys to the surrounding. In the experiments, magnetic field intensity 0.02T was superimposed to the samples during the diamond cutting in order to minimize the material swelling effect on the machined surface. Figures 4.5(a-b) show the micrographs of MFS and NMFS. Clear, obvious and straight swelling marks were exposed linearly on the bottom of cutting surface at the NMFS, in particular to the center of the cutting surface, the swelling marks were the most apparent. It implied the deep swelling effect is dominant over the machined surface. The deep swelling effect concentrated at the bottommost of the machined surface, which the direction of material recovery was located at the bottom area and the solidified materials were expanded upward which is a kind of deep swelling as mentioned in the previous section. On the other hand, side swelling was appeared in the machined groove side, the side surfaces of the cutting groove showed raised and uneven, even some cracks were appeared on the groove edge. It signified the bur formation and material recovery were localized and they appeared at the cutting edge sidelong. Titanium alloys showed a high level of

material swelling on the machined surface after diamond cutting. For the MFS under the same cutting condition, it's machined surface demonstrated smooth and unclear swelling marks, the bottom surface of cutting groove showed horizontal lamella vein surface texture with few vertical swelling marks, suggesting the smooth and small levels of deep swelling. Also, the groove side showed straight and had nearly no crack in comparison to the NMFS, the MFS showed the remarkable reduction of side swelling under the magnetic field influence.

For the width of cut groove, the groove width of MFS was 230μm while that of NMFS was 158μm; With the assigned cutting width 220μm, the cutting width error of MFS counted for only 4.5% which was smaller than that of NMFS 28.2%. The side swelling introduced the larger volume of material at the groove side and therefore the groove width in the NMFS became much smaller than the assigned one. Actually, as titanium alloys have low thermal conductivity and low elastic modulus, almost one third of removal materials at the side position was recovered for the NMS after diamond cutting according to the experimental results. The higher degree of material recovery of titanium alloys causes the rejection of precision production of these valuable alloys. Under the magnetic field influence, the cutting width error of MFS lowered to only 4.5% with only 10μm error with assigned cutting width, side swelling of machined groove was highly suppressed under the magnetic influence, which was reflected by

high accuracy of machined groove width generated in the presence of magnetic field.

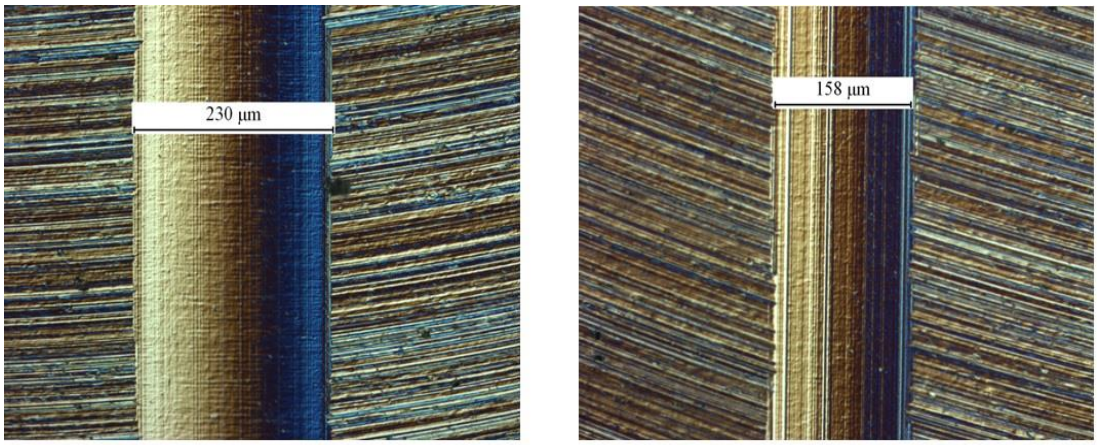

Figure 4.5 The micrographs of cutting groove of (a) MFS and (b) NMFS.

The groove profiles of NMFS and MFS are shown in Figures 4.6(a-b), depth of cut and radius of curvature of cutting profile of MFS were about 2.96µm and 1.513mm (RadCrV in Figures 4.6(a-b)) respectively which were extremely close to the assigned depth of cut 3µm and the diamond tool radius 1.514mm. Furthermore, the cutting edge of MFS showed smooth radius curve with less obvious wavy and vibration characteristics. Adversely, due to the dominant of material swelling effect, the materials were expanded after a diamond cutting, ragged and crude profile was displayed on the machined surface of NMFS, the shape of cutting profile of NMFS was even distorted which deviated largely from the actual tool shape. Moreover, its depth of cut and the radius of curvature of cutting profile were 1.9 µm and 1.883mm, indicating a significance of deep swelling on the machined surface.

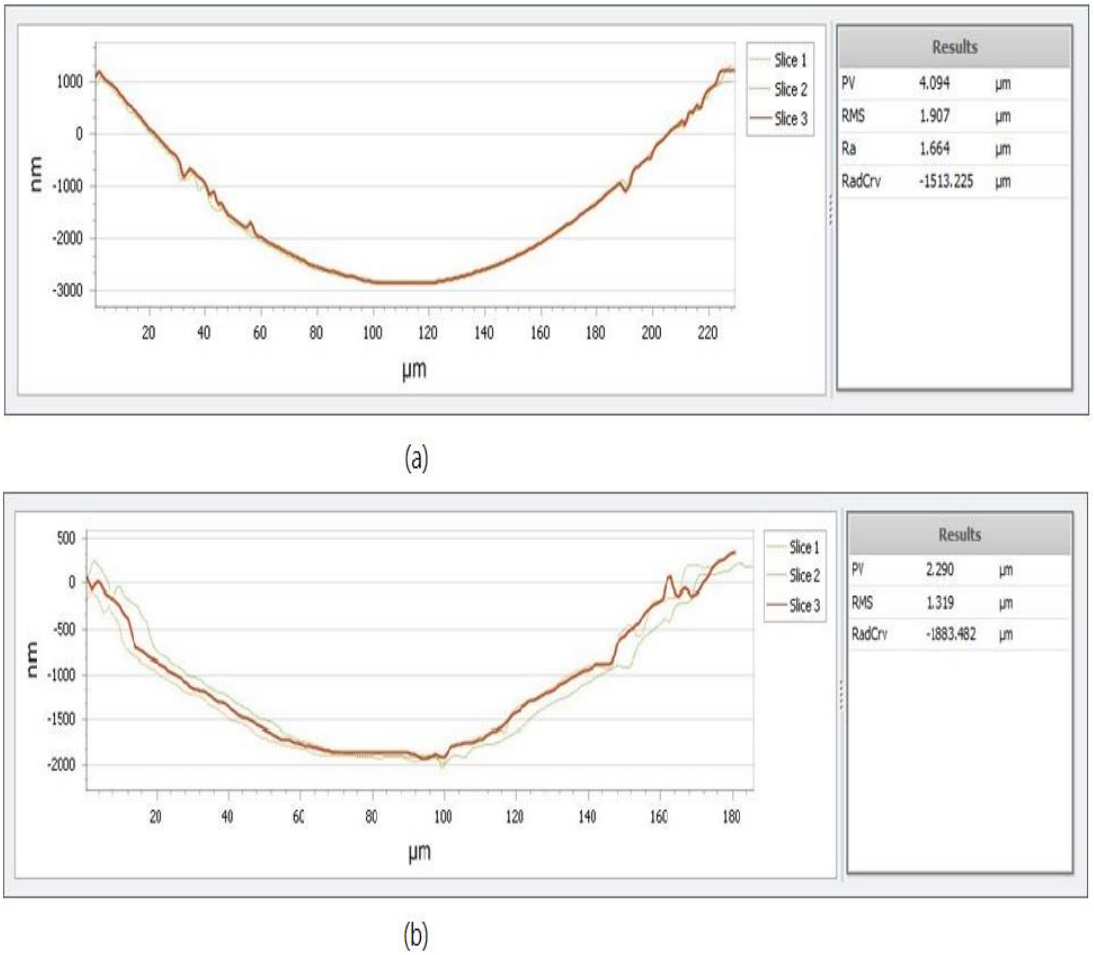

Figure 4.6 The cutting profiles of cutting grooves of (a) MFS and (b) NMFS.

The burs caused by side material swelling are analyzed by AFM as shown in Figures 4.7 (a-b), which they captured the figures of groove side area. The comparison of AFM between the NMFS and MFS showed that fewer Poisson burs were formed for the latter. The MFS illustrated a manifestly smaller bur size and shorter bur height in comparison to that of NMFS. The width of uplift material at the groove side of NMFS was larger and the burs were showed separately with obvious crests.

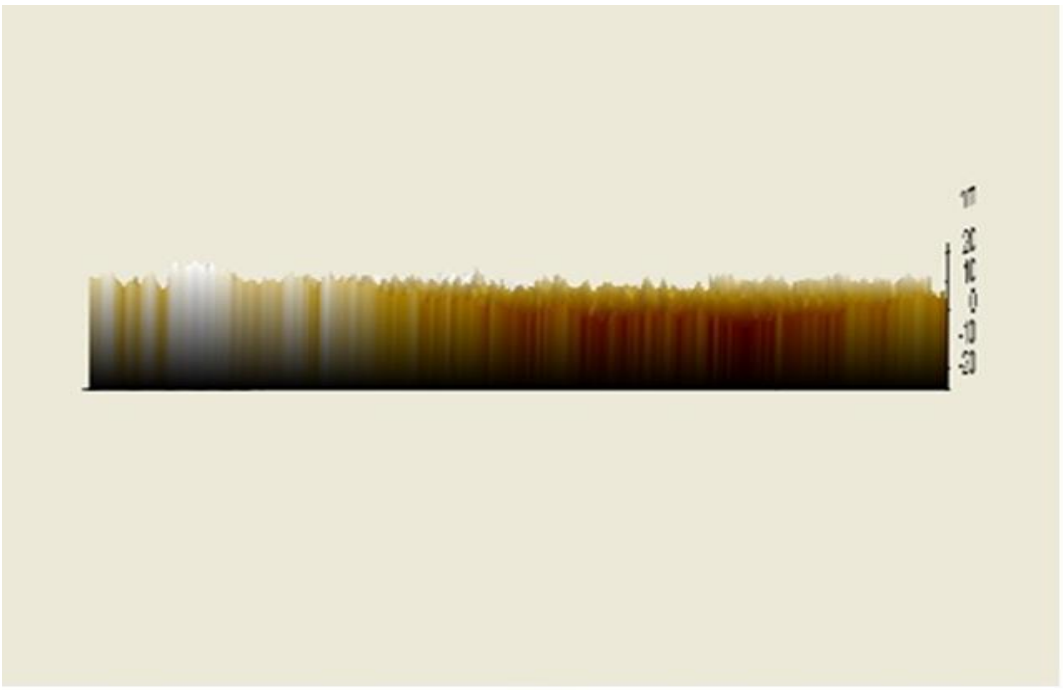

(a)

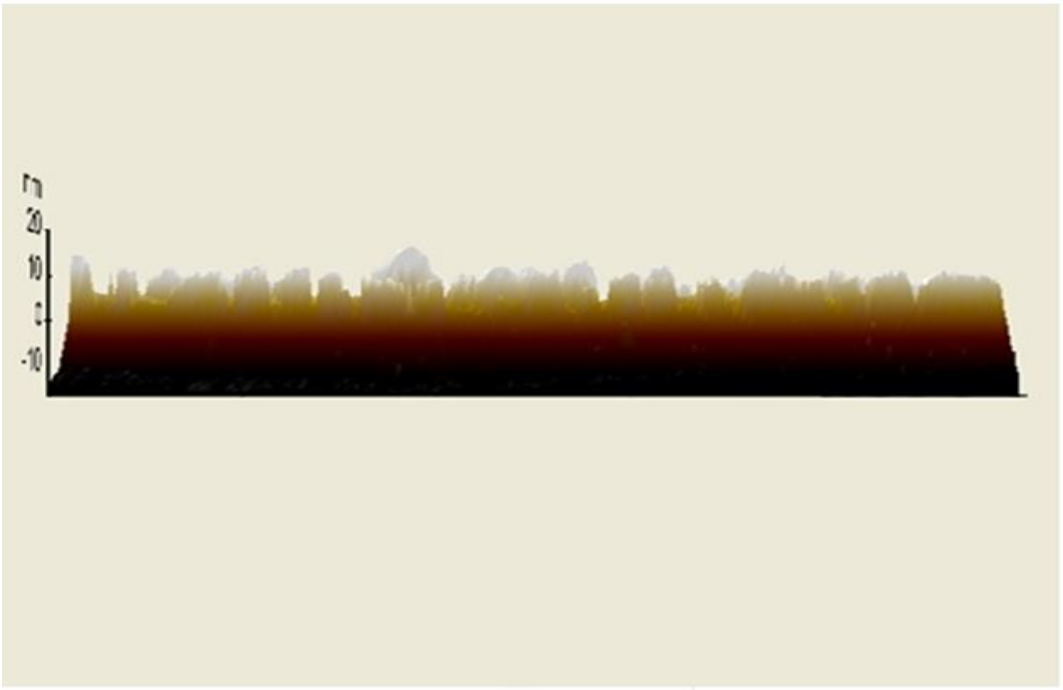

(b)

Figure 4.7 AFMs of bur formation at the groove side of (a) MFS and (b) NMFS.

More supporting results of the enhancement of form accuracy and surface finishing of the machined groove in the presence of magnetic field are shown in Figures 4.8-4.10. Figures 4.8 show surface roughness of grooves in the plane view, the MFS

showed few changes in the radical color of surface roughness at two groove sides in comparison of that of NMFS, which suggested the small difference of bur height and distance between every bur along the cutting side, it implied the minimization of side material swelling under the magnetic field influence. In Figures 4.9, it shows bottom surface roughness of MFS which was only 15nm, it was contrary to that of NMFS which surface roughness was 36.58nm, which the improvement percentage of surface roughness of MFS was about 59%. The result is consistent to the previous discussion, stating a significant suppression of deep swelling in the presence of magnetic field. Figures 4.10 show the histograms of groove bottom surface of both MFS and NMFS; X axis of histogram refers to the height of machined surface. The histogram of MFS illustrated that over 1000 pixels was located at 0nm of x axis with less dispersion shape, it is in contrast to the NMFS that only about 250 pixels was located at 0nm of x axis with the highly scattered pattern. The higher concentration of pixel at 0nm for the MFS in the histogram indicated that the higher proportion of measured data point for the surface height is zero, it revealed that the MFS consisted the smooth bottom surface. The above proved that deep material swelling was highly restricted in the presence of magnetic field.

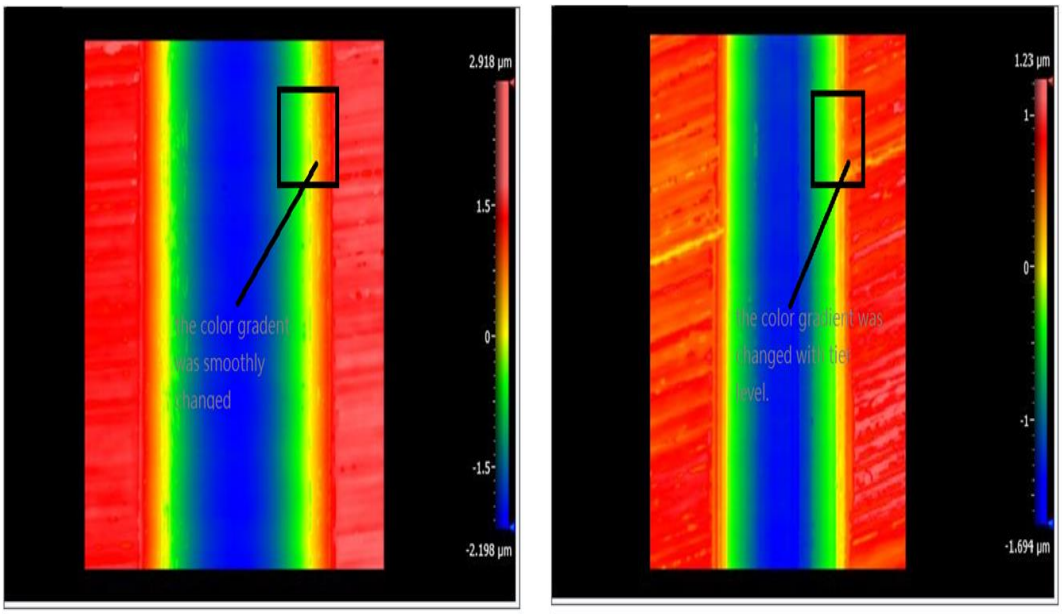

Figure 4.8 The plane views of surface roughness of (a) MFS and (b) NMFS.

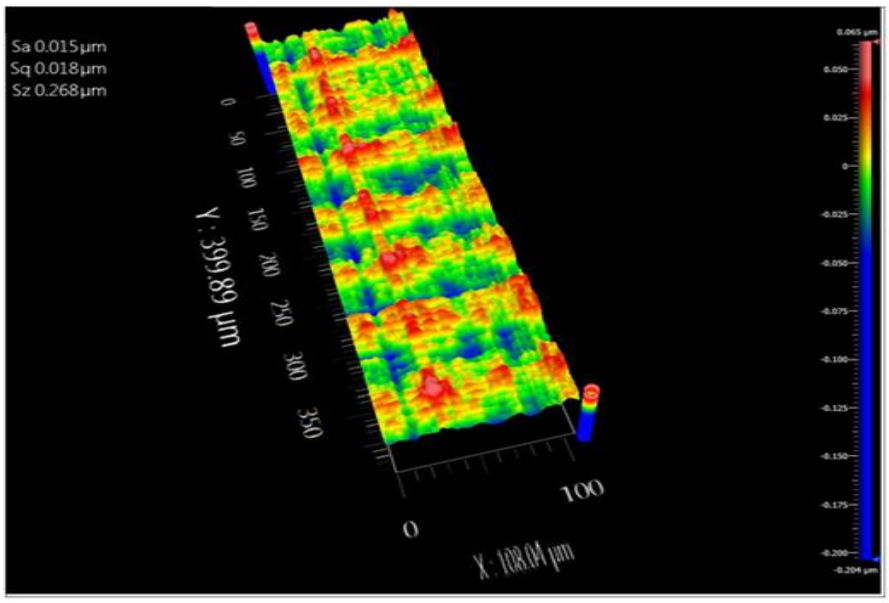

(a)

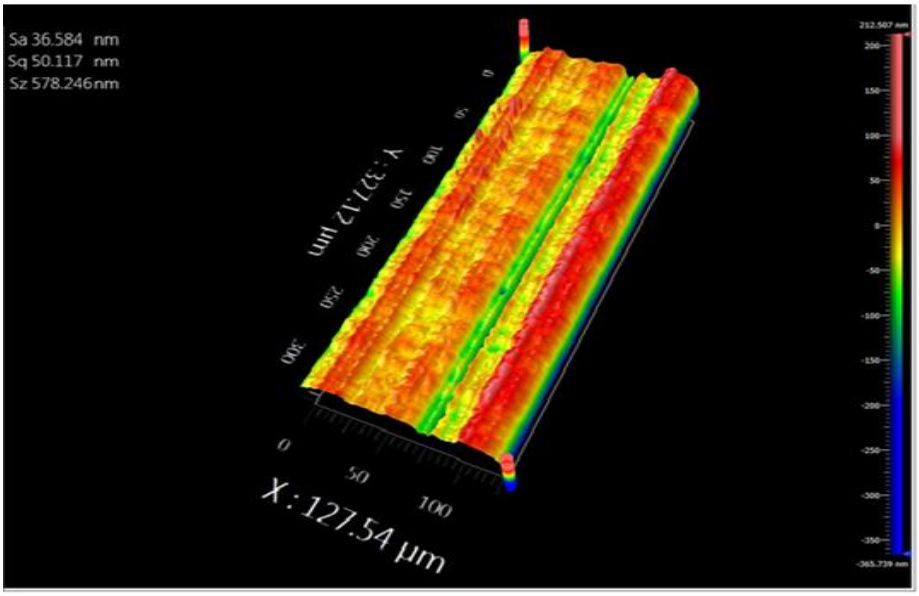

(b)

Figure 4.9 The surface roughness of bottom surface of (a) MFS -15nm and (b) NMFS – 36.58nm.

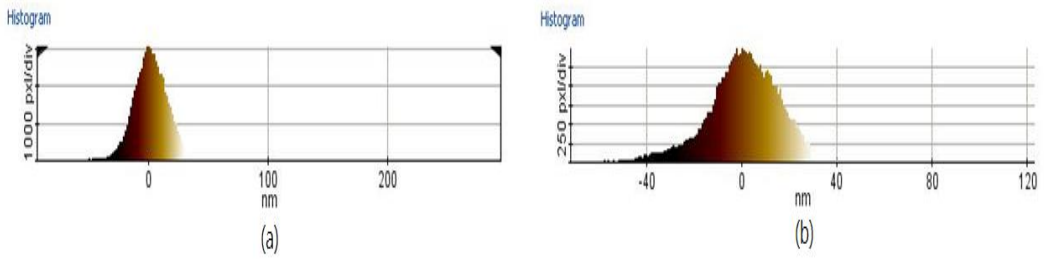

Figure 4.10 The Histograms of bottom surface of (a) MFS and (b) NMFS.

4.3.4 Tool wear

The tools of MFS and NMFS were new before the cutting test. On the other hand, the tool conditions of MFS and NMFS were measured after each cutting test, which these could ensure that tool wear was not the cause for the appearance of crack and uneven surface on the machined groove of NMFS. Figures 4.11(a-b) show the flank and rake faces of diamond tool after diamond cutting respectively. As the cutting tool distance in the cutting tests was extremely short which was only 15mm, therefore tool wear was not serious and the cutting tool edges for both MFS and NMFS were nearly "no worn" condition with only little adhesive tool wear as displayed in Figures 4.11(a-b).

As literature reported previously, the cutting temperature generated in machining titanium alloys was extremely high, therefore tool wear occurred in machining titanium alloys is mainly adhesive wear, meaning that titanium alloys melt and diffuse into the cutting edge (Jawaid et al., 1999; Wang et al., 2005). Refer to Figures 4.11(a-b), titanium alloys were welded on the tool tips of diamond tools of both MFS and NMFS, also, both of tools displayed bur formation on the rake faces because of attachment of welded chip on the rake face under the high cutting temperature, which is agree with the previous reported.

The diamond tool conditions of MFS and NMFS actually were not largely different as shown in Figures 4.11(a-b), therefore, the tool marks induced by tool wear from the

tools of MFS and NMFS should not be large variate too. As a result, the obvious differences between the experimental results of NMFS and MFS showed in this chapter (material swelling in term of surface roughness, form accuracy, depth of cut and cutting width) were not caused by tool wear.

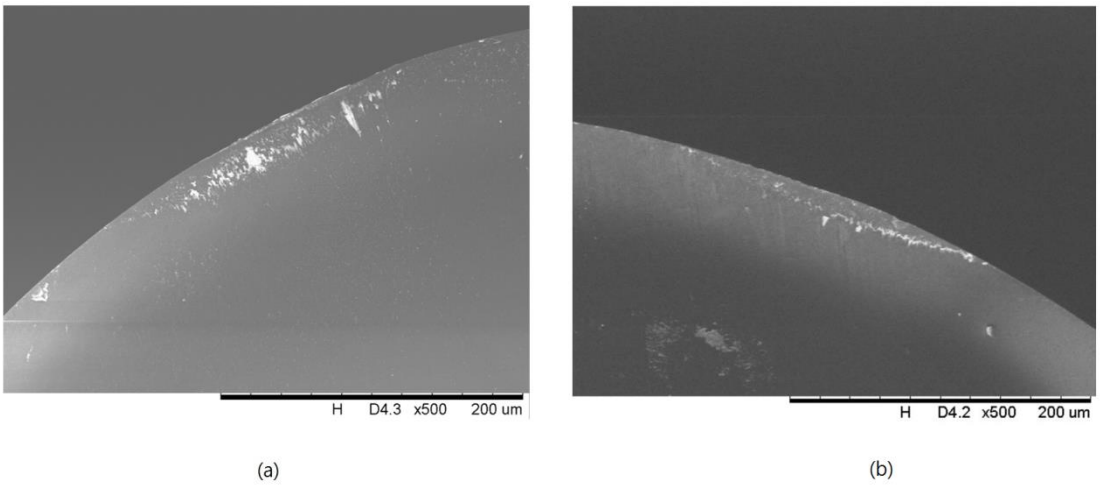

Figure 4.11 The SEMs of tool flank face of (a) MFS and (b) NMFS after the cutting tests.

4.4 Summary

Especially for titanium alloys which the materials have a low thermal conductivity and low elastic modulus, the material swelling and recovery effects are intensified on the machined surface after UPM. Therefore, material swelling is always the underlying reason for the poor machinability of titanium alloys in UPM. In this part of thesis, the problematic material swelling/ recovery, which unavoidably occurs in UPM, was minimized under the magnetic field influence. UPM of titanium alloys takes advantages of the magnetic field influence, which the magnetic particles on the machined surface

are able to migrate as the highly conductive chain structures. The diamond cut surface under the magnetic field influence achieved the excellent surface roughness and form accuracy. The errors of cutting width, depth of cut and cutting radius of cutting groove were improved significantly under the magnetic field influence, their values in term of absolute differences and percentage errors are summarized in Tables 4.2 and 4.3. In the absence of magnetic field, depth of cut, cutting width and profile radius were 1.9μm, 158μm and 1.883mm respectively; while in the presence of magnetic field, the respective measurements improved to 2.96μm, 192μm and 1.513mm. Noting that the machined surface in the absence of magnetic field constituted almost 25-37 percent percentage errors between the assigned and actual results for all of the form accuracy indicators, while the sample in the presence of magnetic field achieved a under 4 percent error for all of these.

The application can be further extended to other medical alloys as long as their magnetic susceptibility is positive. The potential alloys are nickel titanium alloys as they have elastic behavior dominantly, which are expected to have a high degree of material recovery on the machined surface after UPM. Furthermore, the proposed machining technology did not utilize complicated pre-treatments and equipment, we simply employed extra two permanent magnets with only 0.02T magnetic field intensity in the diamond cutting process to solve the material swelling/ recovery

problems. The small size of magnets enables them to be adjusted freely inside UPM machine which it overcomes the problem of inadequate space of UPM machines, the technique can contribute to high precision products in the future.

Table 4.2 The designed machining parameters and experimental results of NMF and MF samples.

	Designed parameters	Experimental results of NMF	Experimental results of MFS
Depth of Cut (μm)	3	1.9	2.9
Cutting Width (μm)	220	158	230
Cutting Radius (mm)	1.514	1.883	1.513
Bottom Surface Roughness (nm)	-	36.58	15

Table 4.3 The absolute differences and relative percentage error between the designed parameters and experimental results of MFS and NMFS.

	MFS			NMF		
	Depth of Cut	Cutting Width	Cutting Radius	Depth of Cut	Cutting Width	Cutting Radius
Absolute differences	0.1μm	10μm	0.001	1.1μm	62μm	0.369

between the designed parameters and experimental results						
Percentage error (%)	3.33	4.5	0.07	36.7	28.2	36.9

Chapter 5 Diamond tool life enhancement using a magnetic field

5.1 Introduction

Titanium alloys are widely applied in the biomedical industry for manufacturing precise components because of their excellent material properties. However, titanium alloys are difficult to cut because of their low thermal conductivity and high sustainability of work hardening at the elevated temperature, resulting a high level of tool wear and unsatisfactory surface integrity, which inevitably lead to high machining costs and energy consumptions. On the other hand, uses of fluid lubricant in machining processes of titanium alloys are sizable in order to provide an effective cooling media to dissipate high cutting heat generated in machining. Although the use of lubricant has been discouraged because of the drew damages to the environment and health, dry machining of titanium alloys is not practical currently as the high friction force and the cutting temperature induced from the dry machining environment which further accelerate and worsen tool life. Therefore, the environmental concerns cover a feasibility of dry machining of titanium alloys. In this part of thesis, a novel machining technology, a magnetic field was applied in dry single point diamond turning (SPDT) of titanium alloys to enhance diamond tool life. A rotating titanium alloy was placed in between of two magnets in order to suffer from an eddy current damping effect and a magnetic field effect during dry SPDT. Under the influence of magnetic field, experimental

results showed reductions of adhesive wear, flank wear and built up edge of tool as well as the machining vibration during dry SPDT. The uncut materials and concave areas of machined surface decreased as a suppression of machining vibration using an eddy current damping effect. The machining performances of titanium alloys in dry SPDT were facilitated in term of tool life and surface integrity by using a magnetic field, showing a feasibility of environmental friendly dry SPDT of titanium alloys in practical applications for sustainable manufacturing. Dry SPDT is firstly implemented in machining area and this part of thesis acts as the preliminary guideline for dry ultra-precision machining (UPM), contributing the instruction and direction of clean production for UPM in the future.

5.2 Machining difficulties of single point diamond turning in the dry machining environment

Titanium alloys are widely applied in biomedical industry because of their superior material properties such as high strength to weight ratio and corrosion resistance (Liu et al., 2004; Rack and Qazi, 2006; Niinomi, 2003). However, titanium alloys are low thermal conductivity and hold high sustainability of work hardening at the elevated temperature, which cause them difficult to machine especially in SPDT of ultra-precision machining (UPM). The high turning temperature is generated and trapped at the tool/workpiece interface during SPDT of titanium alloys, causing adhesive tool

wear and short diamond tool life.

Diamond tool life of difficult to cut materials in SPDT was reported to be short and problematic (Zhang et al. 2017). Fang et al. (2003) indicated that flank wear in SPDT of optical glasses reached to 70μm after the cutting distance 4km. Jia and Zhou (2012) discovered diamond tool wear started quickly after the relative short cutting distance 50m in machining glass soda lime. For diamond cutting of silicon carbide, Yan et al. (2003) stated that diamond tool wear occurred after the cutting distance 1km in SPDT of single crystal silicon. In contrast to the difficult to cut materials, diamond tool life of easy to cut materials such as aluminum alloys and copper was demonstrated to be longer; tool wear occurred at the cutting distances over thousand km (Zhang et al. 2016). Therefore, diamond tool life is highly depended on the machined materials. For the difficult to cut materials especially titanium alloys, diamond tool life is expected to be short.

As the machining difficulties exist, there have been many literature concerns on resolving tool wear in machining difficult to cut materials in order to minimize the elicited impacts to the environment. Sarikaya et al. (2016) reported serious tool wear happened during machining of a difficult to cut material Haybes 25 superalloys, they used minimum quantity lubrication approach together with the statistical analysis to reduce tool wear as well as the amount of cutting fluids used in the cutting process, the

amount of cutting oil unitized in the cutting process was successfully reduced while the machinability of Haybes 25 superalloys was enhanced. Wang et al. (2017) employed ecofriendly method, oil on the water, to reduce tool wear and the environmental pollution in machining of difficult to cut material compacted graphite cast iron. Fan et al. (2015) investigated the tool wear mechanism of Nickel-based alloy Inconel 718 which is a difficult to cut material, they compared different lubrication conditions. They discovered that water vapor plus air lubrication condition would increase the chemical rate and growth rate of oxide films, they offered a better lubrication effect at the tool/chip interface and thus reduced tool wear. Zhang et al. (2012) proposed dry cutting and minimum quantity cooling lubrication cutting of Inconel 718 with biodegradable vegetable oil. They suggested that minimum quantity cooling lubrication with biodegradable vegetable oil enabled to enhance the machinability of Inconel 718 in term of an increase in tool life and a decrease of cutting force, the machining outcomes fulfilled the increasing demands for cleaner manufacturing of Inconel 718. Researches demonstrated various environmental friendly methods to resolve the problematic tool wear and the environmental impacts of lubricant uses in machining processes of various difficult to cut materials. In this part of thesis, an environment friendly machining technology was proposed to machine difficult to cut titanium alloys in UPM under the dry machining condition, which aims to contribute the reduction of

environmental impacts brought from SPDT process.

Dry machining is one of the important machining technologies to minimize the damages and wastes induced from machining processes. However, due to the absence of lubricant or coolant, dry machining always generates a high amount of heat energy and friction force during machining processes which accelerate tool failure and cause unsatisfactory surface integrity of machined component. Integrating the subsequences of low thermal conductivity of titanium alloys in dry machining, dry SPDT of titanium alloys is almost infeasible as it further worsens diamond tool life and deteriorates the surface integrity, making rejections of final products from the industries. Machining processes containing cooling lubricants generally show better machining performances than dry machining (Devillez et al., 2011; Sreejith and Ngoi, 2000). The high cutting temperature at the tool/workpiece interface is dissipated and taken away from the workpiece by the flow of lubricants (Varadarajan et al. 2002), adhesive wear is significantly reduced because of the heat reduction at the cutting edge, preventing early tool failure. However, drawbacks remain valid for wet machining; lubricants and material particles pollute water sources and those contaminated sources damage the environment in the disposal processes (Davoodi and Tazehkandi, 2014).

Previous literature indicated that titanium alloys melts under the condition of high cutting heat, melted titanium alloys weld on the tool edge and thus adhesive wear occurs.

Researchers reported that there was strong adhesion between the tool and workpiece materials during machining of titanium alloys, it caused a high degree of adhesive tool wear (Zoya and Krishnamurthy, 2000; Wang et al., 2005). Due to the machining difficulties of titanium alloys and resulting tool wear in dry SPDT, few researches have showed successive implementations of titanium alloys in dry SPDT, as well as proposing measures to reduce diamond tool wear in dry SPDT of such low thermal conductivity alloys. Moreover, the demand of high precise components has remarkably increased, the corresponding machining impacts to the environment unavoidably increase at the same time, therefore, for sustainable manufacturing, an effective dry SPDT is urged to adopt which enables to benefit both environment and quality of precise products. In this part of thesis, a novel machining technology, an eddy current eddy damping effect and a magnetic field effect were employed into dry SPDT of titanium alloys in UPM to reduce tool wear in the dry machining environment. A rotating titanium alloy was placed in between of two magnets in order to suffer from an eddy current damping effect and a magnetic field effect during experiments. The resulting tool wear in dry SPDT of titanium alloys was significantly reduced under the influences of eddy current damping effect and magnetic field. Moreover, the proposed machining technology only employed extra two magnets which are low cost and environmental friendly. The proposed machining technology seeks to contribute to

provide a feasibility of dry SPDT of titanium alloys in practical applications for sustainable manufacturing.

5.3 Theory

5.3.1 Reduction of turning vibration using an eddy current damping effect

When a conductive metal suffers from a magnetic field and rotates in between of the magnetic field, an eddy current is generated inside the moving conductor due to the varying static magnetic field. Eddy current further generates its own magnetic field with the direction against the external magnetic field. The kinetic energy of vibration motion in the mechanical system will be dissipated in the form of heat to heat up the conductor. The processes of creating an eddy current and dissipating the vibration energy suppress the vibration in the mechanical system (Sodano and Bae, 2004; Sodano et al., 2006; Bae et al., 2005). Actually, an eddy current damping effect has been applied to many practical uses, showing the positive outcomes of the mechanical vibration reduction and uplifting operational performances of particular device; the examples include automobiles (Cadwell, 1996; Nagaya et al., 1984) and elevators (Jou et al., 2006).

Applying the same theory of eddy current damping effect to this study, titanium alloys were rotated in between of two permanent magnets and influenced by an eddy current damping effect. The overall turning vibration in dry machining environment as well as the tool vibration was then suppressed by transferring the kinetic energy of

vibration into the heat energy, thus reduced tool wear. Consequently, the surface integrity of machined titanium alloys was improved in dry SPDT.

5.3.2 Enhancement of thermal conductivity of titanium alloys under a magnetic field influence

Literature indicated that the thermal conductivity of ferrometals/ferrofluid was enhanced under the magnetic field influence. Summarized reasons of literature are, the ferroparticles inside ferrometals/ferrofluid are aligned in the presence of external magnetic field. In the absence of magnetic field, the ferroparticles are randomly orientated because of van der Waals force and dipole-dipole interactions. Once an external magnetic field exists, the ferroparticles tend to align along with the direction of physical field as the positive value of magnetic susceptibility of ferroparticles. Aligned ferroparticles then become continuous chains which are highly conductive, serving as the paths for the quick heat transference and dissipation (Gavili et al., 2012; Ghofraniet et al., 2013; Lajvardi et al., 2010; Odenbach, 2003). The information of increase in thermal conductivity by the magnetic field could be revealed theoretically. In the absence of external magnetic field, magnetic particles may attach to each other because of van der Waals forces and dipole-dipole interactions. However, once the magnetic field presence, the dipole moments like to align with an external applied

magnetic field. The dipole-dipole interaction energy U_d between the magnetic particles is termed as:

$$U_d(ij) = -\frac{3(m_i \cdot r_{ij})(m_j \cdot r_{ij})}{{r_{ij}}^5} - \frac{(m_j \cdot m_i)}{{r_{ij}}^3}\ ,\ r_{ij} = r_i - r_j \quad (5.1)$$

where r is the distance between the magnetic particles i and j, m is the mass of magnetic particle, i and j denotes to the i-th and j-th magnetic particles. The coupling constant is equal to

$$L = U_d(ij)/k_B T \quad (5.2)$$

which defines an effective attraction between two magnetic particles, where K_B is Brownian constant and T is the temperature respectively. In the absence of magnetic field, the magnetic particles are oriented in random directions and follow with Brownian motion as L is in smaller value. When applying a magnetic field, the magnetic dipole interaction energy turns to be large enough and the value of L increases, leading the initiation of magnetic particle alignments parallel to the direction of magnetic field. As the magnetic field increases, the magnetic particles begin to group as short chains along the direction of the magnetic field, the chain structures of magnetic particle enhance the thermal conductivity of materials (Philip et al., 2007; Philip et al., 2008), the aligned particles act as linear chains which are highly conductive paths for transferring heat and the fast heat transference along the conductive paths occurs.

As the magnetic susceptibility of titanium alloys is 14.6ppm which is a positive value, titanium alloys enable to react toward a magnetic field as long as an existence of magnetic field. The titanium alloys' particles could be aligned in the presence of magnetic field. Applying the same theory into this study, the titanium alloys' particles inside melted titanium alloys generated in dry SPDT were enabled to form conductive chains for the heat dissipation. When titanium alloys were exposed to a magnetic field in dry SPDT, the trapped heat was efficiently dissipated by the conductive chains of titanium alloys particles, tool wear especially adhesive wear can be minimized because of the cutting heat reduction, consequently eliminating the weakened mechanical properties of diamond tool by adhered materials at the high cutting temperature.

5.4 Experimental study of the magnetic field and eddy current damping effects on tool wear in dry single point diamond turning

5.4.1 Experimental setup

Two phase titanium alloys, Ti6Al4V were used as materials for the experiments. Ti6Al4V have 6% aluminum, 4% of beta phase stabilizer vanadium, 0.25% of iron, 0.2% of oxygen and remaining parts of titanium. Titanium alloys were in rod shapes with the length 40mm and diameter 16mm. Two samples underwent dry SPDT without lubricants. One sample processed dry SPDT in the absence of magnetic field, named as dry non-magnetic field sample (DNMFS), while another sample processed dry SPDT

in the presence of magnetic field, named dry magnetic field sample (DMFS). A self-developed fixture was used for holding two permanent magnets in an ultra-precision turning machine, DMFS was turned in between of two magnets in order to suffer from an eddy current damping effect and a magnetic field during dry SPDT.

In dry SPDT, single point diamond cutting tool was used and is made of single crystal diamond which offers a high accuracy microscopic process to workpieces. The grain size of single point diamond tool would not be changed throughout the whole experiment as the single crystal natural of the used diamond tool. The radius and height of diamond tool were 1.468mm and 10.172mm respectively. The force sensor Kistler 9256C was used to measure the cutting force which would be transferred to Fast Fourier transform (FFT) analysis. Moore Nanotech 350FG (4 axis Ultra-precision machine) was used as the equipment for diamond turning. Surface roughness of machined samples was measured by Wyko NT8000 Optical Profiling System. The experimental setup is shown in Figure 5.1. The turning parameters for both DNMFS and DMFS were set as spindle speed: 1500rpm; feedrate: 8mm/min; depth of cut: 5μm. For the extremely small turning parameters (depth of cut and feedrate) used in dry SPDT, small vibration force would be generated in dry SPDT, therefore, a relatively small magnetic field intensity 0.02T was chosen as the valuable parameter to provide an adaptive eddy current damping effect for suppressing the turning vibration.

The tool wear condition of titanium alloys in dry SPDT became significant at the cutting distance 75m in the pilot experiments under the same machining condition. Therefore, in this experiment, the tool conditions at the cutting distances 75m,150m, 225m and 300m were chosen and observed under SEM. At each cutting distance, tool wear of both samples was evaluated by the observations of rake and flank faces. Flank and rake faces of both tools were cleaned by hydroflouridic acid before taking SEM so that resulting tool wear was accurate without a distortion.

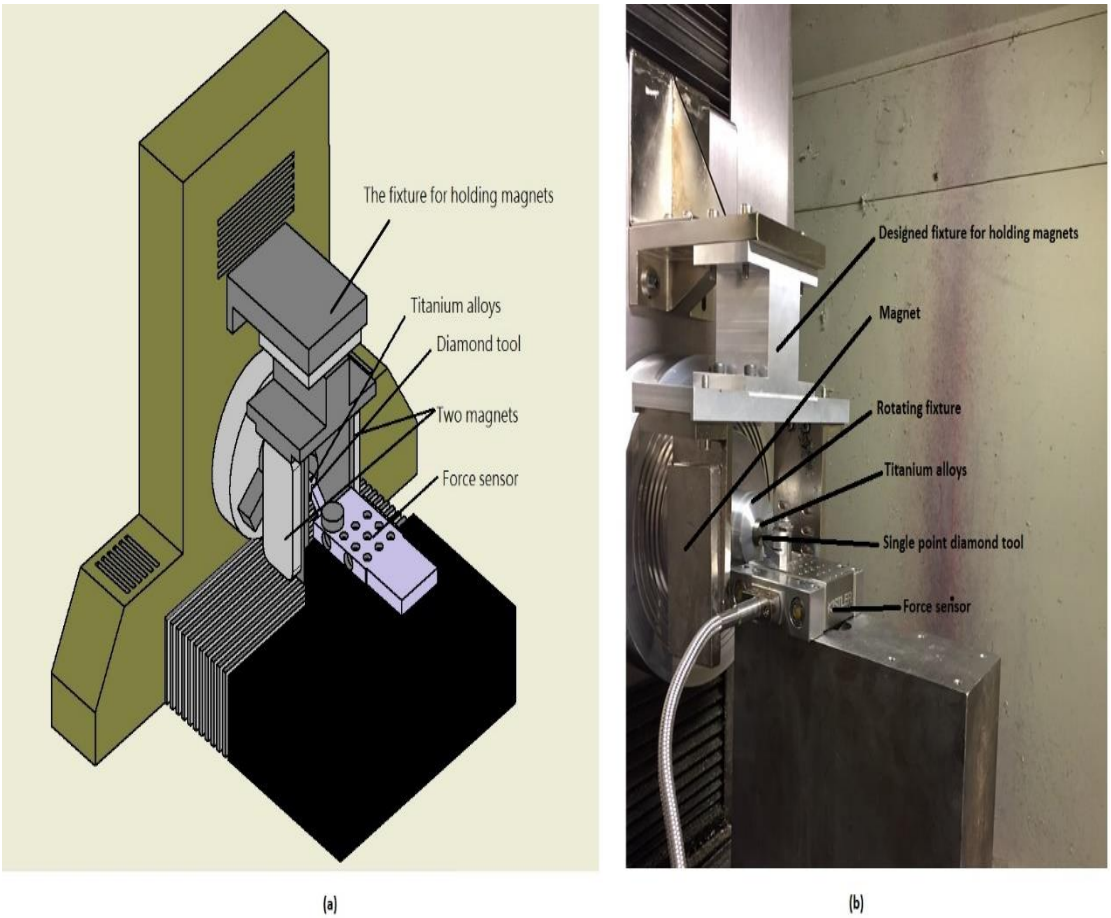

Figure 5.1 The experiment setup of proposed magnetic assisted diamond turning.

5.4.2 Validation of turning vibration suppression in dry SPDT of titanium alloys under an eddy current damping effect and a magnetic field effect

The machining vibration of turning system generated in dry SPDT was examined through Fast Fourier transform (FFT) of cutting force parallel to the feed direction as shown in Figures 5.2 and 5.3. The vibration amplitudes of turning system could be reflected into FFT which Fourier analysis converts the cutting force signal from a time domain to a frequency domain. The sample frequency of FFT is 50KHz. The y axis of the graph represents the amplitude of vibration force while x axis represents the corresponding frequency. The scales of x axis and y axis are the same.

Under an eddy current damping effect, the kinetic energy of vibration motion in the turning system would be converted to the heat energy to heat up titanium alloys, which minimized the amplitudes of turning vibration. Therefore, the vibration amplitudes in dry SPDT of titanium alloys are expected to be lower for DMFS. Comparing between the peak amplitudes of both samples in the relative frequency of FFT shown in Figures 5.2 and 5.3, at all cutting distances (75m - 300m), all peak amplitudes of DMFS in FFT were lower than that of DNMFS in the relative frequency, the above provided the solid evidence that the overall turning vibration was suppressed by an eddy current damping effect.

Generally, a significance of tool wear increases with the cutting distance increase, therefore, to evaluate the turning vibration contributed by diamond tool wear in the experiments, FFT generated at the larger cutting distance of both samples under the same machining condition was compared. As shown in Figures 5.2 and 5.3, the difference of vibration amplitudes between two samples increased with the cutting distance increase. Especially at the last cutting distance 300m, the maximum peak amplitude in FFT of DMFS was noteworthily smaller than that of DNMFS, the maximum peak amplitude of DMFS was only 0.00142N while that of DNMFS was 0.0039N, which the maximum peak amplitude of DNMFS was at least 2.76 times of DMFS, it showed the turning vibration at the longer cutting time was significantly reduced under an eddy current damping effect and a magnetic field effect, which possibly caused by the reduction of tool wear.

Moreover, previous literature reported that tool wear would produce the tool vibration in relatively high frequency, an increase in tool flank wear caused the vibration amplitudes increased in a relatively high frequency range (Kopač and Šali, 2001; Toh, 2004). Referring to FFT of both samples at all cutting distances, the vibration amplitudes located at a relatively high frequency were lower for the DMFS in comparison to that of DNMFS, which explained that tool wear was remarkably reduced in dry SPDT with assistances of eddy current damping effect and a magnetic field effect.

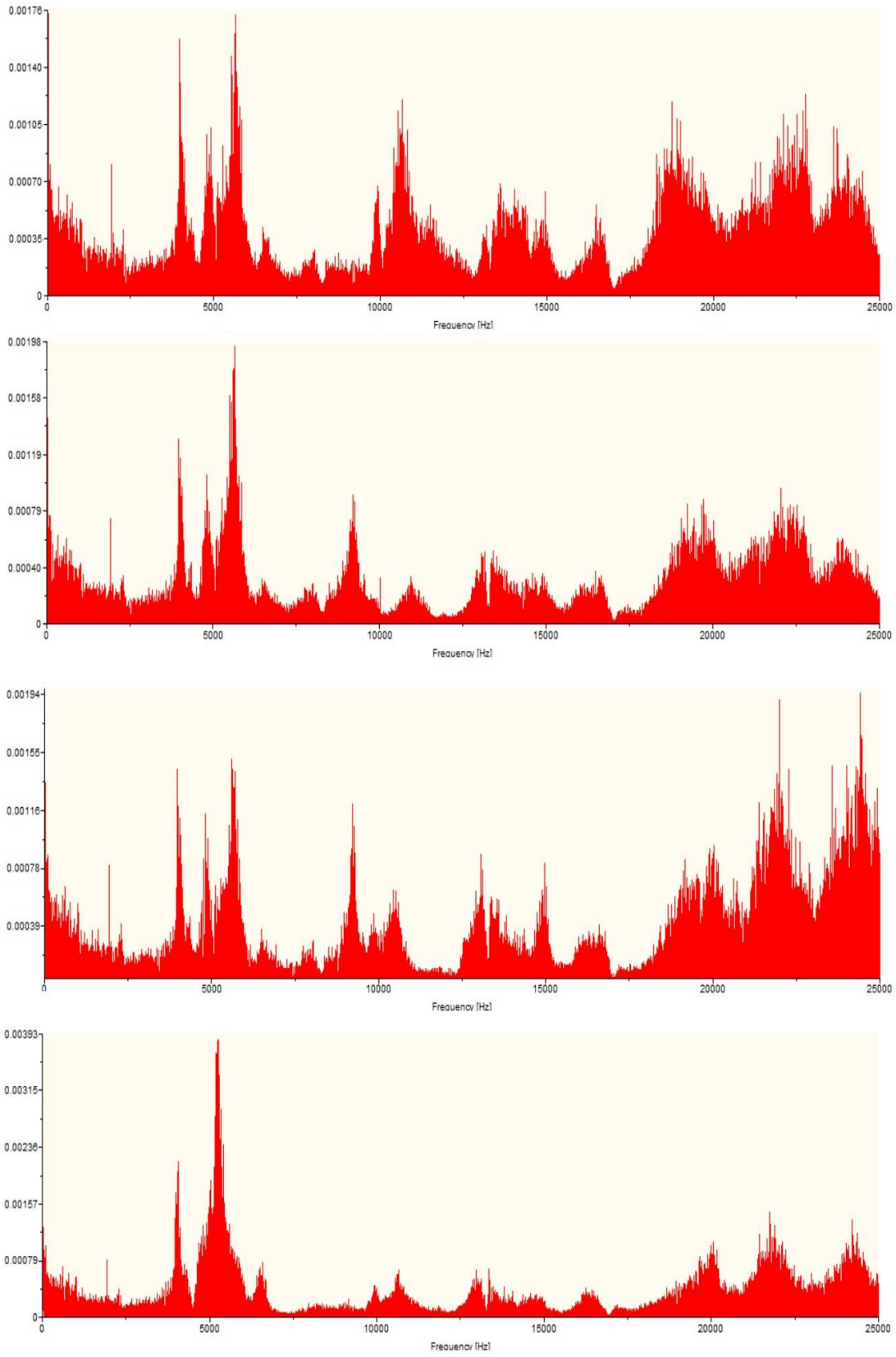

Figure 5.2 FFT of feed force generated in DNMFS at the cutting distances (a) 75m, (b) 150m, (c) 225m, (d) 300m.

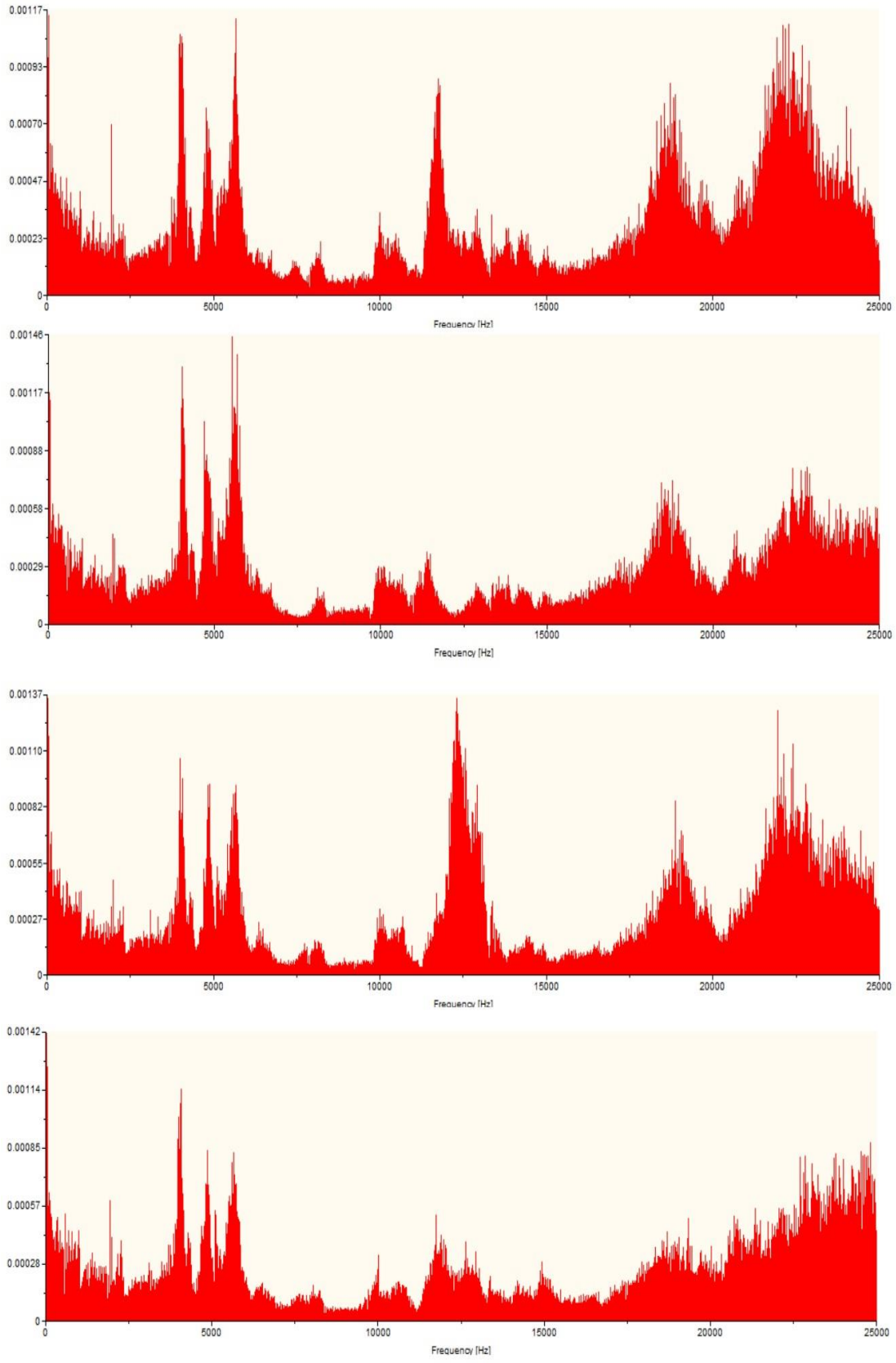

Figure 5.3 FFT of feed force generated in DMFS at the cutting distances (a) 75m, (b) 150m, (c) 225m, (d) 300m.

5.4.3 Analysis on rake wear

Actually, titanium alloys are classified as difficult to cut materials and proven to be low machinability due to their low thermal conductivity, which restricts the dissipation of cutting heat from the tool/workpiece interface (Bordin et al., 2015; Narutaki et al., 1983; Che-Haron, 2001) as a result, there is strong adhesion between the tool and workpiece materials, which affects the tool adversely. In comparison to other materials, the cutting temperature in machining titanium alloys is comparatively high (Ezugwu et al., 2003), the cutting temperature of titanium alloys was reported to achieve over 1000K under the particular machining condition (Li et al., 2017). Under turning at the extremely high cutting temperature, chips melt and stay contacts with the rake and flank faces of diamond tool, resulting serious adhesive wear. Adhesive wear was reported to be the dominant wear mechanism in machining of titanium alloys (Rahim and Sadahara, 2011; Da Silva et al., 2013; Huang et al., 2012), and mainly happened on the tool rake face (Dearnley and Grearson, 1986). Therefore, adhesive wear on the rake face of diamond tool would be observed in the detail in this part of thesis.

Figures 5.4 and Figures 5.5 show SEMs of rake faces of both tools in dry SPDT. As shown in Figure 5.4(a) and Figure 5.5(a), at the first cutting distance 75m, the melted titanium alloys generated in dry SPDT had already been attached to the cutting edge of DNMFS tool. In the case of low thermal conductivity materials in dry machining

condition, extremely high cutting heat was generated and localized at the cutting edge, titanium alloys melted and welded on the tool edge consequently. The shiny melted titanium alloys were formed as a layer on the diamond tool tip of DNMFS tool, showing an occurrence of chipping on the tool edge and adhesive tool wear. Actually, chipping originally happens before adhesive wear and normally at the beginning of cutting process, which is induced by the high cutting temperature (Kikuchi, 2009), and it is the common drawback in dry machining of low thermal conductivity materials (Dhar et al., 2006). In contrast to the DMFS tool, fewer shinny titanium alloys were attached on the tool edge of DMFS tool, only flaked fragments of titanium alloys were adhered on the cutting edge of DMFS tool in comparison to the DNMFS tool. The underlying reason for the reduction of titanium alloys adhesion of DMFS tool is that, the thermal conductivity of titanium alloys is enhanced under the influence of magnetic field, due to the quicker heat transfer, cutting heat trapped at the tool/workpiece interface could be dissipated sufficiently, the tool/workpiece interface was suffered from the lesser heat. With the tool vibration reduction benefited from an eddy current damping effect, the tool motion would be continuous and smooth with few vibrations, thus the melted titanium alloys could be flowed from the tool/workpiece interface by the aerodynamic force generated from the rotating workpiece/fixture, as a result, the chips did not adhere on the tool edge and adhesive tool wear was reduced under the magnetic field influence.

The significance of adhesive tool wear of DNMFS tool became serious at the cutting distance 150m. At the cutting distance 150m, due to the low thermal conductivity of materials and high turning vibration, titanium alloys melted and welted to the cutting edge continuously which the tool wear mechanism was as same as the previous cutting distance 75m, the newly melted titanium alloys welded on the top of adhered titanium alloys generated before, the accumulative welded materials increased the volume of adhesive titanium alloys and hence enlarged adhesive tool wear, a larger volume and thicker layer of titanium alloys showed at the DNMFS tool as Figure 5.5(b) shown. For the DMFS tool at the same cutting distance, due to the fast heat transfer effect and tool vibration reduction conveyed by the magnetic field, the cutting friction and cutting heat at the tool/workpiece interface decreased, hence, adhesive tool wear just began, a thin adhesive titanium alloys layer was observed on the cutting edge, in comparison to the DNMFS tool at the same cutting distance, the volume of adhered material at the DMFS tool was much smaller.

At the cutting distance 225m, for DNMFS tool, as the physical strength of diamond tool was degraded by the welded materials at the cutting edge, therefore, due to the continuously inserted load at the cutting edge, the diamond materials were pulled off in the subsequent turning processes and the DNMFS tool appeared cracking, the cutting edge of DNMFS tool displayed a crack as shown in Figure 5.5(c), the location of crack

was previously the location of adhesive area at the cutting distance 150m. Actually, when tool materials at the cutting edge are removed under the continuous cutting process, the removal process involves the abrasion process due to the cutting friction generated between the material particles and tool rake face (Gómez-Parra et al., 2013). When the cutting edge persists in the continuous abrasion process, the worn tool appears cracks and the loss of tool geometry finally. The overall process of tool wear in machining titanium alloys is adhesive wear following with the abrasion process. In comparison to the DMFS tool shown in Figure 5.4(c), thanks to an increase in thermal conductivity by a magnetic field, only a small amount of titanium alloy was welded on the cutting edge accumulatively, adhesive tool wear became only slightly stronger than that at the cutting distance 150m; with the reduction of turning vibration by an eddy current damping effect, abrasion between the diamond tool and the workpiece particles decreased, therefore, there was no observation of crack and enlargement of adhesive layer on the cutting edge of DMFS tool.

At the final cutting distance 300m, for the DNMFS tool, more amount of tool materials were drew out, one more crack displayed, the number of crack increased to two as shown in Figure 5.5(d), the area of defect is magnified in Figure 5.6 for showing the cracks clearly. In contrast to the DMFS tool, the area of adhesive titanium alloys on the cutting edge of DMFS tool slowly increased and not intensified dramatically as the

cutting heat was dissipated from the cutting zone effectively, there was no obvious difference of rake wear between the cutting distance 225m and 300m for the DMFS tool.

To conclude, due to the thermal conductivity enhancement of titanium alloys and the turning vibration reduction by the magnetic field, a high amount of heat was dissipated to the outside environment, leading fewer volumes of melted and welded titanium alloys at the cutting edge and thus minimized adhesive tool wear. In addition, an eddy current damping effect suppressed the turning vibration as well as the tool vibration; the tool shift, friction force and friction heat at the tool/workpiece interface were highly reduced, minimizing the abrasion processes at the tool/workpiece interface, all of the above were favor to the diamond tool condition.

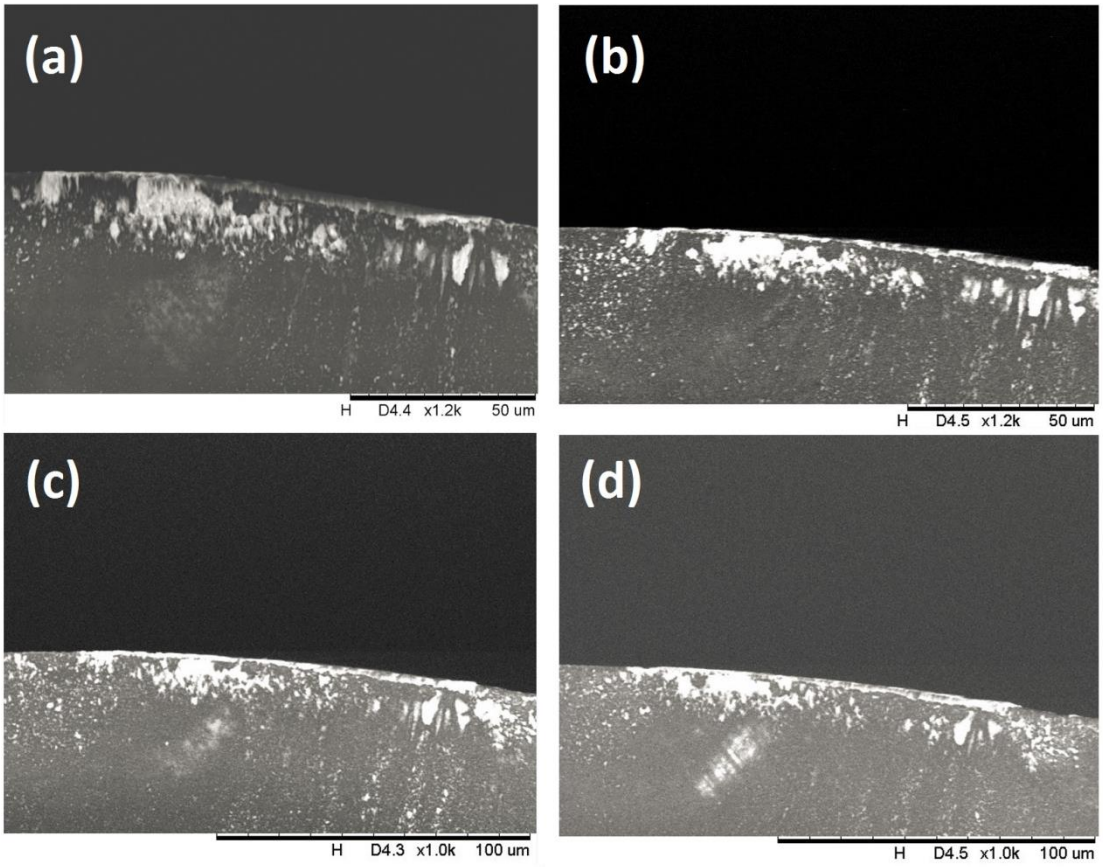

Figure 5.4 SEMs of tool rake face of DMFS at the cutting distance (a) 75m, (b) 150m, (c) 225m and (d) 300m.

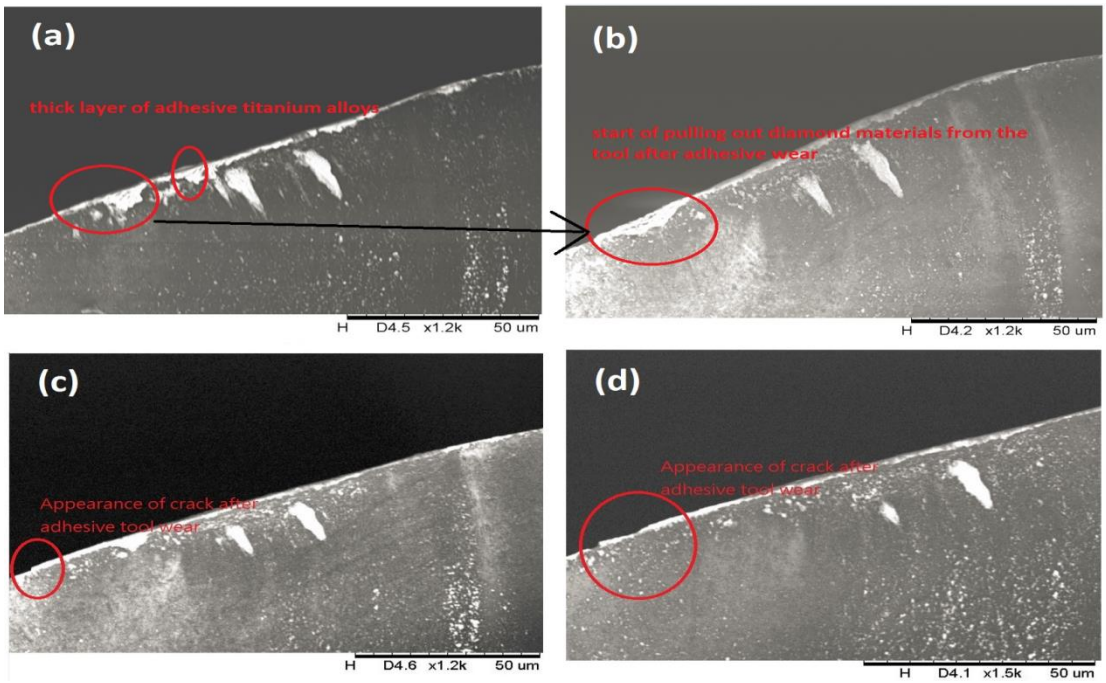

Figure 5.5 SEMs of tool rake face of DNMFS at the cutting distance (a) 75m, (b) 150m, (c) 225m and (d) 300m.

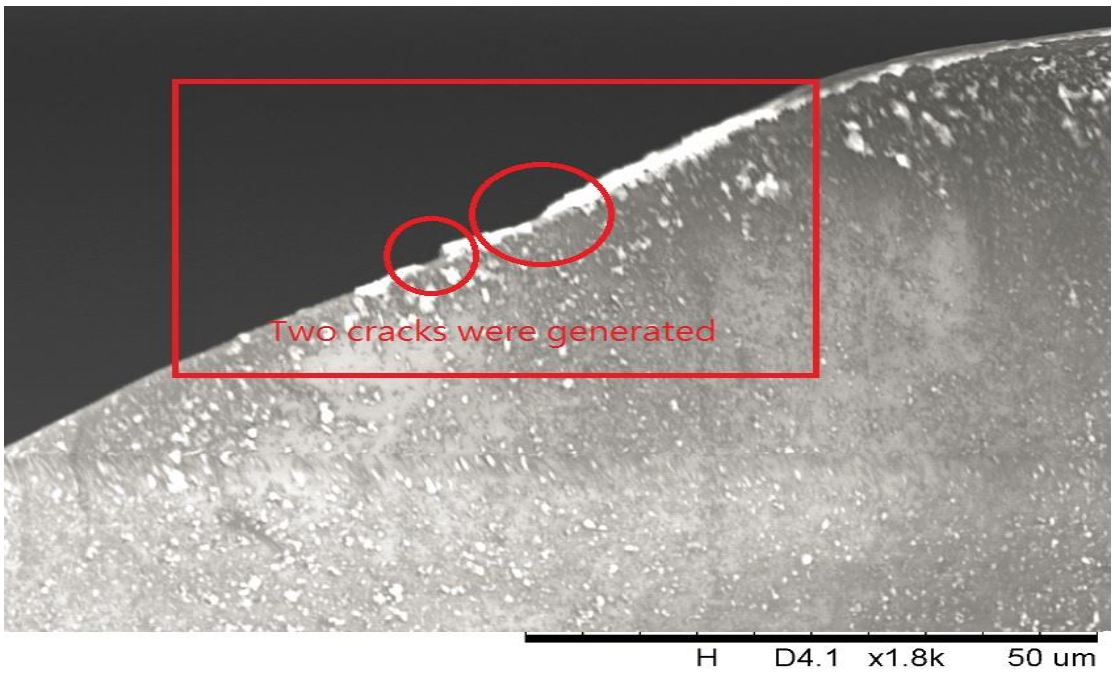

Figure 5.6 The closer viewer of defected area of cutting edge in Figure 5.5(d).

5.4.4 Analysis on flank wear and built up edge

Flank wear of both DNMFS and DMFS tools was examined. SEMs of flank faces of both tools are shown in Figures 5.7 and Figures 5.8. Incomplete removal of chip causes adhesion of chips on the rake face, giving rise to built-up edge. In addition, a rapid increase in the cutting temperature in the dry machining environment significantly reduces the strength of diamond tool and promotes the growth of built-up edge, which attributes to the plastic deformation of cutting edge. As the high cutting heat remained at the removal chips causes the built up edge formation, the built up edge formation is one of the indicators for evaluating the performance of magnetic field on transferring heat in dry SPDT. At the beginning cutting distance 75m, built up edge was discovered at the cutting edge of DNMFS tool as shown in Figure 5.8(a). When the diamond tool

edge moved along on the machined surface without lubricants, extremely high temperature remained in the removal chips, causing chip adhesion on the tool rake surface, forming as built up edge at the flank face of DNMFS tool. In the contrast to the DMFS tool, as the enhancement of thermal conductivity of titanium alloys in the presence of magnetic field, the chips were sheared away efficiently from the workpiece without sticking to the rake face, consequently built-up edge was minimized. Refer to Figure 8.7(a), there was no observation of built up edge on the flank surface of DMFS tool under the influence of magnetic field.

At the cutting distances 150m and 225m, for the DNMFS tool, adhesive wear developed quickly, a larger volume of titanium alloy was welded on the rake face which covered the whole cutting edge, an utilization of this degraded tool edge would lead to an unacceptable surface quality of machined surface. In the continuous turning process, the thickness of adhered materials successively increased, the newly melted titanium alloys plastically attached along the tool flank face, built up edge turned to become built up edge layer on the tool edge which displayed on the flank face of DNMFS tool as Figure 5.8(b) and 5.8(c). For the flank face of DMFS tool at the same cutting distance, the worn area in the tool edge was similar to that generated at the previous cutting distance 75m; only few growths of welded titanium alloys were on the tool edge but no built up edge was found, implying a lower amount of cutting heat at the tool/workpiece

interface, which reduced the volume of melted titanium alloys and caused a relatively low growth rate of titanium alloy adhesive layer.

At the final cutting distance 300m, for the DNMFS tool, as the cutting process was carried out for a longer time, built-up layer was continuously formed because the newly melted titanium alloys constantly welded on the tool edge. Because of this, the features of this built up layer was very similar to that at the cutting distances 150m - 225m. For the DMFS tool at the cutting distance 300m, under the influence of quick heat conduction by the magnetic field and the turning vibration reduction, fewer titanium alloys melted and were attached to the tool edge. Therefore, although the volume of adhesive titanium alloys increased, the adhesive materials only covered to the diamond tool edge partly, a part of tool edge was still uncovered with titanium alloys, it became as the smooth diamond edge which enabled to contribute to an effective cutting for the further turning processes, lengthening the utilization time of diamond tool for sustainable manufacturing.

To conclude, as the high cutting temperature and the friction force generated in the dry machining environment, built up edge started to form on the rake face of DNMFS tool at the beginning cutting distance 75m. The volume of adhesive materials was enlarged attached to the tool edge in the continuous turning. In the further cutting distance, built up edge was accumulated, the accumulative built up edge generated built

up layer which fully covered the tool edge. For the DMFS tool, under the influence of a magnetic field, there was no built up edge on the rake face at the beginning distance, only few adhesive titanium alloys were found at the cutting edge, and the volume of adhesive titanium alloys increased in a slow rate with the cutting distance increase. Even at the final cutting distance 300m, the tool edge was not covered fully by titanium alloys, there remained the fresh diamond tool edge which could contribute to the further turning process. The significances of flank wear and built up edge of DMFS tool were obviously lower than the DNMFS tool.

A common way of presenting flank wear is by the parameter VB, which is denoted as the maximum width of wear mark on the flank face. Figure 5.9 and Table 5.1 show the maximum flank wear width of DNMFS and DMFS tools, as the cutting depth in dry SPDT was 5μm, so the maximum flank wear width was accordingly small and in the micron range. Comparing VB between DNMFS and DMFS tools, VB of DNMFS tool was remarkably larger than the DMFS tool at the whole cutting distances 75m - 300m, particular to the longer cutting distance 300m, VB of DNMFS tool was even larger than that of DMFS about 123%. The above fully proved that flank wear of DMFS tool was successfully reduced by a magnetic field assistance.

Also, the slope of maximum flank wear width against the accumulative cutting distance was larger for the DNMFS tool, it showed that the adhesive rate of titanium

alloys in the presence of magnetic field was smaller than that in the absence of magnetic field, possibly caused by the decrease of cutting heat as well as the friction force. Increasing the cutting distance from 150m to 225m, the DNMFS tool showed a dramatic increase of maximum flank wear width, this was the signal that associated with the change in tool wear condition, integrating the information of Figures 5.5(b-d), the causes of dramatic increase of VB would be due to the cracks on the DNMFS tool. For the DMFS tool, as an effective heat transfer and a reduction of tool vibration, the maximum flank wear width displayed a steady growth with the accumulative cutting distance, the maximum flank wear width did not show a rapid increase throughout the whole cutting distances; it revealed the stable growth of adhesive materials on the tool edge without generating an obvious defect which was consistent with the results shown in Figure 5.4(a-d).

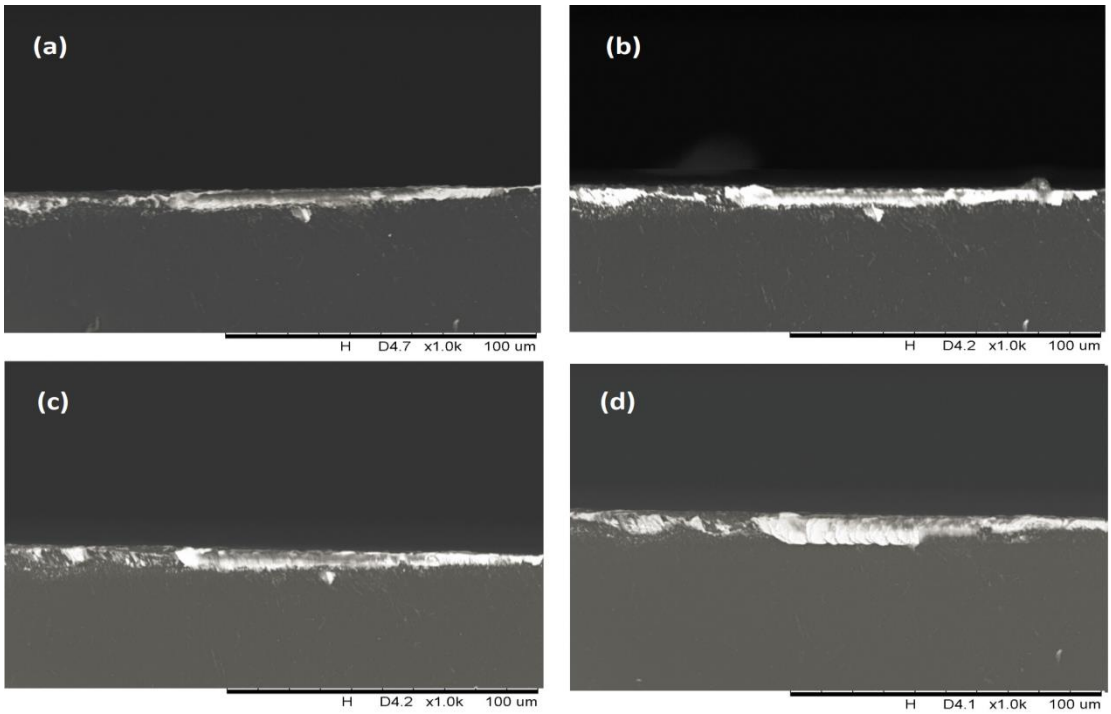

Figure 5.7 SEMs of the flank face of DMFS tool at cutting distance (a) 75m, (b) 150m, (c) 225m and (d) 300m.

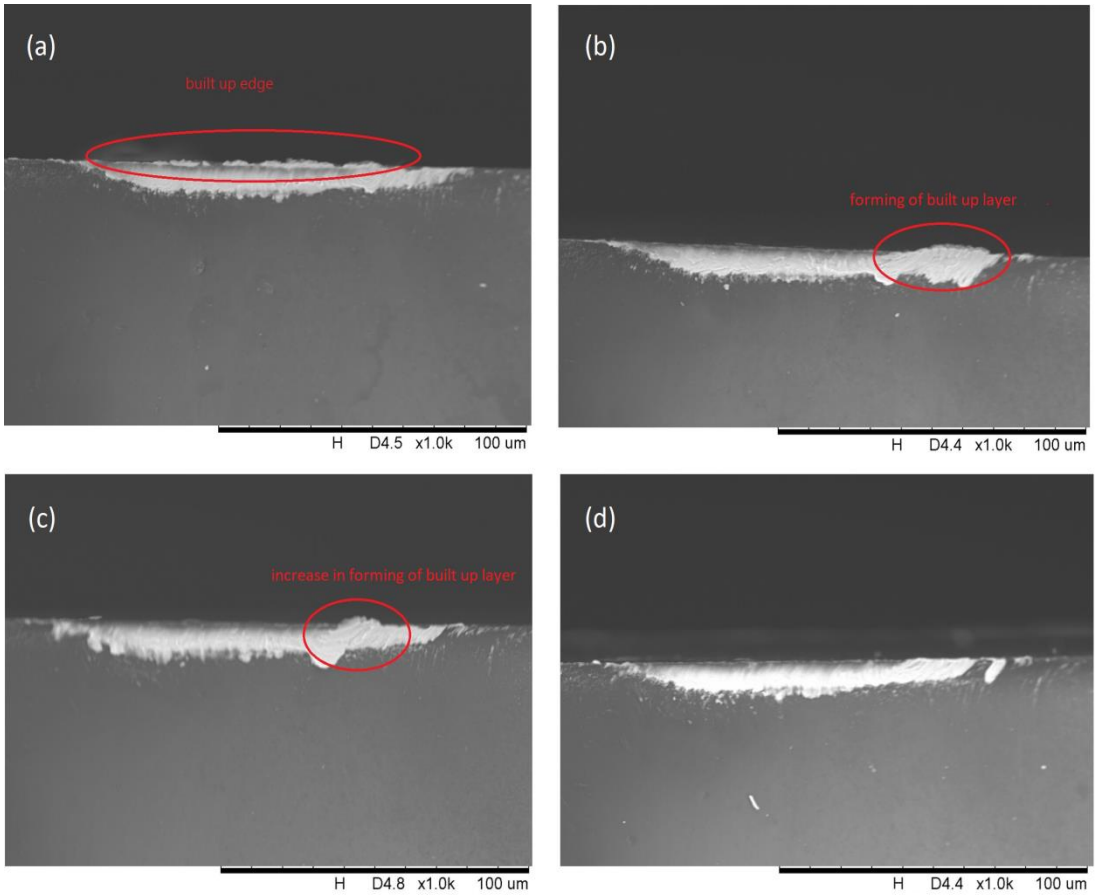

Figure 5.8 SEMs of the flank face of DNMFS tool at cutting distance (a) 75m, (b) 150m, (c) 225m and (d) 300m.

Table 5.1 The maximum flank wear width VB of DNMFS and DMFS tools at different cutting distances.

Cutting distance(m)	Maximum flank wear width VB (μm)	
	DMFS	DNMFS
75	5.16	11.2
150	5.46	12.4
225	6.5	15.5
300	8.6	19.2

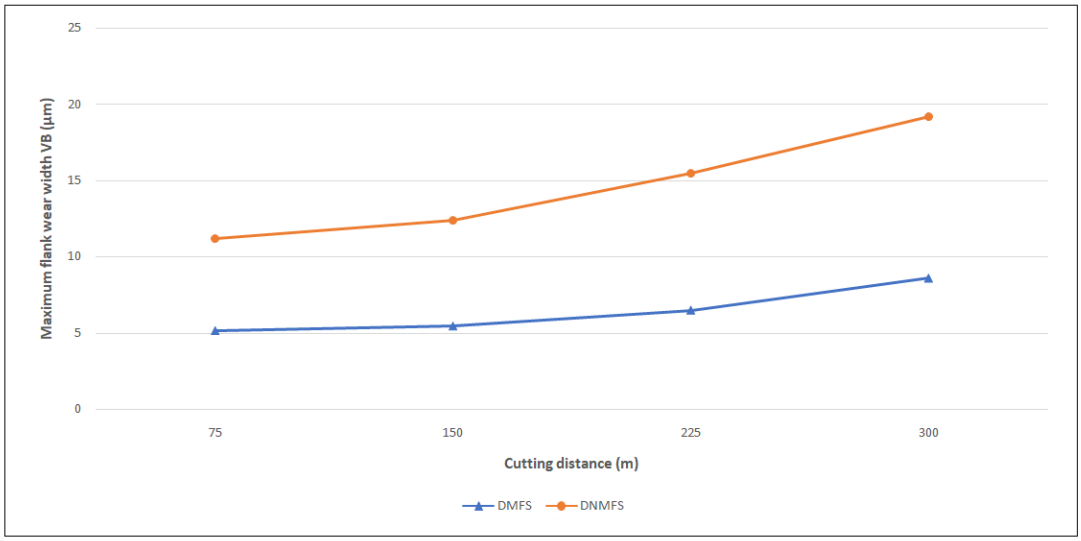

Figure 5.9 The maximum flank wear width of DNMFS and DMFS tools at different cutting distances.

5.4.5 Machined surface analysis

Researchers presented an advanced study about the significant impacts of tool wear on the surface integrity of machined surface, therefore, the machined surfaces by both DNMFS and DMFS tools were measured and are shown in Figures 5.10. Refer to

Figure 5.10(a), there were many uncut materials left on the machined surface of DNMFS. Uncut materials were randomly distributed on the machined surface and ragged above the average height of machined surface, leading the relatively poor surface finishing. In comparison to the machined surface of DMFS as shown in Figure 5.10(b), the machined surface displayed nearly none of uncut material which was far fewer than that of DNMFS, and the size of uncut materials was exceptionally small in contrast to that of DNMFS. Theoretically, the uncut materials on the turned surface are mainly due to the phase shift of tool vibration induced from the high cutting temperature and the friction force in machining processes, which is believed to intensify in the dry machining environment. The geometric illustration of generation of uncut materials and corresponding tool marks is shown in Figure 5.11. For an ideal turned profile, the diamond tool radius should be sufficiently large to generate continuous tool marks which offer small surface roughness without uncut materials. However, in the dry machining environment, the high cutting temperature and the friction force are resulted always and induce a high level of tool vibration. For the DNMFS generated in dry SPDT, diamond tool continuously shifted backward and forward due to the tool vibration. As a result, the end of two adjacent tool marks was not connected continuously, causing separations or overlaps of two adjacent tool marks. The overlapping adjacent tool marks provided excessive cuts of materials which caused the machined area below the average

surface height, which was indicated by the concave surface on the machined surface (the red circles in Figure 5.10(a)), while the separations of adjacent tool marks induced the ragged materials on the machined surface which were notified as the uncut materials on the machined surface (white circles in the Figure 5.10(a)). They contributed to poor surface finishing on the machined surface of DNMFS. In addition, the widths of tool mark of DNMFS were about 2.29μm - 3.16μm while that of DMFS was about 980nm. The widths of tool marks on the DMFS were reduced by 57.2% - 68.99% in comparison to the DNMFS. The better performance of surface integrity of DMFS proved the effectiveness of suppression tool vibration using an eddy current damping effect in dry SPDT, achieving a reduction of tool wear and an improvement the surface integrity simultaneously in dry SPDT under the magnetic field influence.

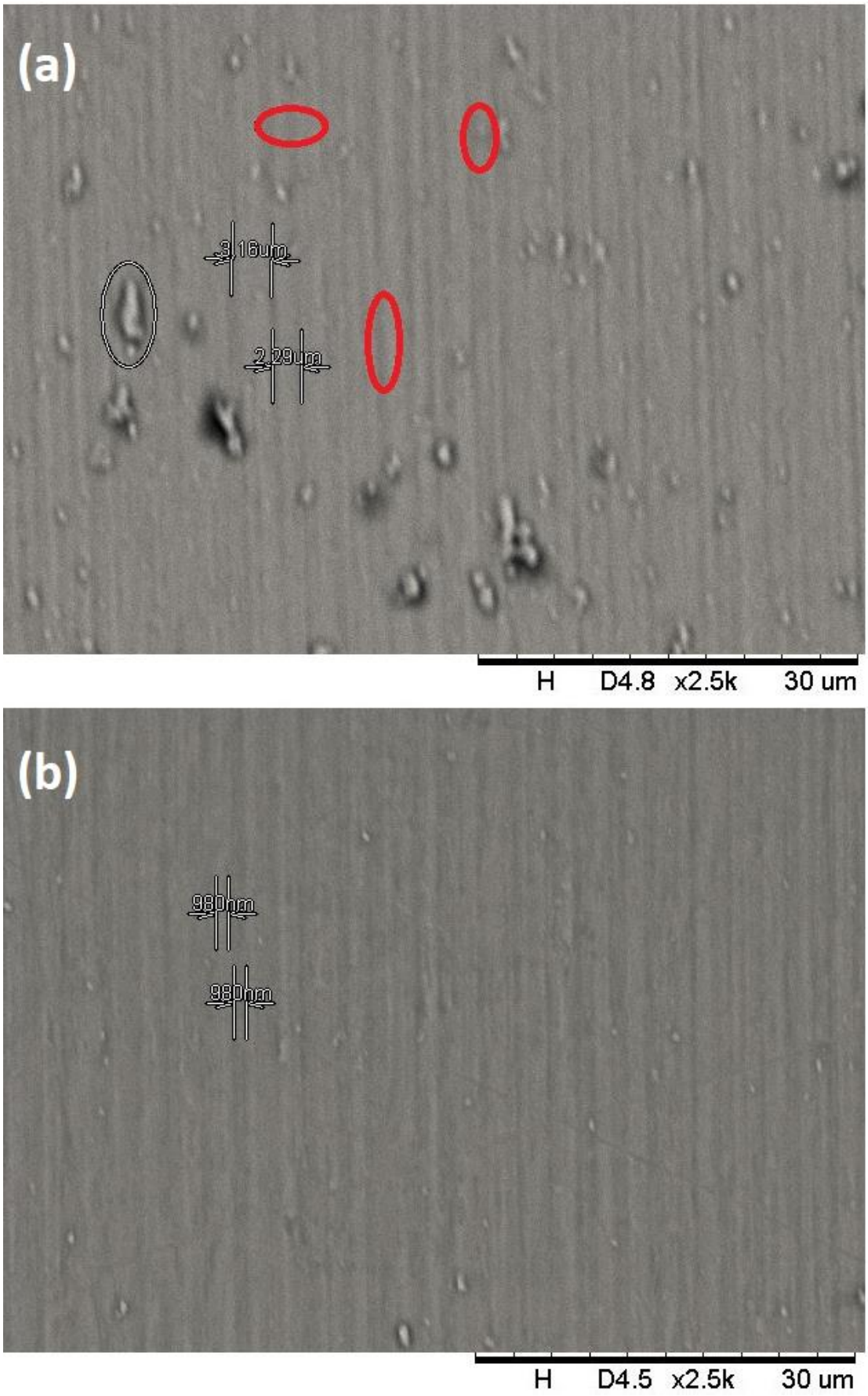

Figure 5.10 SEMs of turned surface of (a) DNMFS and (b) DMFS.

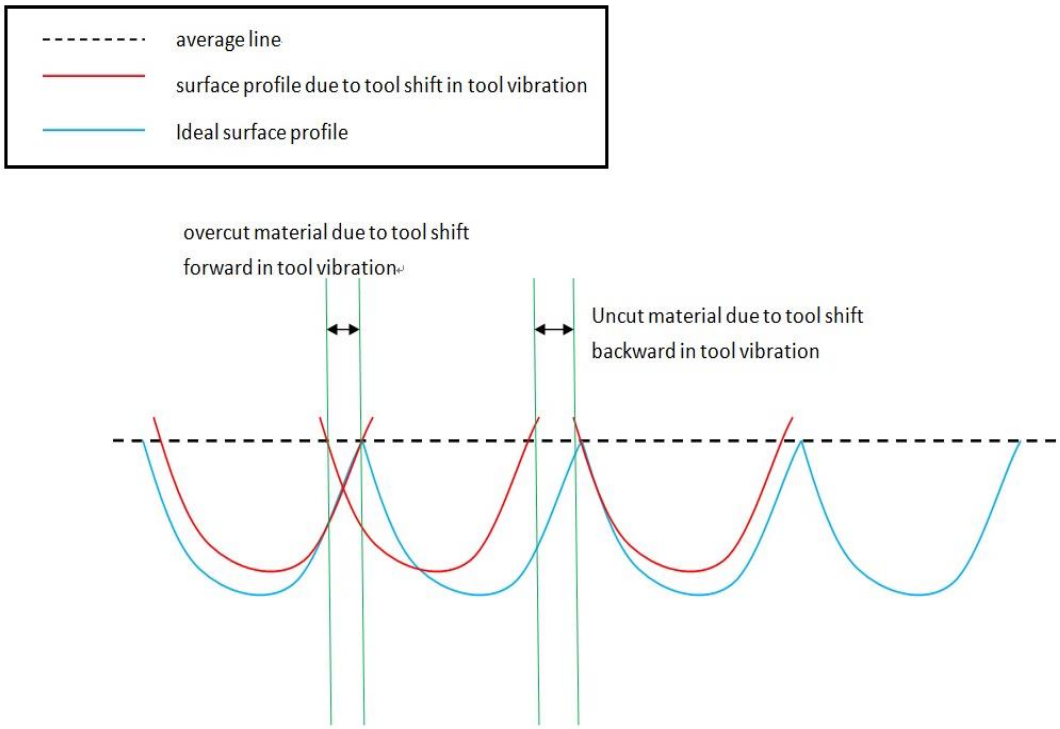

Figure 5.11 The illustration graph of tool shift induced by tool tip vibration in dry SPDT.

5.5 Summary

In this part of thesis, a novel machining technology was introduced, a magnetic field was firstly applied in dry SPDT of titanium alloys to reduce diamond tool wear. Normally, diamond tool wear was found to be much serious in dry machining of titanium alloys because of the combination effect of low thermal conductivity of materials and high cutting temperature in the dry machining environment. Through the experimental results, diamond tool in dry SPDT in the presence of magnetic field showed the lower degree of adhesive wear, built up edge, cracking and ragged/concave machined surface in comparison to that in the absence of magnetic field. The machining difficulties in term of serious tool wear and poor surface integrity in dry SPDT of

titanium alloys are minimized using the magnetic field and an eddy current damping effects, allowing the feasibility of dry SPDT of titanium alloys in the practical uses. Without employing complicated equipment, the proposed machining technology reduces the negative environmental impacts resulted from dry SPDT, simultaneously, the machined components of titanium alloys show the better surface integrity. The principle and the consequences of proposed machining technology on diamond tool wear in dry SPDT are summarized step by step in Figure 5.12. To conclude, few points below should be noted:

1. A rotating titanium alloys was placed in between of two permanent magnets in the experiments, the vibration amplitudes in dry SPDT shown in FFT were lowered under the influence of eddy current damping effect at all cutting distances, it proved the tool vibration was highly reduced using an eddy current damping effect.
2. Adhesive tool wear is the dominant wear mechanism in dry SPDT of titanium alloys because of the low thermal conductivity of titanium alloys. As the enhancement of thermal conductivity at the tool/workpiece interface in dry SDPT of titanium alloys in the presence of magnetic field, adhesive wear of diamond tool was overall minimized, no crack and built up edge was observed on the DMFS tool.
3. The maximum flank wear width of DNMFS tool was remarkably larger than

DMFS tool at the entire turning process, particular at the longer cutting distance 300m, the maximum flank wear of DNMFS tool was even larger than that of DMFS about 123%. The maximum flank wear width of diamond tool was largely reduced under the influence of magnetic field.

4. The machined surface generated in the absence of magnetic field displayed many uncut materials and concave area which were induced by the tool vibration. In comparison to the machined surface influenced by an eddy current damping effect, as a suppression of tool vibration, the amount of uncut materials and concave area showed fewer on the machined surface also, the widths of tool marks on the machined surface were much small. The surface integrity of machined titanium alloys in dry SPDT was highly enhanced in the presence of magnetic field.

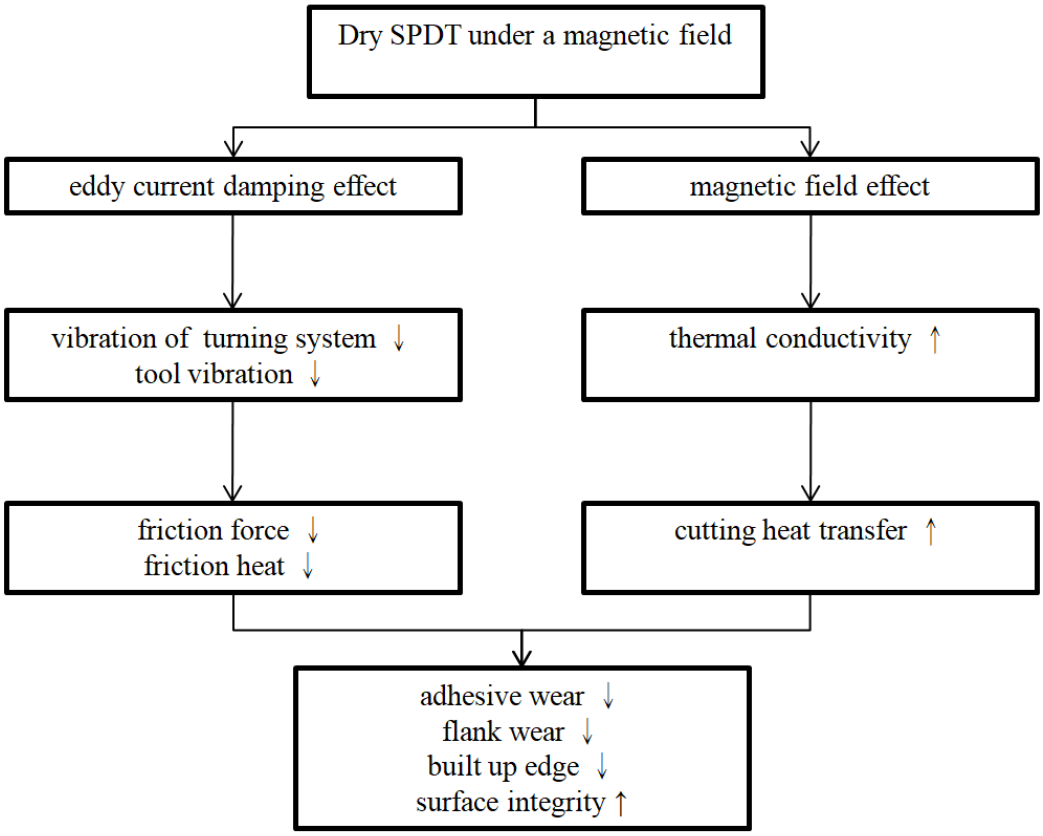

Figure 5.12 The principles and the consequences of proposed machining technology on diamond tool wear and surface integrity.

Chapter 6 Conclusions and suggestions for future studies

6.1 Conclusions

Because of the superior material properties of two phase titanium alloys Ti6Al4V including high strength-to-weight ratio and excellent corrosion resistance, they are intensively applied in the medical industry. They are valuable materials and the price of them is relatively higher than other traditional alloys as the considerable challenges on extracting or machining processes of these alloys. On the other hand, titanium alloys are well known difficult to cut materials especially in ultra-precision machining. The material properties of titanium alloys such as low thermal conductivity at the elevated temperature and low elastic modulus induce the extensive difficulties in the machining processes. The low thermal conductivity causes the trap of high cutting heat at the tool/workpiece interface in the machining processes; the cutting heat is unable to dissipate out from the machined surface effectively, as a result, the cutting heat is localized and concentrated at the cutting zone, which accelerates tool wear. Under the continuous machining process, the cutting heat is accumulated which the extremely high cutting heat and the friction heat affected the tool edge, causing early tool failure ultimately. Serious tool wear worsens the surface integrity consequently. As a result, the high level of tool wear and poor surface integrity are obtained, which compensate the precise effect in UPM, subsequently high machining costs are induced because of

rapid tool wear in UPM of titanium alloys. The precise machining of titanium alloys' components becomes unpractical because of the limitations of machining cost and machined surface quality.

On the other hand, environmental issues related to UPM are still in the progress stage, which there are needs of evolutional machining technology to minimize the negative impacts from UPM to the environment, and so the clean production can be integrated into UPM area. Utilizing of liquid lubricant with the heat dissipation effect had been proposed as an alternative to solve the problem of heat localization in machining of titanium alloys. Lubricants enforce the ability of heat transfer at the tool/workpiece interface to the surrounding environment. However, the validity of lubricants for heat dissipation is doubtful in ultra-precision machining, which literature reported the high level of diamond tool wear and unsatisfactory surface integrity remained existence in UPM of titanium alloys although lubricants use. All of the above imply that the environmental problems of machining titanium alloys still endure, the evolution of UPM of titanium alloys is needed for ensure the precise production of titanium alloys' components with a clean production condition simultaneously.

To upper the machinability and minimize the environmental impacts of titanium alloys in UPM, in this thesis, a novel machining technique, a magnetic field combined with UPM, was firstly introduced to deliver positive influences on the machining

outcomes in UPM of titanium alloys. In general, the low thermal conductivity of titanium alloys is the main source to cause the poor machinability of these valuable alloys, which the low thermal conductivity causes high cutting heat, a high machining vibration and s high level of tool wear. In response to the underlying source of poor machinability of titanium alloys and its subsequences, an application of magnetic field provides three major functions which aim to reduce the effectiveness of subsequences induced from the low thermal conductivity of titanium alloys. The three main contributions using the magnetic field influences in UPM are summarized as follow:

(1) The thermal expansion effect is directly proportional to the degree of heat absorption of the materials. The thermal expansion effect of the material increases with an increase in residual heat at the materials. Therefore, the thermal expansion effect is dominant and obvious for the materials with low thermal conductivity. Consequently, for titanium alloys with extremely low thermal conductivity, the thermal expansion effect of titanium alloys is intensified in the solidification process. The thermal expansion effect causes the problematic material swelling/recovery effect in UPM of titanium alloys. The resulting machined surface of titanium alloys in UPM is always high surface roughness and lack of form accuracy because of material swelling effect. The phenomenon of material swelling is related to the material properties, which the degree of recovery is proportional to

the coefficient of thermal expansion, they are unavoidable and uncontrollable unless titanium alloys are undergone a change of chemical composition or change of cutting parameters in machining processes. Therefore, a better machining approach should be adopted to fill up the research gap of minimizing the material swelling of titanium alloys.

A magnetic field places the effect directly on the localized heat source generated in UPM, which it enables to increase the thermal conductivity at the tool/workpiece interface. It is proven that thermal conductivity of nanofluid containing ferroparticles /magnetite particles could be enhanced in the presence of magnetic flied. In the presence of magnetic field, the magnetic dipolar energy inside the molecules is sufficient to come over the thermal energy, the ferroparticles inside the nanofluid align along with the direction of the external field as the positive value of magnetic susceptibility of ferroparticles. The aligned particles become chained structures, which are highly conductive paths for transferring heat. Under the same logic, the enhancement of thermal conductivity of materials in the presence of magnetic field could be extended to UPM of titanium alloys. The magnetic susceptibility of titanium alloys is 14.6ppm, which titanium alloys are paramagnetic materials. The reaction tendencies of titanium alloys toward the magnetic field exist as long as the magnetic field is presence. The magnetic moments of titanium alloys

enable to move in the presence of external magnetic field. Therefore, UPM of titanium alloys is befitted to the magnetic field assistance, which the thermal conductivity of titanium alloys is enhanced by forming the chained structures in the liquid state of melted titanium alloys in the UPM process. The highly conductive chained particles on the machined titanium alloys' surface dissipate the cutting heat effectively, the material swelling / recovery consequently is reduced under the condition of less heat energy inside the machined surface.

The magnetic field influence enables to suppress the material swelling by increasing the thermal conductivity at the tool/titanium alloys interface in UPM. The diamond cut surface under the magnetic field influence achieved the excellent surface roughness and form accuracy which mentioned in Chapter 4. Accuracy of cutting width, depth of cut and cutting radius of the machined groove was improved significantly under the magnetic field influence. The machined surface in the absence of magnetic field constituted almost 25% - 37% error between the assigned and actual results for all of the form accuracy indicators, while the machined titanium alloys' surface in the presence of magnetic field achieved under 4 percents error for all of these.

(2) Apart from the problematic high cutting temperature in UPM of titanium alloys, the machining vibration is another main factor that worsens the surface quality and

machining performance in UPM of titanium alloys.

The low thermal conductivity of titanium alloys causes the localized cutting heat at the cutting zone and a high level of material recovery on the machined surface, both of these adverse effects indirectly lead to a high degree of machining vibration as well as the tool tip vibration in UPM. Therefore, the suppression of machining vibration of titanium alloys becomes the main issue for enhancing the machining performance of titanium alloys.

In response to the machining vibration in UPM, an eddy current damping effect which is generated by the magnetic field influence is applied into suppressing the vibration amplitude and vibration energy in SPDT. Once a conductive material rotates or moves within a magnetic field, an eddy current is generated through the stationary magnetic field inside the conductor. The generated eddy current further creates its own magnetic field with the direction opposite to the applied magnetic field, it causes the repulsive force with the opposite direction to the movement of rotational metal. The repulsive force is called Lorentz force which increases with the rotational velocity of conductive metal. In SPDT of titanium alloys, titanium alloys rotate in order to provide the interactive motion for the material removal process by the diamond tool. The material properties of conductivity of titanium alloys and the characteristics of rotational motion in SPDT could be utilized

integrally for generating an eddy current damping effect, which suppresses the machining vibration in SPDT. An eddy current damping has never been applied in the machining area especially in UPM to provide exceptional effects to increase the machining performance of difficult to cut materials in SPDT. In Chapter 3 of this thesis, it reported the application of eddy current damping effect on SPDT. A magnetic field was superimposed into rotating titanium alloys in SPDT in order to suffer the influence of an eddy current damping effect. The effects of eddy current damping on SPDT were investigated in the thesis. By employing the eddy current damping effect in SPDT, the suppression of cutting force variation, the continuous chip formation and the reduction of adhesive tool wear were achieved successfully in comparison to normal SPDT, which all are the signal of enhancing machinability of titanium alloys in UPM. Under the influence of eddy current damping effect, the machining vibration as well as the tool vibration of SPDT of titanium alloys is highly suppressed. The surface integrity of machined surface under an eddy current effect is also enhanced too.

According to the experimental results, the maximum vibration amplitude of nonmagnetic sample in the particular frequency in FFT showed 87.2% higher than that of magnetic sample. The total vibration energy of non-magnetic sample was up to 25.3% higher than that of magnetic sample. For the chip formation, the length of

chip generated from the magnetic sample was surprisingly long while the powder and fragment chips were formed for the nonmagnetic sample. On the other hand, the cutting force variation of magnetic sample was found to be smaller than that of nonmagnetic sample, which there was no dramatic increase/decrease of thrust force throughout the whole turning process for the magnetic sample. The particular area of surface roughness of the magnetic sample achieved to 9nm, which achieved the requirement of nano-surface generation. Average surface roughness of magnetic sample was 13nm which was relatively higher than that of nonmagnetic sample. Furthermore, tool life of nonmagnetic sample tool was 79.4mins in SPDT of titanium alloys only, which was lower than that of magnetic sample tool. The effectiveness of an eddy damping current effect on improving the machinability of titanium alloys in SPDT is proven experimentally in this thesis.

(3) The environmental issue related to machining is always concerned by the public. Especially for UPM of titanium alloys, a high level of tool wear and ineffectiveness of using traditional lubricants in machining processes intensified the negative effects to the environment brought from the machining processes. Dry machining is one of the important green machining technologies to minimize the damages from machining processes. However, under the condition of absence of lubricant, a high amount of heat energy and friction force are generated in machining processes

which speed up tool wear and worsen the surface integrity. With the material properties of low thermal conductivity of titanium alloy, dry SPDT of titanium alloys is nearly infeasible as it further promotes the damage of diamond tool which finally deteriorates the surface integrity, making unacceptable of surface quality and inevitably high machining costs. In this thesis, a magnetic field is utilized to resolve the mentioned impacts induced from dry UPM to the environment. In this thesis. titanium alloys would be undergone SPDT in dry machining environment under the magnetic field influence, aiming to provide the guideline for the feasibility of dry SPDT of difficult to cut materials.

In chapter 5 of the thesis, it reported about the investigation of machinability of titanium alloys in dry SPDT experimentally. A rotating titanium alloy was placed in between of two magnets in dry SPDT in order to suffer from an eddy current damping effect and a magnetic field effect. Under the influences of magnetic field and eddy current damping effects, even for the relatively long cutting distance 300m in the dry machining environment, the maximum peak amplitude of machining vibration of magnetic sample was only 0.00142N, which was only 0.36 time of that of non magnetic sample.

The experimental results showed the reductions of adhesive wear, flank wear and built up edge of tool as well as the machining vibration during dry SPDT. Adhesive

tool wear is the dominant wear mechanism in dry SPDT of titanium alloys because of the low thermal conductivity of titanium alloys. As the enhancement of thermal conductivity at the tool/workpiece interface in dry SDPT in the presence of magnetic field, adhesive wear of diamond tool was overall minimized, no crack and built up edge was observed on the magnetic sample tool. On the other hand, the maximum flank wear of magnetic sample tool was only 0.81 time of nonmagnetic sample tool at the relatively long cutting distance. Also, the surface integrity of machined titanium alloys in dry machining environment showed excellent; the uncut materials and concave area on the machined surface reduced, which are the evidence of vibration suppression of dry SPDT using an eddy current damping effect and the magnetic field influence.

The machining performances of titanium alloys in dry SPDT were facilitated in term of tool life and surface integrity by using a magnetic field, showing a feasibility of environmental friendly dry SPDT of titanium alloys in practical applications for sustainable manufacturing. In this thesis, SPDT is firstly implemented in the dry environment and reported as successful improvements in term of tool life and surface quality. This part of thesis can be treated as an instruction for implementing dry cutting in UPM, providing the direction of green production for precise products in the future.

6.2 Suggestions for the future work

The researches in this thesis provide all around investigations including theoretical and experimental basis of magnetic field assisted UPM. The utilization of magnetic field in UPM could be further extended to deliver other positive machining outcomes in UPM. The suggestions for the future work related to magnetic field assisted UPM are:

(1) The feasibility of machining materials in the proposed machining technology are not limited to ferromagnetic and paramagnetic materials. The proposed machining technology can even be extended to nonmagnetic/anti-ferromagnetic materials. Non-magnetic materials such as bulk metallic glass is planned to utilize the magnetic field influence to improve the its machinability. A thin film made by magnetic materials will be pre-coated on the workpiece so that the surface of workpiece acts positively toward a magnetic field. The coated magnetic film acts toward a magnetic field positively and thus the positive magnetic field effects could effectively influence the non magnetic workpiece. The potential materials for coating of non magnetic materials in the proposed machining technology are copper and aluminium.

(2) Researchers have investigated deeply about artificial and functional surfaces. They normally use the approach of altering the weighting of chemical elements of molecules and metals, which supports the fabrication of the novel structures. The

fabrication methods of those artificial and functional surfaces include: imprinting, self-assembly and etching. However, the precise levels of fabricated nanostructures/microstructures by the existing techniques are still not satisfied in the aspect of hierarchical level. Therefore, a new fabrication approach should be adapted which aims to generate nanostructures/microstructures precisely and independently.

With the effectiveness of uplifting the machining performance and machinability of machined materials using a magnetic field, some micro-patterns are planned to fabricate under the magnetic field to increase form accuracy and the precise level of the micro patterns. The machined micro-patterns are expected to have minimum bur and high form accuracy under the suppressions of machining vibration and cutting heat localization at the tool/workpiece interface in the presence of magnetic field. Hierarchical structures, superhydrophobic surfaces, microdot array and other bio-inspiration surfaces are planned to fabricate by UPM under the magnetic field influence.

References

Altan, C. L., Elkatmis, A., Yüksel, M., Aslan, N., Bucak, S. (2011). Enhancement of thermal conductivity upon application of magnetic field to Fe3O4 nanofluids. Journal of Applied Physics, 110(9), 093917.

American National Standards Institute. (1986). Tool Life Testing with Single-point Turning Tools. American Society of Mechanical Engineers.

Bae, J. S., Kwak, M. K., Inman, D. J. (2005). Vibration suppression of a cantilever beam using eddy current damper. Journal of Sound and Vibration, 284(3), 805-824.

Bai, J., Bai, Q., Tong, Z., Hu, C., He, X. (2016). Evolution of surface grain structure and mechanical properties in orthogonal cutting of titanium alloy. Journal of Materials Research, 31(24), 3919-3929.

Barry, J., Byrne, G. (2002). The mechanisms of chip formation in machining hardened steels. Journal of Manufacturing Science and Engineering, 124(3), 528-535.

Bayoumi, A. E., Xie, J. Q. (1995). Some metallurgical aspects of chip formation in cutting Ti-6Al-4V alloy. Materials Science and Engineering: A, 190(1), 173-180

Bhatt, A., Attia, H., Vargas, R., Thomson, V. (2010). Wear mechanisms of WC coated and uncoated tools in finish turning of Inconel 718. Tribology International, 43(5), 1113-1121.

Bomberger, H. B., Froes, F. H. (1984). The melting of titanium. JOM, 36(12), 39-47.

Bordin, A., Bruschi, S., Ghiotti, A., & Bariani, P. F. (2015). Analysis of tool wear in cryogenic machining of additive manufactured Ti6Al4V alloy. Wear, 328, 89-99.

Brinksmeier, E., Mutlugünes, Y., Klocke, F., Aurich, J. C., Shore, P., Ohmori, H. (2010). Ultra-precision grinding. CIRP Annals-Manufacturing Technology, 59(2), 652-671

Cadwell, L. H. (1996). Magnetic damping: analysis of an eddy current brake using an airtrack. American journal of physics, 64(7), 917-923.

Calamaz, M., Coupard, D., Girot, F. (2008). A new material model for 2D numerical simulation of serrated chip formation when machining titanium alloy Ti–6Al–4V. International Journal of Machine Tools and Manufacture, 48(3), 275-288.

Che-Haron, C. H. (2001). Tool life and surface in turning titanium alloy. Journal of Materials Processing Technology, 118(1), 231-237.

Chen, W., Jiang, J., Liu, J., Bai, S., Chen, W. (2013). A passive eddy current damper for vibration suppression of a force sensor. Journal of Physics D: Applied Physics, 46(7), 075001.

Chen, X., Rowe, W. B., Cai, R. (2002). Precision grinding using CBN wheels. International Journal of Machine Tools and Manufacture, 42(5), 585-593

Chen, Y. H., Lee, Y. S., Fang, S. C. (1998). Optimal cutter selection and machining plane determination for process planning and NC machining of complex surfaces. Journal of Manufacturing Systems, 17(5), 371-388.

Cheng, C. P., Wu, K. L., Mai, C. C., Hsu, Y. S., Yan, B. H. (2010). Magnetic field-assisted electrochemical discharge machining. Journal of Micromechanics and Microengineering, 20(7), 075019.

Cheung, C. F., Kong, L. B., Ho, L. T., To, S. (2011). Modelling and simulation of structure surface generation using computer controlled ultra-precision polishing. Precision Engineering, 35(4), 574-590

Cheung, C. F., Lee, W. B. (2000a). A theoretical and experimental investigation of surface roughness formation in ultra-precision diamond turning. International Journal of Machine Tools and Manufacture, 40(7), 979-1002.

Cheung, C. F., Lee, W. B. (2000b). Study of factors affecting the surface quality in ultra-precision diamond turning. Materials and Manufacturing Processes, 15(4), 481-502.

Choi, E. S., Brooks, J. S., Eaton, D. L., Al-Haik, M. S., Hussaini, M. Y., Garmestani, H., Li, D., Dahmen, K. (2003). Enhancement of thermal and electrical properties of carbon nanotube polymer composites by magnetic field processing. Journal of Applied physics, 94(9), 6034-6039.

Colafemina, J. P., Jasinevicius, R. G., Duduch, J. G. (2007). Surface integrity of ultra-precision diamond turned Ti (commercially pure) and Ti alloy (Ti-6Al-4V). Proceedings of the Institution of Mechanical Engineers, Part B: Journal of Engineering Manufacture, 221(6), 999-1006.

Da Silva, R. B., Machado, Á. R., Ezugwu, E. O., Bonney, J., Sales, W. F. (2013). Tool life and wear mechanisms in high speed machining of Ti–6Al–4V alloy with PCD tools under various coolant pressures. Journal of Materials Processing Technology, 213(8), 1459-1464.

Davis, L. C., Reitz, J. R. (1971). Eddy currents in finite conducting sheets. Journal of Applied Physics, 42(11), 4119-4127.

Davoodi, B., Tazehkandi, A. H. (2014). Experimental investigation and optimization of cutting parameters in dry and wet machining of aluminum alloy 5083 in order to remove cutting fluid. Journal of cleaner production, 68, 234-242.

Dearnley, P. A., Grearson, A. N. (1986). Evaluation of principal wear mechanisms of cemented carbides and ceramics used for machining titanium alloy IMI 318. Materials Science and Technology, 2(1), 47-58.

Devillez, A., Le Coz, G., Dominiak, S., Dudzinski, D. (2011). Dry machining of Inconel 718, workpiece surface integrity. Journal of Materials Processing Technology, 211(10), 1590-1598.

Devillez, A., Lesko, S., Mozer, W. (2004). Cutting tool crater wear measurement with white light interferometry. Wear, 256(1), 56-65.

Dhar, N. R., Kamruzzaman, M., Ahmed, M. (2006). Effect of minimum quantity lubrication (MQL) on tool wear and surface roughness in turning AISI-4340

steel. Journal of materials processing technology, 172(2), 299-304.

Ebrahimi, B., Khamesee, M. B., Golnaraghi, F. (2010). Permanent magnet configuration in design of an eddy current damper. *Microsystem Technologies*, 16(1-2), 19.

El Mansori, M., Pierron, F., Paulmier, D. (2003). Reduction of tool wear in metal cutting using external electromotive sources. Surface and Coatings Technology, 163, 472-477.

Elbuken, C., Khamesee, M. B., Yavuz, M. (2006). Eddy current damping for magnetic levitation: downscaling from macro-to micro-levitation. Journal of Physics D: Applied Physics, 39(18), 3932.

Ezugwu, E. O., Bonney, J., Yamane, Y. (2003). An overview of the machinability of aeroengine alloys. Journal of materials processing technology, 134(2), 233-253.

Ezugwu, E. O., Wang, Z. M. (1997). Titanium alloys and their machinability—a review. Journal of materials processing technology, 68(3), 262-274.

Fan, Y., Hao, Z., Lin, J., Yu, Z. (2015). New observations on tool wear mechanism in machining Inconel 718 under water vapor+ air cooling lubrication cutting conditions. Journal of Cleaner Production, 90, 381-387.

Fan, Y. H., Zheng, M. L., Zhang, D. Q., Yang, S. C., Cheng, M. M. (2011). Static and Dynamic Characteristic of Cutting Force when High-Efficiency Cutting Ti-6Al-4V. In Advanced materials research (Vol. 305, pp. 122-128). Trans Tech Publications.

Fan, Z., Wang, T., Zhong, L. (2004). The mechanism of improving machining accuracy of ECM by magnetic field. Journal of materials processing technology, 149(1), 409-413.

Fang, F. Z., Liu, X. D., & Lee, L. C. (2003). Micro-machining of optical glasses—A review of diamond-cutting glasses. Sadhana, 28(5), 945-955.

Ferreira, J. M., Maple, M. B., Zhou, H., Hake, R. R., Lee, B

. W., Seaman, C. L., Kuric, M. V., Guertin R. P. (1988). Magnetic field alignment of high-T c superconductorsRBa 2 Cu 3 O 7–δ (R= rare earth). Applied Physics A: Materials Science & Processing, 47(1), 105-110.

Gavili, A., Zabihi, F., Isfahani, T. D., Sabbaghzadeh, J. (2012). The thermal conductivity of water base ferrofluids under magnetic field. Experimental Thermal and Fluid Science, 41, 94-98.

Genta, G., Delprete, C., Tonoli, A., Rava, E., Mazzocchetti, L. (1992). Analytical and experimental investigation of a magnetic radial passive damper.

Ghofrani, A., Dibaei, M. H., Sima, A. H., Shafii, M. B. (2013). Experimental investigation on laminar forced convection heat transfer of ferrofluids under an alternating magnetic field. Experimental Thermal and Fluid Science, 49, 193-200.

Goel, S., Luo, X., Reuben, R. L. (2013). Wear mechanism of diamond tools against single crystal silicon in single point diamond turning process. Tribology

International, 57, 272-281

Gómez-Parra, A., Álvarez-Alcón, M., Salguero, J., Batista, M., Marcos, M. (2013). Analysis of the evolution of the Built-Up Edge and Built-Up Layer formation mechanisms in the dry turning of aeronautical aluminium alloys. Wear, 302(1), 1209-1218.

Gonnet, P., Liang, Z., Choi, E. S., Kadambala, R. S., Zhang, C., Brooks, J. S., Wang, B., Kramer, L. (2006). Thermal conductivity of magnetically aligned carbon nanotube buckypapers and nanocomposites. Current Applied Physics, 6(1), 119-122.

Gosline, A. H., Hayward, V. (2008). Eddy current brakes for haptic interfaces: Design, identification, and control. IEEE/ASME Transactions on Mechatronics, 13(6), 669-677.

Han, Z., Fina, A. (2011). Thermal conductivity of carbon nanotubes and their polymer nanocomposites: a review. Progress in polymer science, 36(7), 914-944.

Hayes, F. H., Bomberger, H. B., Froes, F. H., Kaufman, L., Burte, H. M. (1984). Advances in titanium extraction metallurgy. JOM, 36(6), 70-76.

Heald, M. A. (1988). Magnetic braking: Improved theory. American journal of physics, 56(6), 521-522.

Horton, M., Hong, H., Li, C., Shi, B., Peterson, G. P., Jin, S. (2010). Magnetic alignment of Ni-coated single wall carbon nanotubes in heat transfer nanofluids. Journal of Applied Physics, 107(10), 104320.

Hu, L. H., Zhou, M. (2016). Experimental Study on the Wear of Single Crystal Diamond Tools in Ultra-Precision Cutting of Titanium Alloy. Key Engineering Materials, 693, 1015.

Huang, C.Vilar, R., Shen, J. (2012). Dry sliding wear behavior of laser clad TiVCrAlSi high entropy alloy coatings on Ti–6Al–4V substrate. Materials & Design, 41, 338-343.

Huang, C. Z., Wang, J., Feng, Y. X., Zhu, H. T. (2006). Recent development of abrasive water jet machining technology. Key Engineering Materials, 315, 396-400.

Ikawa, N., Donaldson, R. R., Komanduri, R., König, W., McKeown, P. A., Moriwaki, T., Stowers, I. F. (1991). Ultraprecision metal cutting—the past, the present and the future. CIRP Annals-Manufacturing Technology, 40(2), 587-594.

Jackson, M. J., Novakov, T., Whitfield, M., Robinson, G., Handy, R., Sein, H., Ahmed, W. (2017). VFCVD diamond-coated cutting tools for micro-machining titanium alloy Ti6Al4V. The International Journal of Advanced Manufacturing Technology, 1-38.

Jasinevicius, R. G., De Campos, G. P., Montanari, L., Tsukamoto, R., Garcia, J. P., Camargo, R., Duduch, J. G., Porto, A. J. V. (2003). Influence of the mechanical and metallurgical state of an Al-Mg alloy on the surface integrity in ultraprecision machining. Journal of the Brazilian Society of Mechanical Sciences and Engineering, 25(3), 222-228.

Jawaid, A., Che-Haron, C. H., & Abdullah, A. (1999). Tool wear characteristics in

turning of titanium alloy Ti-6246. Journal of Materials Processing Technology, 92, 329-334.

Jia, P., Zhou, M. (2012). Tool wear and its effect on surface roughness in diamond cutting of glass soda-lime. Chinese Journal of Mechanical Engineering, 25(6), 1224-1230.

Joshi, S., Govindan, P., Malshe, A., Rajurkar, K. (2011). Experimental characterization of dry EDM performed in a pulsating magnetic field. CIRP Annals-Manufacturing Technology, 60(1), 239-242.

Jou, M., Shiau, J. K., & Sun, C. C. (2006). Design of a magnetic braking system. Journal of Magnetism and Magnetic Materials, 304(1), e234-e236.

Kainuma, R., Imano, Y., Ito, W., Sutou, Y., Morito, H., Okamoto, S., Fujita, A., Kanomata, T., Ishida, K. (2006). Magnetic-field-induced shape recovery by reverse phase transformation. Nature, 439(7079), 957-960.

Karakoc, K., Suleman, A., Park, E. J. (2014). Optimized braking torque generation capacity of an eddy current brake with the application of time-varying magnetic fields. IEEE Transactions on Vehicular Technology, 63(4), 1530-1538.

Karnopp, D. (1989). Permanent magnet linear motors used as variable mechanical dampers for vehicle suspensions. Vehicle System Dynamics, 18(4), 187-200.

Khettabi R, Fatmi L, Masounave J, Songmene V. (2013) On the micro and nanoparticle

emission during machining of titanium and aluminum alloys. CIRP J Manufacturing Sci Technology 6:175–180

Kikuchi, M. (2009). The use of cutting temperature to evaluate the machinability of titanium alloys. Acta biomaterialia, 5(2), 770-775.

Komanduri, R., Von Turkovich, B. F. (1981). New observations on the mechanism of chip formation when machining titanium alloys. Wear, 69(2), 179-188.

Kong, L. B., Cheung, C. F., To, S., Lee, W. B. (2009). An investigation into surface generation in ultra-precision raster milling. Journal of materials processing technology, 209(8), 4178-4185.

Kong, M. C., Lee, W. B., Cheung, C. F., To, S. (2006). A study of materials swelling and recovery in single-point diamond turning of ductile materials. Journal of materials processing technology, 180(1), 210-215.

Kopač, J., Šali, S. (2001). Tool wear monitoring during the turning process. Journal of Materials Processing Technology, 113(1), 312-316.

Lajvardi, M., Moghimi-Rad, J., Hadi, I., Gavili, A., Isfahani, T. D., Zabihi, F., Sabbaghzadeh, J. (2010). Experimental investigation for enhanced ferrofluid heat transfer under magnetic field effect. Journal of Magnetism and Magnetic Materials, 322(21), 3508-3513.

Lee, E. C., Nian, C. Y., Tarng, Y. S. (2001). Design of a dynamic vibration absorber

against vibrations in turning operations. Journal of Materials Processing Technology, 108(3), 278-285.

Lee, K., Park, K. (1999). Optimal robust control of a contactless brake system using an eddy current. Mechatronics, 9(6), 615-631.

Li, C. J., Li, Y., Gao, X., Duong, C. V. (2014). Ultra-precision machining of Fresnel lens mould by single-point diamond turning based on axis B rotation. The International Journal of Advanced Manufacturing Technology, 1-7.

Li, G. R., Li, Y. M., Wang, F. F., Wang, H. M. (2015). Microstructure and performance of solid TC4 titanium alloy subjected to the high pulsed magnetic field treatment. Journal of Alloys and Compounds, 644, 750-756.

Li, H. Y., Liu, J., Lajvardi, M., Gavili, A., Zabihi, F., Isfahani, T. D., Hadi, I., Sabbaghzadeh, J. Mechanical Engineering Series-Enhanced Heat Transfer-Vol. 1. Science Network, 2012

Li, N., Chen, Y., Kong, D., Tan, S. (2017). Experimental investigation with respect to the performance of deep submillimeter-scaled textured tools in dry turning titanium alloy Ti-6Al-4V. Applied Surface Science, 403, 187-199.

Lin, Y. C., Lee, H. S. (2008). Machining characteristics of magnetic force-assisted EDM. International journal of machine tools and manufacture, 48(11), 1179-1186.

Liu, C. Y., Jiang, K. J., Zhang, Y. (2011). Design and use of an eddy current retarder in

an automobile. International Journal of Automotive Technology, 12(4), 611-616.

Liu, K., Melkote, S. N. (2006). Effect of plastic side flow on surface roughness in micro-turning process. International Journal of Machine Tools and Manufacture, 46(14), 1778-1785.

Liu, X., Chu, P. K., Ding, C. (2004). Surface modification of titanium, titanium alloys, and related materials for biomedical applications. Materials Science and Engineering: R: Reports, 47(3), 49-121.

Long, L., Baoji, M. A., Ruifeng, W., Lingqi, D. (2017). The coupled effect of magnetic field, electric field, and electrolyte motion on the material removal amount in electrochemical machining. The International Journal of Advanced Manufacturing Technology, 1-12.

Lu, X., Zhang, Q., Weng, D., Zhou, Z., Wang, S., Mahin, S. A., Ding, S., Qian, F. (2017). Improving performance of a super tall building using a new eddy-current tuned mass damper. Structural Control and Health Monitoring, 24(3).

Lütjering, G. (1998). Influence of processing on microstructure and mechanical properties of (α+ β) titanium alloys. Materials Science and Engineering: A, 243(1), 32-45.

Malhotra, R., Saxena, I., Ehmann, K., Cao, J. (2013). Laser-induced plasma micro-machining (LIPMM) for enhanced productivity and flexibility in laser-based micro-

machining processes. CIRP Annals-Manufacturing Technology, 62(1), 211-214.

Matsuzaki, Y., Ishikubo, D., Kamita, T., Ikeda, T. (1997). Vibration control system using electromagnetic forces. Journal of Intelligent Material Systems and Structures, 8(9), 751-756.

Maurotto, A., Siemers, C., Muhammad, R., Roy, A., Silberschmidt, V. (2014). Ti alloy with enhanced machinability in UAT turning. Metallurgical and Materials Transactions A, 45(6), 2768-2775.

Nagaya, K., Kojima, H., Karube, Y., Kibayashi, H. (1984). Braking forces and damping coefficients of eddy current brakes consisting of cylindrical magnets and plate conductors of arbitrary shape. IEEE Transactions on Magnetics, 20(6), 2136-2145.

Narutaki, N., Murakoshi, A., Motonishi, S., Takeyama, H. (1983). Study on machining of titanium alloys. CIRP Annals-Manufacturing Technology, 32(1), 65-69.

Nicholas, D. J., Boon, J. E. (1981). The generation of high precision aspherical surfaces in glass by CNC machining. Journal of Physics D: Applied Physics, 14(4), 593.

Niinomi, M. (1998). Mechanical properties of biomedical titanium alloys. Materials Science and Engineering: A, 243(1), 231-236.

Niinomi M (2003) Recent research and development in titanium alloys for biomedical applications and healthcare goods. Sci Technol Adv Mater 4:445–454

Nkurikiyimfura, I., Wang, Y., & Pan, Z. (2013). Heat transfer enhancement by magnetic

nanofluids—a review. Renewable and Sustainable Energy Reviews, 21, 548-561.

Nogawa, H. (1988). Ceramics Processing: State of the Art of R & D in Japan. ASM International, Metals Park, Ohio 44073, USA, 1988.

Odenbach, S. (2003). Ferrofluids—magnetically controlled suspensions. Colloids and Surfaces A: Physicochemical and Engineering Aspects, 217(1), 171-178.

Oliaei, S. N. B., Karpat, Y. (2016). Investigating the influence of built-up edge on forces and surface roughness in micro scale orthogonal machining of titanium alloy Ti6Al4V. Journal of Materials Processing Technology, 235, 28-40.

Pa, P. S. (2009). Super finishing with ultrasonic and magnetic assistance in electrochemical micro-machining. Electrochimica Acta, 54(25), 6022-6027.

Parekh, K., Lee, H. S. (2010). Magnetic field induced enhancement in thermal conductivity of magnetite nanofluid. Journal of Applied Physics, 107(9), 09A310.

Park, K. H., Beal, A., Kwon, P., Lantrip, J. (2011). Tool wear in drilling of composite/titanium stacks using carbide and polycrystalline diamond tools. Wear, 271(11), 2826-2835.

Patt, P. (1985). Design and testing of a coaxial linear magnetic spring with integral linear motor. IEEE Transactions on Magnetics, 21(5), 1759-1761.

Paul, E., Evans, C. J., Mangamelli, A., McGlauflin, M. L., Polvani, R. S. (1996).

Chemical aspects of tool wear in single point diamond turning. Precision Engineering, 18(1), 4-19.

Peacor, S. D., Cohn, J. L., & Uher, C. (1991). Effect of magnetic field on thermal conductivity of YBa 2 Cu 3 O 7− δ single crystals. Physical Review B, 43(10), 8721.

Pervaiz S, Rashid A, Deiab I, Nicolescu M (2014) Influence of tool materials on machinability of titanium and nickel-based alloys: a review. Mater Manuf Process 29(3):219–252

Philip, J., Shima, P. D., Raj, B. (2007). Enhancement of thermal conductivity in magnetite based nanofluid due to chainlike structures. Applied physics letters, 91(20), 203108.

Philip, J., Shima, P. D., Raj, B. (2008). Evidence for enhanced thermal conduction through percolating structures in nanofluids. Nanotechnology, 19(30), 305706.

Pramanik, A. (2014). Problems and solutions in machining of titanium alloys. The International Journal of Advanced Manufacturing Technology, 70(5-8), 919-928.

Rack, H. J., Qazi, J. I. (2006). Titanium alloys for biomedical applications. Materials Science and Engineering: C, 26(8), 1269-1277.

Rahim, E. A., Sasahara, H. (2011). A study of the effect of palm oil as MQL lubricant on high speed drilling of titanium alloys. Tribology International, 44(3), 309-317.

Rao, B. C., Shin, Y. C. (1999). A comprehensive dynamic cutting force model for

chatter prediction in turning. International Journal of Machine Tools and Manufacture, 39(10), 1631-1654.

Ruibin, X., Wu, H. (2016). Study on cutting mechanism of Ti6Al4V in ultra-precision machining. The International Journal of Advanced Manufacturing Technology, 86(5-8), 1311-1317.

Sales, W. F., Schoop, J., & Jawahir, I. S. (2017). Tribological behavior of PCD tools during superfinishing turning of the Ti6Al4V alloy using cryogenic, hybrid and flood as lubri-coolant environments. Tribology International, 114, 109-120.

Sarıkaya, M., Yılmaz, V., & Güllü, A. (2016). Analysis of cutting parameters and cooling/lubrication methods for sustainable machining in turning of Haynes 25 superalloy. Journal of Cleaner Production, 133, 172-181.

Sata, T., Li, M., Takata, S., Hiraoka, H., Li, C. Q., Xing, X. Z., Xiao, X. G. (1985). Analysis of surface roughness generation in turning operation and its applications. CIRP Annals-Manufacturing Technology, 34(1), 473-476.

Saxena, I., Wolff, S., Cao, J. (2015). Unidirectional magnetic field assisted laser induced plasma micro-machining. Manufacturing Letters, 3, 1-4.

Schieber, D. (1974, February). Braking torque on rotating sheet in stationary magnetic field. In Proceedings of the Institution of Electrical Engineers (Vol. 121, No. 2, pp. 117-122). IET.

Schieber, D. (1975). Optimal dimensions of rectangular electromagnet for braking purposes. IEEE Transactions on magnetics, 11(3), 948-952.

Schmid, M., Varga, P. (1992). Analysis of vibration-isolating systems for scanning tunneling microscopes. Ultramicroscopy, 42, 1610-1615.

Schneider, F., Lohkamp, R., Sousa, F. J. P., Müller, R., Aurich, J. C. (2014). Analysis of the surface integrity in ultra-precision cutting of cp-titanium by investigating the chip formation. Procedia CIRP, 13, 55-60.

Semlitsch, M. (1987). Classic and new titanium alloys for production of artificial hip joints. Titanium Development Association, 721-740.

Shaw, M. C., Vyas, A. (1998). The mechanism of chip formation with hard turning steel. CIRP Annals-Manufacturing Technology, 47(1), 77-82.

Shimada, S., Tanaka, H., Higuchi, M., Yamaguchi, T., Honda, S., Obata, K. (2004). Thermo-chemical wear mechanism of diamond tool in machining of ferrous metals. CIRP Annals-Manufacturing Technology, 53(1), 57-60.

Shimotomai, M., Maruta, K., Mine, K., Matsui, M. (2003). Formation of aligned two-phase microstructures by applying a magnetic field during the austenite to ferrite transformation in steels. Acta Materialia, 51(10), 2921-2932.

Shiou, F. J., Ciou, H. S. (2008). Ultra-precision surface finish of the hardened stainless mold steel using vibration-assisted ball polishing process. International Journal of

Machine Tools and Manufacture, 48(7), 721-732.

Siekmann, H. J. (1955). How to machine titanium. Tool Eng, 34(1), 78-82.

Smith, S., Tlusty, J. (1990). Update on high-speed milling dynamics. Journal of Engineering for Industry, 112(2), 142-149.

Sodano, H. A., Bae, J. S. (2004). Eddy current damping in structures. Shock and Vibration Digest, 36(6), 469.

Sodano, H. A., Bae, J. S., Inman, D. J., Belvin, W. K. (2005). Concept and model of eddy current damper for vibration suppression of a beam. Journal of Sound and Vibration, 288(4), 1177-1196.

Sodano, H. A., Bae, J. S., Inman, D. J., Belvin, W. K. (2006). Improved concept and model of eddy current damper. Journal of Vibration and Acoustics, 128(3), 294-302.

Sommerfeld, A. (1889). Proceedings of the London Mathematical Society, Vol. 28, 395

Sreejith, P. S., Ngoi, B. K. A. (2000). Dry machining: machining of the future. Journal of materials processing technology, 101(1), 287-291.

Suenaga, M. (1984). A source book of titanium alloy superconductivity: by EW Collings; published by Plenum, New York, 1983; 512 pp.; price, US $69.50.

Sundar, L. S., Singh, M. K., Sousa, A. C. (2013). Investigation of thermal conductivity and viscosity of Fe 3 O 4 nanofluid for heat transfer applications. International communications in heat and mass transfer, 44, 7-14.

Taniguchi, N. (1983). Current status in, and future trends of, ultraprecision machining and ultrafine materials processing. CIRP Annals-Manufacturing Technology, 32(2), 573-582.

Teimouri, R., Baseri, H. (2013). Experimental study of rotary magnetic field-assisted dry EDM with ultrasonic vibration of workpiece. The International Journal of Advanced Manufacturing Technology, 1-14.

Teshima, H., Tanaka, M., Miyamoto, K., Nohguchi, K., Hinata, K. (1997). Effect of eddy current dampers on the vibrational properties in superconducting levitation using melt-processed YBaCuO bulk superconductors. Physica C: Superconductivity, 274(1), 17-23.

Tlusty G. Manufacturing Processes and Equipment. Prentice Hall, New York: 2000.

To, S., Cheung, C. F., Lee, W. B. (2001). Influence of material swelling on surface roughness in diamond turning of single crystals. Materials science and technology, 17(1), 102-108.

Toh, C. K. (2004). Vibration analysis in high speed rough and finish milling hardened steel. Journal of Sound and Vibration, 278(1), 101-115.

Tolbert, S. H., Firouzi, A., Stucky, G. D., Chmelka, B. F. (1997). Magnetic field alignment of ordered silicate-surfactant composites and mesoporous silica. Science, 278(5336), 264-268.

Ullakko, K., Huang, J. K., Kantner, C., O'handley, R. C., Kokorin, V. V. (1996). Large magnetic-field-induced strains in Ni2MnGa single crystals. Applied Physics Letters, 69(13), 1966-1968.

Vagnorius, Z., Rausand, M., Sørby, K. (2010). Determining optimal replacement time for metal cutting tools. European Journal of Operational Research, 206(2), 407-416.

Varadarajan, A. S., Philip, P. K., Ramamoorthy, B. (2002). Investigations on hard turning with minimal cutting fluid application (HTMF) and its comparison with dry and wet turning. International Journal of Machine Tools and Manufacture, 42(2), 193-200.

Wang, C., Lin, H., Wang, X., Zheng, L., Xiong, W. (2017). Effect of different oil-on-water cooling conditions on tool wear in turning of compacted graphite cast iron. Journal of Cleaner Production, 148, 477-489.

Wang, H., To, S., Chan, C. Y. (2013). Investigation on the influence of tool-tip vibration on surface roughness and its representative measurement in ultra-precision diamond turning. International Journal of Machine Tools and Manufacture, 69, 20-29.

Wang, H., To, S., Chan, C. Y., Cheung, C. F., Lee, W. B. (2010). A theoretical and experimental investigation of the tool-tip vibration and its influence upon surface generation in single-point diamond turning. International Journal of Machine Tools and Manufacture, 50(3), 241-252.

Wang, K. (1996). The use of titanium for medical applications in the USA. Materials

Science and Engineering: A, 213(1), 134-137.

Wang, Y. H., Zhao, Y. C., Wang, M. Z., Zang, J. B. (2003). Structure and properties of diamond grits coated with corundum micron powders. Key Engineering Materials, 250, 94-98.

Wang, Z. G., Rahman, M., Wong, Y. S. (2005). Tool wear characteristics of binderless CBN tools used in high-speed milling of titanium alloys. Wear, 258(5), 752-758.

Wichmann, W., Von Ammon, K., Fink, U., Weik, T., Yasargil, G. M. (1997). Aneurysm clips made of titanium: magnetic characteristics and artifacts in MR. American journal of neuroradiology, 18(5), 939-944.

Wiederick, H. D., Gauthier, N., Campbell, D. A., Rochon, P. (1987). Magnetic braking: Simple theory and experiment. American Journal of Physics, 55(6), 500-503.

Wolff, S., Saxena, I. (2014). A preliminary study on the effect of external magnetic fields on laser-induced plasma micromachining (LIPMM). Manufacturing Letters, 2(2), 54-59.

Yan, J., Syoji, K., Tamaki, J. I. (2003). Some observations on the wear of diamond tools in ultra-precision cutting of single-crystal silicon. Wear, 255(7), 1380-1387.

Yeo, S. H., Murali, M., Cheah, H. T. (2004). Magnetic field assisted micro electro-discharge machining. Journal of Micromechanics and Microengineering, 14(11), 1526.

Younes, H., Christensen, G., Luan, X., Hong, H., Smith, P. (2012). Effects of alignment,

p H, surfactant, and solvent on heat transfer nanofluids containing Fe2O3 and CuO nanoparticles. Journal of Applied Physics, 111(6), 064308.

Zareena AR, Veldhuis SC (2012) Tool wear mechanisms and tool life enhancement in ultra-precision machining of titanium. J Mater Process Technol 212(3):560–570

Zhang, S., Li, J. F., Wang, Y. W. (2012). Tool life and cutting forces in end milling Inconel 718 under dry and minimum quantity cooling lubrication cutting conditions. Journal of Cleaner Production, 32, 81-87.

Zhang, S. J., To, S., Zhang, G. Q. (2017). Diamond tool wear in ultra-precision machining. The International Journal of Advanced Manufacturing Technology, 88(1-4), 613-641.

Zhang, G., To, S., Xiao, G. (2014). Novel tool wear monitoring method in ultra-precision raster milling using cutting chips. Precision Engineering, 38(3), 555-560.

Zhang, Y., Zhou, Z., Wang, J., & Li, X. (2013). Diamond tool wear in precision turning of titanium alloy. Materials and Manufacturing Processes, 28(10), 1061-1064.

Zhecheva, A., Sha, W., Malinov, S., Long, A. (2005). Enhancing the microstructure and properties of titanium alloys through nitriding and other surface engineering methods. Surface and Coatings Technology, 200(7), 2192-2207.

Zhu, H. T., Huang, C. Z., Wang, J., Li, Q. L., Che, C. L. (2009). Experimental study on abrasive waterjet polishing for hard–brittle materials. International Journal of Machine

Tools and Manufacture, 49(7), 569-578.

Zhu, Y. H., To, S., Lee, W. B., Zhang, S. J., Cheung, C. F. (2010). Ultra-precision raster milling-induced phase decomposition and plastic deformation at thesurface of a Zn–Al-based alloy. ScriptaMaterialia, 62(2), 101-104.

Zhu, Z., Sun, J., Li, J., Huang, P. (2016). Investigation on the influence of tool wear upon chip morphology in end milling titanium alloy Ti6Al4V. The International Journal of Advanced Manufacturing Technology, 83(9-12), 1477-1485.

Zoya, Z. A., & Krishnamurthy, R. (2000). The performance of CBN tools in the machining of titanium alloys. Journal of Materials Processing Technology, 100(1), 80-86.